AD A102093

14/ NOO-SP-265

WESTERN ROSS SEA

AND
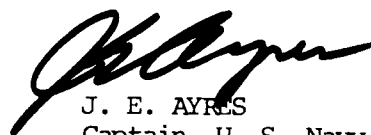
McMURDO SOUND

ICE FORECASTING GUIDE

R. J. PERCHAL

JUNE 1975

NAVAL OCEANOGRAPHIC OFFICE
WASHINGTON, D.C.   20373

FOREWORD

Since 1955, when Operation DEEP FREEZE began, the U. S. Navy has provided support for the Antarctic programs sponsored by the National Science Foundation. Most logistical support of this scientific activity has been conducted by transport vessels. Resupply operations have been centered at McMurdo Station, which has served as the main staging site for other scientific stations on the continent.

This study summarizes sea ice forecasting techniques applicable to the western Ross Sea and McMurdo Sound and sea ice conditions encountered by the resupply ships and escort icebreakers during the 16 resupply seasons from DEEP FREEZE I through DEEP FREEZE 71. Data on means and ranges of ice conditions expand on past investigations of austral summer conditions. Procedures and examples for preparing sea ice forecasts by relating the use of historical and real-time ice data to environmental factors are given.

J. E. AYRES
Captain, U. S. Navy
Commander

Accession For	
NTIS GRA&I	☒
DTIC TAB	☐
Unannounced	☐
Justification	
By	
Distribution/	
Availability Codes	
Dist	Avail and/or Special
A	

ACKNOWLEDGMENTS

CONTENTS

CONTENTS (con.)

FIGURES

EQUATIONS

APPENDIXES

x

Frontispiece— Breakout of fast ice from the southern end of McMurdo Sound, 6 March 1958. Looking north, Hut Point Peninsula and McMurdo Station are in the foreground, Cape Royds and the slopes of Mount Erebus are in the background.

I. INTRODUCTION

Participation by the United States in the international program of scientific investigation in Antarctica has required the deployment of considerable men and materiel. The U.S. Navy is responsible for logistical support of our permanent facilities on the continent. The main staging site, McMurdo Station to which the vast majority of various resupply cargoes are delivered by ship during the austral (southern hemisphere) summer, is located in the southwestern sector of the Ross Sea. To reach McMurdo Station, the resupply vessels must steam through ice congested waters. A knowledge of the prevailing and expected sea ice conditions is required to ensure maximum operational efficiency and safety.

Transits of the Ross Sea have been too infrequent for the accumulation of detailed historical ice data. Ice conditions vary considerably from year-to-year, as well as within the same resupply season. Therefore, the Naval Officer assigned to assess prevailing ice conditions or to prepare ice forecasts is faced with a difficult task.

The purpose of this publication is to provide procedures for forecasting the distribution of sea ice in the western Ross Sea and McMurdo Sound. Analyses of observed ice conditions and related environmental factors also are given to provide useful background information. The sea ice data and forecasting procedures will be for the austral summer because the information was obtained in conjunction with resupply operations. Although many of the sea ice features are quantified and/or located by geographic coordinates with time, the observational period of record in McMurdo Sound and the Ross Sea is brief. Therefore, some modification of these statistics with the collection of additional data may be expected. Similar changes in mean values of various environmental factors are also probable.

The procedures used to prepare any forecast must be objective. However, the subjectivity used in formulating the input values of various environmental factors causes the resulting forecast to be subjective. This is especially true in an area as large as the Ross Sea where, for example, the observed and forecast surface pressure (wind) distributions are based directly on only four land station observations and possibly one or two ship reports. Using such sparse observations, the presence of a storm in the central portion of the Ross Sea might well be undetected, or it may be inferred, but its location cannot be determined very accurately. The vortex pattern of clouds observed by satellite may be used to indicate the upper level position of the storm center with much greater accuracy but its sea level position and intensity must be estimated in order to form an opinion concerning the sea level distribution of wind direction and speed. Furthermore, much remains to be learned about the relationships between the environment and the distributions of sea ice in such an isolated region. Therefore, the subjectivity in forecasting the drift and disintegration of sea ice in the Ross Sea should be readily apparent even though objective tables and graphs are used in part of the forecasting procedures.

This publication will be concerned with ice forecasts of two distinct durations. These are the long-range estimates that give an overall estimate of ice conditions during the ensuing 30 days or longer; and

1

short-range forecasts for 24- or 48-hour durations that emphasize detailed
ice conditions in areas where ship operations are underway or shortly
planned.

II. BACKGROUND DATA

Any discussion which seeks understanding of growth, drift and
disintegration of sea ice in a particular area must include a brief
description of the related environmental factors. This section describes
the most important of these factors, which include wind velocity and
storm tracks, air temperature, ocean currents, and geography of the area.

Some background knowledge of average ice conditions and their
variance during the austral summer is also necessary. Owing to the large
variability indicated by past ice observations, maximum and minimum as
well as median and mean values are given when possible, as well as the
number of years of data upon which mean values are based.

A. Physical Features

The Antarctic Continent (fig 1) is commonly divided into two
parts, East Antarctica and West Antarctica, by a line running along the
western boundary of the Ross Ice Shelf, north of the Horlick, Thiel, and
Pensacola Mountains, and along the eastern edge of the Filchner Ice Shelf.
The Ross Ice Shelf straddles the International Date Line, but lies in West
Antarctica which lies mostly in the western hemisphere; East Antarctica is
situated mostly in the eastern hemisphere.

The Ross Sea is one of the large embayments that borders on West
Antarctica. It extends from Victoria Land eastward to Cape Colbeck and
is located mostly over the continental shelf; depths range generally from
350 to 750 m (191 to 410 fm) but occasionally exceed 900 m (492 fm).
Pennell Bank, located on the shelf near 74.5°S 180°, shoals to 106 m (58 fm)
below sea level. McMurdo Sound, in the southwest corner of the Ross Sea,
ranges from 50 to 75 km (27 to 41 nmi) wide and has a maximum length of
approximately 90 km (49 nmi). Depths in the eastern portion of the sound
range generally from 650 to 900 m (355 to 492 fm) south to the Dellbridge
Islands (fig 15); depths of approximately 550 m (301 fm) extend southward
to the ice shelf. The western portion of McMurdo Sound has shallower
depths which range generally from 200 to 450 m (109 to 246 fm).

The Ross Ice Shelf covers approximately the southern half or about
540,000 km^2 (157,464 nmi^2) of the Ross Sea (Zumberge and Swithinbank, 1962),
is approximately 850 km (459 nmi) wide along its northern edge or barrier,
and extends southward almost 800 km (432 nmi) from the Bay of Whales. The
shelf generally rises from 30 to 40 m (98 to 131 ft) above sea level along
the barrier to the east of the Bay of Whales and from 40 m (131 ft) to
approximately 55 m (180 ft) to the west. It increases in elevation to 100 m
(328 ft) about 225 km (122 nmi) from its southernmost extremity (Bentley,
1962). In the vicinity of Little America V (78°10'S,162°13'W, 1958 position),
the shelf located 15 km (8 nmi) from its northern edge is about 250 m (820 ft)
thick; thinning toward the edge occurs between 3 and 4 m (10 to 13 ft) per
kilometer (Crary, 1961). The Ross Ice Shelf increases in thickness to as
much as 1000 m (3281 ft) at the junction with land ice (Crary and Van der

2

Hoeven, 1961); it is mostly afloat south to its southern limits. Large portions of the shelf periodically break off and drift seaward as tabular icebergs. Most icebergs have horizontal dimensions between a few hundred meters and several kilometers, but icebergs 30 to 40 km (16 to 22 nmi) long are not uncommon; the largest on record was observed 185 km (100 nmi) long (Zumberge and Swithinbank, 1962). Few measurements of absolute movement of the barrier have been made. However, Debenham (1923) computed a minimum rate of movement of 1300 m/yr (4265 ft/yr) between 173°W and 179°E by comparing the 1902 Discovery survey of the ice front with the 1911 Terra Nova survey. Crary (1961) indirectly calculated a movement of 1400 m/yr (4593 ft/yr) in the vicinity of 168°W which he states may be 3 to 4 times as fast as movement of the barrier to the east of Roosevelt Island (79°S, 162°W). Estimates of the movement of the ice front in the Bay of Whales sector have been collected by Wexler (1960) who quotes speeds between 322 and 458 m/yr (1056 and 1503 ft/yr).

Perhaps the most important environmental factor affecting McMurdo Sound and the Ross Sea, winter air temperature, is related to East Antarctica topography. East Antarctica is nearly four times as large as West Antarctica and consists of an almost unbroken undulating plateau of snow and ice that reaches an interior height of more than 4 km (13,000 ft). This expanse of ice (more than 3.5 km (11,500 ft) thick in places) gradually slopes to an elevation of 2 km (6,500 ft) some 100 to 400 km (54 to 216 nmi) from the north coasts. East of 125°E, from 72°S inland nearly to the central dome, the ice surface slopes eastward toward the western edge of the Ross Sea and Ross Ice Shelf an average between 1:1000 and 2:1000. This gentle slope, however, is terminated along Victoria Land and the western edge of the Ross Ice Shelf by the chain of high mountains forming a portion of the border of East Antarctica.

Ross Island forms the eastern side of McMurdo Sound and is about 78 km (42.1 nmi) wide (east-west) between Cape Royds and Cape Crozier and about 77 km (41.6 nmi) long (north-south) between Cape Bird and Cape Armitage (fig 15). The island is dominated by Mount Erebus (3,795 m, 12,450 ft) from which a ridge extends eastward to Mount Terra Nova (1,829 m, 6,000 ft) and Mount Terror (3,094 m, 10,150 ft) and northward to Mount Bird (1,719 m, 5,640 ft).

B. Storm Tracks

Storms that affect Ross Sea and McMurdo Sound (U.S. Navy Weather Research Facility, 1960) follow three main tracks as indicated in figure 2. These are:

(1) Major cyclones that frequently originate near western Australia, move south of Tasmania, and thence southeastward into the eastern Ross Sea (track 1).

(2) Small cyclones or vortices that follow an eastward track approximately 300 nmi (556 km) off the Antarctic coast and enter the Ross Sea near 70°S, 180°S (track 2).

(3) Storms that enter the Antarctic continent near 155°E, cross Victoria Land, and move southeastward over the southern sector of the

Ross Sea onto the Ross Ice Shelf (track 3).

Cyclones which follow track 1 and track 2 may continue on an eastward trajectory within 300 nmi (556 km) of the coast, or travel inland near the eastern portion of the Ross Ice Shelf. Storms that travel inland may then follow a trajectory that recurves toward the west over the Ross Ice Shelf; storms following this track are referred to as the retrograde type. Although the three tracks imply that storms pass out of the Ross Sea, low pressure centers tend to stagnate or even develop in the Ross Sea embayment.

Cyclones that originate near western Australia attain lower central pressures (deepen) along their southeastward trajectory and reach a maximum intensity as they cross the Antarctic Convergence near 55°S. These systems (track 1) then usually display a decaying condition and a higher central pressure (filling) as they merge into the semi-permanent low pressure in the eastern Ross Sea. Low pressure is customarily found there because the Ross Sea is one of the principal cyclone graveyards in the Antarctic.

The small cyclonic vortices that approach the Ross Sea from the west (track 2) are thought to be major perturbations along the Antarctic front; that is, along the northern edge of cold air which has moved from the continent over coastal water during the austral summer. Some are also thought to be decayed ocean storms which continue eastward upon reaching the Antarctic front.

The merging of these coastal vortices (track 2) with major cyclones (track 1) produces violent Antarctic storms which may last several days and in which central pressures as low as 923 to 940 mb have been observed.

C. Sea Level Pressure

The distribution of mean monthly sea level pressure over the Ross Sea and adjacent areas (Taljaard et. al., 1969) is presented in Appendix A, figures A-1 through A-12. Over the water regions adjacent to coastal stations or along the commonly used sea routes, the pressure charts were based primarily on pressure data taken at those locations. Analyses over land were drawn strictly according to the mean reduced pressure values. Over the remainder of the area, a best fit of the isobars was obtained by comparison of grid point pressure values with charts of vector winds contained in different climatic atlases.

The pressure patterns strongly reflect the frequency and location of tracks and intensity of cyclones which approach and exit from the Ross Sea. Additionally, the closed, generally circular, isobars confirm the tendency for cyclones to stagnate and decay in the Ross Sea. During early spring (September and October), the semi-permanent low pressure area is located farthest southward and has the lowest central pressure. The highest central pressure occurs during the austral summer (December and January), when its mean position is displaced north of the Ross Sea. The large-scale sea level circulation implied by the mean pressure distributions is generally toward the north over the western Ross Sea during May through

4

October when ice growth is abundant. In the eastern Ross Sea, large-scale circulation is toward the southwest from May through June. From July through October circulation along the coast is very light; farther offshore, circulation is toward the northeast.

From November through April which spans the ice disintegration season, the large-scale circulation over the western Ross Sea generally is toward the northwest. Dominant east winds are found over the central and eastern portion of the Ross Sea. Spacing of the isobars over McMurdo Sound indicates mean monthly south to southeast geostrophic winds of approximately 5 kn (9 km/hr) in January to 18 kn (33 km/hr) in October (chart scale 1:11,000,000). However, prevailing 10 to 15 kn (19 to 28 km/hr) easterly winds recorded at McMurdo Station throughout the year emphasize the large non-geostrophic component of surface wind over land and the effects of local topography. The predominance of easterly wind at Hut Point is caused by the deflection of the southeasterly air stream as it strikes the southern edge of Ross Island. The surface air motion in the eastern portion of McMurdo Sound probably varies from east to south. Winds should be mainly southeast to southerly over the western portion of the sound; south winds should prevail at the western limits owing to the north-south orientation of the Royal Society Range which rises to a mean elevation of 2.75 km (9,000 ft) with peaks extending to 4.25 km (14,000 ft).

D. Surface Air Temperature

The distribution of mean monthly air temperature (degrees Celsius) over the Ross Sea and adjacent areas (Taljaard et. al., 1969) is presented in Appendix B in figures B-1 through B-12. Surface values for points over water were derived from comparison of air temperatures given in different marine climatic atlases. Irregular isopleths in some areas were minimized by constructing curves of the annual variation of temperature at grid points. Inspection of the curves at a group of neighboring points indicated the most probable smooth curve of the annual march of temperature at the innermost point. The analysis of surface air temperatures over land was difficult because of complicated topography and insufficient stations to draw isotherms objectively. However, the analyses were made by relating available values to smoothed regional topography.

Probably the best known distinguishing feature of Antarctica is its extremely low mean surface temperature which is reflected by cold summers and severe winters. Because snow covers more than 98% of the continent (Thiel, 1962), little solar energy is absorbed and its own heat is readily radiated. Subsidence over the continent results in a clear sky which, in turn, facilitates the radiation. Heat loss is greatest during winter and cooling occurs primarily at the surface; summer heating occurs at the surface as well as aloft. Heating of the surface air in summer, however, depends much more on the temperature of the earth's surface, with which the air is in contact, than on the direct rays of the sun since they never are strong enough to melt the snow even when the sun is at its greatest altitude. Therefore, the mean temperature of the warmest month is below 0°C almost everywhere in Antarctica.

5

Mean monthly temperature values for McMurdo Station, compiled through 1970 from U.S. Navy and National Weather Service data, are included on each figure. Some difference is apparent between these data and interpolated values between isotherms because the periods of record are different.

The normal march of mean monthly air temperature is probably quite similar at all Antarctic stations. The major temperature decrease occurs by May after which temperatures continue to fall slowly owing to a continuing radiation heat loss. The general pattern of the annual temperature profile shows a broad flat minimum during the austral winter. It has been suggested (U.S. Navy Weather Research Facility, 1960) that, owing to the effect of newly formed pack ice to the north during mid-winter, the lowest surface temperatures usually occur well after the winter solstice; that is, in August or as late as September. However, a minimum with slightly higher temperatures also often occurs about July. During spring the steepest rise in temperature occurs in October. During November, December, and January, temperatures increase owing to increased incoming radiation, but at a much slower rate.

Advection of cold air from the interior over McMurdo Sound and the Ross Sea is thought to occur as a result of the invasion of storm centers from lower latitudes in other quadrants which impinge on lobes or separate centers of the cold air mass over the plateau. The resulting outflow of cold air also may be aided by down-sloping topography. According to Ball (1960), katabatic winds may be expected to predominate over gradient winds where the slope is 2:1000, and can still be important on less steep slopes. Slopes of this order are present west of the Ross Sea and Ross Ice Shelf to 125°E. Drainage of surface air from this sector of the interior over the Ross Sea, however, may be diminished by the Coriolis deflection and by the presence of the high mountains along eastern Victoria Land and the western limits of the Ross Ice Shelf.

E. Surface Currents

A generalized distribution of surface currents over the Ross Sea and adjacent waters is given in figure 3. Current directions and magnitudes in heavy print were taken directly from U.S. Navy Hydrographic Office Pub. 705, (1957). Directions in lighter print and magnitudes in parenthesis have been estimated for use in ice forecasting.

The surface current over the Ross Sea, called the East Wind Drift, is dominated by prevailing easterly and southeasterly winds. Current speeds range from 1 to 3 kn (1.9 to 5.6 km/hr) along the Ross Ice Shelf, where data are adequate, to estimated speeds of 0.2 kn (0.4 km/hr) at the Antarctic Divergence, where data are sparse. Along Victoria Land, the westgoing current is deflected to the north.

North of the Antarctic Divergence, which is a zone of general upwelling, is the eastgoing West Wind Drift which transports large volumes of surface water. A zone exists within the West Wind Drift, the Antarctic Convergence, which probably separates the generally easterly sets to the north from the northeasterly sets to the south. However, the

current regime is uncertain in this region, and the slow surface drifts are subject to considerable variation. Therefore, surface currents around the Antarctic Convergence are not well defined.

F. Pack Ice

During winter, sea ice completely surrounds the Antarctic Continent and extends northward hundreds of miles in a fairly continuous sheet. Only during summer does the sea ice disintegrate in some areas to permit access to land areas and broad ice shelves. Some coastal areas of the continent remain, for the most part, inaccessible to vessels even during summer months.

One coastal area that is always accessible in summer is adjacent to most of the Ross Sea. The ice edge reaches its maximum northward extent during late September primarily owing to current and wind drift of pack ice to the north but also as the result of freezing of the open sea. This northward drift which is especially evident over the western sector of the Ross Sea causes a movement of ice away from the area adjacent to the Ross Ice Shelf. Therefore, the latter area probably never freezes over to any great extent because of the constant drift of ice far to the north of the continent. Probably as a result of dispersal of ice northward and regrowth of new ice in colder areas adjacent to the continent, sea ice formed in the Ross Sea is relatively thin compared to drift ice found in other sectors surrounding Antarctica. Sea ice formed in the Ross Sea probably attains an average end-of-winter thickness of approximately 2 to 4 ft (0.6 to 1.2 m) with pressure ridges an average of 5 ft (1.5 m) thick. Sea ice found along the Ross Ice Shelf in winter probably consists of new and young ice up to 1 ft (0.3 m) thick.

During summer, the prevailing wind drift of ice over the western area of the Ross Sea is toward the northwest. This drift, similar to winter drift causes a movement of ice away from the area adjacent to the Ross Ice Shelf. The latter sector is the first to clear during the austral summer and the ice free area enlarges to the north in the western portion of the Ross Sea. The northern edge of the pack ice concurrently recedes southward and, usually during late January, the ice free areas merge near the northwest portion of the Ross Sea. An ice-free passage to the Ross Ice Shelf in the western sector of the Ross Sea is then possible.

Owing to the Coriolis deflection to the left (southern hemisphere), the mean direction of ice drift is more directly onto the Victoria Land coast during summer than during winter, when the large-scale circulation is northward. Advection of ice against Victoria Land during summer is evident by a band of close to compact sea ice that remains there after much of the western Ross Sea has cleared.

Dominant westward current and wind drift over the central and eastern portions of the Ross Sea from November through April are thought to advect thick ice into those sections and frequently into the western sector of the Ross Sea from the area east of Cape Colbeck. Observations made between 160°W and 180°, including satellite imagery, indicate that large amounts of heavy pack remain in that sector of the Ross Sea into late

austral summer. It is probable that large areas of very open pack and some open pack belts and patches of hummocky floes remain in that sector to the beginning of freezeup in April.

1. North Pack Edge

Ship observations of the location of the northern edge of pack ice were extracted from post-operational reports of the various icebreakers which transited the Ross Sea from DEEP FREEZE (DF) I through DF 71. Observations by resupply vessels were included for unescorted transits. Locations of the edge observed by aerial reconnaissance from DF 61, when observations began, through DF 71 were also included.

a. Procedure

Positions of the northern edge of pack ice observed during each austral summer were plotted, and ice edges at the beginning and middle of each month from 15 October through 15 January were interpolated between observations from 170°E to 180°. In a few instances, locations of edges obviously inconsistent with other data taken within the same year were rejected. Latitudes of interpolated edges at even longitudes were recorded as far as 3° of longitude from an observation. Additionally, interpolated edges were recorded only within 18 days of an observed edge. Latitudes of extrapolated ice edges were recorded when an observation was made within 12 days of the 1st or the 15th of each month. Average and median values at half-monthly intervals were calculated from the recorded latitudes and are summarized in figure 4. Average and median values, latitude ranges, and frequency of data also are given separately for each period in figures 5 through 8.

The northern edge of pack ice was defined by 1 okta or more of ice concentration. Therefore, a few discrepancies of latitude of the pack edge occurred when an encounter with heavier pack was reported as the northern pack edge after lighter ice concentrations were transited.

b. Semi-Monthly Positions and Ranges

Usually, the northern pack edge in the western Ross Sea was located approximately at 62°45'S by 15 October (fig 5). Average and median values indicate the pack edge receded southward along each longitude at a fairly uniform rate. By 15 December, the edge had receded approximately to 66°S (fig 7); by 15 January, it was located at approximately 67°45'S (fig 8). Average and median positions of the pack edges bent slightly southward between 176°E and 180°. This trend increased slightly at successive half-monthly intervals indicating that usually a more southern latitude can be reached at any time along 180° than along longitudes to the west. However, the location of the inner or southern pack edge and pack concentration analyses should be consulted to determine the most ice free route to the Ross Ice Shelf.

Figures 5 through 8 indicate that the largest latitudinal range variability in north pack edge location was approximately four degrees of latitude in mid-December. The occurrence of largest ranges

8

during this period, except along 170°E, may be related to a greater density of observations. The maximum range along 170°E was observed during late October and early November and also seemed to be related to a data maximum. Latitude ranges should not be taken as the absolute limits of all sea ice since isolated floes of considerable size may drift north of the pack edge. For example, on 6 December 1961 the USS ATKA reported a giant floe at 63°19'S, 177°09'E, which was approximately 100 nmi (185 km) north of the pack edge.

Average and median locations usually were separated by 15 nmi (28 km) or less. The largest separation of 20 nmi (37 km) occurred on 1 December along 174°E, 176°E, and 178°E and can be attributed to location of the pack edge exceptionally far south during DF 69. A comparison of the paired average and median latitudes shows larger southward than northward anomalies of the pack edge position. Almost twice as many cases of more southern average latitudes than median latitudes were observed. Therefore, the ice forecaster should be aware that accelerated southward retreat of the north pack edge occurs more often than retarded recession of the edge. Furthermore, interpolated ice edges always progress southward. Therefore, a more southern latitude always should be given in a 15-day ice forecast even though the edge may drift northward over shorter time intervals.

c. Recession During Individual Seasons

Mean positions of the north pack edge indicate the overall pack recession computed over many years. However, recessions of the edge over monthly intervals during individual resupply seasons probably are more useful as background information to the forecaster for preparing 30-day ice forecasts. These data may be used independently when estimates of environmental trends are not available in preparing the forecast.

A preliminary analysis of the normal (median) locations of the edge on 15 November and 15 December shows that similar anomalous positions of the edge occurred along 174°E, 176°E, 178°E, and 180° during any particular year. Inclusion of data from all longitudes for one year therefore would result in duplicate rather than additional independent data. Accordingly, the ice edge along only one longitude for each resupply season and 30-day period was used in the analysis of monthly edge recession. Four overlapping 30-day periods were used: 1 November to 1 December; 15 November to 15 December; 1 December to 1 January; and 15 December to 15 January. A total of 31 observations (7 to 9 observations per period) was compiled from the interpolated positions used to calculate mean positions of the edge; 26 were along 176°E. Data along 176°E were selected for study over other observations because initial penetration and transit of the pack is usually along that meridian. The following summary may be used if a backlog of annual ice observations is not at hand.

The grouped data indicate all north pack edges 40 nmi (74 km) or more south of normal (8 observations) at the beginning of the 30-day period or on "forecast day" were south of normal one month later. Three observations 90 nmi (167 km) or more south of normal were equally or slightly more south of normal (by 15 to 30 nmi) (28 to 56 km) whereas five locations of the edge 40 to 60 nmi (74 to 111 km) south of normal had retarded

9

recession but the edges remained south of normal.

Ten edges located from 5 to 40 nmi (9 to 74 km) south of normal on forecast day receded to the range from 30 nmi (56 km) south of normal to 20 nmi (37 km) north of normal 30 days later. A larger number of observations of edge recession closer to normal than farther from normal was observed. The largest change from the normal recession rate occurred when the edge 25 nmi (46 km) south of normal became 15 nmi (28 km) north of normal 30 days later.

All positions of the edge from normal to north of normal on forecast day remained normal or north of normal 30 days later. Nine edges located at normal to 30 nmi (56 km) north of normal on forecast day were related to retarded pack edge recession; that is, more occurrences of the edge becoming farther north than closer to normal 30 days later were observed. The largest departure from a normal rate of edge recession occurred when the edge 5 nmi (9 km) north of normal became 55 nmi (100 km) north of normal 30 days later.

Locations of the edge greater than 30 nmi (56 km) north of normal on forecast day (4 observations) were related to accelerated pack edge recession; that is, more occurrences of edge recession closer to normal than farther north of normal 30 days later were observed. The largest departure from a normal rate of edge recession occurred in two cases when the edge 85 and 65 nmi (157 and 120 km) north of normal, 30 days later, became 20 nmi (37 km) and 0 nmi north of normal, respectively.

d. Seasonal Recession Rate

A seasonal position of the edge, which indicates its overall southward recession rate is given in figure 9. An overall median latitude for each period was calculated from the six median values from 170°E to 180°. Median values probably are better indicators of central tendency than average values because they are less dependent on a single observation. The seasonal linear recession rate was approximately 3 1/3 nmi/day (6.2 km/day) from 15 October to 15 January.

2. South Pack Edge

The same data sources and analysis technique used to calculate mean positions of the northern pack edge were used to calculate positions of the inner or southern pack edge in the western Ross Sea at half-monthly intervals from 15 November to 15 January. A composite of average and median values is given in figure 10. Average and median values, latitude ranges, and frequency of data are also given separately for each period in figures 11 through 13.

a. Semi-Monthly Positions and Ranges

Sparse data indicate that pack ice (gray and gray-white) probably lies adjacent to the Ross Ice Shelf on 1 November. By 15 November, the pack westward of 174°E remained generally against the shelf but east of 174°E a large ice free area had formed north of the shelf. The ice-free

area expanded northward most rapidly during the latter half of November; the edge extended to approximately 73°15'S by 1 December. Recession of the pack farther northward then slowed to a fairly steady rate, the edge reaching approximately 70°S by 15 January.

Average and median locations indicate the south pack edge was located farthest north along 178°E by 15 November, 176°E in December, and 174°E during early January. Southward trend of edges along 170°E and 172°E resulted from the remnant pack adjacent to Victoria Land. Similarly, more southern positions calculated along 180° resulted from the general southeastward oriented southern pack edge in the central portion of the Ross Sea.

Figures 11, 12, and 13 indicate that the largest latitudinal range (greatest locational variability) of the southern pack edge occurs from the latter half of December to the first part of January. This feature is similar to observations of the north pack edge and may be related to a greater density of data during the same period. The largest range, almost seven degrees of latitude, occurred during early January along 170°E. This extreme range can be related to the north-south oriented pack edge along the Victoria Land coast which receded west of 170°E during this period.

Average and median locations were usually close to each other. However, the largest difference occurred in mid-November along 172°E and 174°E, where average positions were skewed toward northern latitudes owing to a very rapid northward movement of the south pack edge during DF II. During the other three years when observations were made, the pack remained adjacent to the Ross Ice Shelf. Similarly, the average location along 180° on 15 January was skewed to the south owing to retarded recession of the edge during DF 60; more northerly positions were observed during the other two years. A comparison of the paired median and average positions indicates to the ice forecaster that accelerated and retarded recession from the seasonal recession rate has an almost equal chance of occurrence.

Few observations of a net southward movement of the south pack edge over a 15-day period in DF I through DF 71 were observed. One notable southward movement occurred during early January 1968 (DF 68) when heavy pack ice between 69°S and 72°S drifted westward across the tracks used by ships in transit between McMurdo Station and New Zealand ports. The westward edge of this pack, which drifted from the central part of the Ross Sea, was observed by aerial reconnaissance as extending generally from 69°S 174°E to 72°S 175°E. The USNS ELTANIN reported a very heavy buildup of floes up to 20 ft (6 m) thick along the southern portion of the pack edge and the USCGC WESTWIND reported very heavy east-west belts of ice cakes 10 to 15 ft (3 to 5 m) thick with 5 to 6 ft (1.5 to 1.8 m) of snow cover over portions of the northern sector. This mass of ice threatened to cut off access to the ice-free area north of Ross Ice Shelf by a continued westward drift against the coast south of Cape Adare. Fortunately that did not occur; however, the ice forecaster should be aware of such ice masses and their potential for interference or blockage of shipping.

b. Recession During Individual Seasons

Monthly data on recession of the south pack edge during
individual resupply seasons, like data on the north pack edge recession, probably
are more useful as background information than mean ice edge data for preparing
30-day ice estimates. Data selection was similar to procedures used to study
the north pack edge except that only three overlapping 30-day periods were avail-
able for analysis; 15 November to 15 December, 1 December to 1 January, and
15 December to 15 January.

A total of 14 paired observations were compiled (4 or 5
observations per period) of which 10 were along 176°E. Five observations of
the south pack edge were 60 to 130 nmi (111 to 241 km) south of normal at
the beginning of the 30-day period or on "forecast day." Three observations
over this range indicated that the edge receded northward slightly faster
than normal, as indicated by 30 nmi (56 km) smaller anomalies 30 days later.
Two observations indicated pack edge recession of from 90 to 110 nmi (167
and 204 km) south of the normal position on forecast day to 15 and 170 nmi
(28 and 315 km) north of normal respectively 30 days later. The recession
rate in the latter case is 280 nmi (519 km) greater than the normal recession
of 125 nmi (231 km). Therefore the ice forecaster should be aware that
very rapid northward advection of the south pack edge may follow a much
farther than normal southward position of the edge.

Six observations of the pack edge were within 20 nmi (37 km)
of the normal position at the beginning of the 30-day period. Four obser-
vations showed the pack edge still within 20 nmi (37 km) of the normal
position 30 days later. The other two locations were 90 and 145 nmi (167 and
269 km) south of normal at the end of 30 days on 15 December along 174°E and
were related to retarded northward pack recession from the Ross Ice Shelf.

Three observations of the pack edge 80 to 150 nmi (148 to
278 km) north of normal at the start of the 30-day period (one observation
from each 30-day period), were related to various locations of the pack edge
30 days later. The edge with the most anomalous position receded northward
slightly faster than normal, resulting in a 170 nmi (315 km) anomaly. The
pack in the other two cases receded northward more slowly than normal. The
edge with the 80 nmi (148 km) anomalous position receded to 45 nmi north of
normal whereas the remaining edge, 115 nmi (213 km) north of normal, receded
to 20 nmi (37 km) south of the normal edge position 30 days later.

c. Seasonal Recession Rate

A seasonal position of the edge and indication of its
overall rate of northward recession are given in figure 14. An overall
median latitude for each period was calculated by grouping the four median
values found from 174°E through 180°. Values along 170°E and 172°E were
not included in the computations because they were representative of pack
along Victoria Land and not of the northward recession of the pack in the
western Ross Sea.

The overall recession rate during the latter half of November
was approximately 12 nmi/day (22 km/day). From 1 December to 15 January the
data indicate an overall rate decrease to a little more than 4 nmi/day (7.4
km/day).

12

Much higher recession rates, however, have been observed in specific resupply seasons. During DF 70 the south pack edge was observed at approximately 74°S 176°E on 9 December and at 71°S 176°E on 17 December. Therefore, the recession rate between observations was 22.5 nmi/day (41.7 km/day). However, the intense Ross Sea storm which caused this movement occurred over a 3-day period. The average recession during those 3 days would be approximately 53 nmi/day (98 km/day) assuming the seasonal rate of 4 nmi/day (7.4 km/day) on the remaining 5 days. Strong southerly winds over the southwestern Ross Sea nearly always occur when a deep surface storm center is located in the southern Ross Sea midway between McMurdo Sound and the Bay of Whales. Surface winds accompanying these storms have speeds in the 100 kn (185 km/hr) range with gusts of 20 to 40 kn (37 to 74 km/hr) and normally last from 1 to 3 days. These storms produce the greatest northward recession of the south pack edge. The state of deterioration of the pack probably is another factor, as well as wind stress, which can affect rates of pack recession on a day-to-day basis.

3. Final Pack Disintegration

Figures 8 and 13 indicate that by 15 January the remaining pack ice across the northwestern Ross Sea (172°E to 178°E) generally was located between 68°S and 70°S. Sparse observations suggest that most of the pack in this region disintegrated during the latter half of January. Extrapolation of the overall recession rates of the north and south pack edges indicate that by 1 February remnant pack, if still present, would be located in the vicinity of 69°S. It is possible, however, for remnant belts and patches of pack ice to drift large distances and take considerably longer to disintegrate especially during severe ice years. For example, during DF I, narrow bands of pack ice up to 1 ft (0.3 m) thick were observed from 64°45'S to 65°45'S along 177°E by the USS GLACIER on 27 February 1956.

Pack ice usually is kept against Victoria Land by dominant winds and the irregular coastline. Probably as a result of wave action, ice floes along the edge are usually in a compact band and well broken into brash and small ice cakes. Big and vast floes are usually found in shoreward areas as a result of the breakup of fast ice. Sparse observations indicate that the pack gradually narrows and that by 1 March most of it has disintegrated.

4. Ice Concentration and Large Floe Size

a. Introduction

Mean percentages of ice cover (or concentration) and large floe size were computed for the western Ross Sea from 62°S to 77°S between 160°E and 175°W and are presented in Appendix C. Concentration and floe-size data were analyzed for each one-degree square during each half-monthly (15-day) period by considering data covering the four one-half degree quadrangles surrounding the intersection of each integer latitude and longitude. Aerial reconnaissance conducted from DF 62 (1961-62) through DF 69 (1968-69) was the primary source of data for both studies. Icebreaker reports, mostly in the northern portion of the study area, also were used. In addition, satellite data supplemented aircraft and icebreaker observations, but only to determine ice concentrations because floe sizes presently cannot be determined from satellite data. Thermal expansion and contraction as well as

13

collisions and pressure between floes are thought to be the major factors associated with the breakup of pack into smaller floes. Collisions caused by wave action result in increased breakup of floes along pack edges.

The concentration and floe-size charts give a better idea of the severity of ice conditions when used together than if concentration charts were used alone. For example, some areas containing seven or eight oktas ice concentration may contain only a small percentage of large floes, whereas some areas of lesser concentrations may contain mostly big floes or larger. Utilization of both charts for each period should provide a better understanding of the breakup of ice in the western Ross Sea. Therefore, ice concentration and large-floe percentage charts were grouped by successive 15-day periods to facilitate use by the ice forecaster.

b. Procedures

Available ice concentration data in oktas (eighths of surface area covered) were tabulated for each one-degree square by half-monthly periods from 1 October to 31 January. When several observations were available for a 15-day period in a particular year, the greatest weight was given to the concentration observed during the middle portion of the period for that particular one-degree square. Concentration data representative of each one-degree square and DEEP FREEZE season were then averaged and the resultant values were plotted and analysed. Figures C-1, C-3, C-5, C-7, C-9, C-11, C-13, and C-15 give these analyses for successive half-monthly periods. Numerals within each area represent the concentration in oktas of surface area covered. A concentration value of 9 represents an area of fast ice or an area of eight oktas of ice with no openings. A value of 8 denotes an area with eight oktas concentration with openings.

Data on the amount of big, vast, and giant floes (>500 m or 1640 ft in extent) which collectively are called large floes in this study were tabulated for each one-degree square and half-monthly period commencing 1 October and ending 15 January. The 16 to 31 January chart was omitted owing to data insufficiency. A weighting factor for determining the representative percentage of large floes similar to the procedure for finding representative concentration values was employed. Representative percentages of big floes or greater for each one-degree square and DEEP FREEZE season were then averaged and the resultant values were plotted and analyzed for each 15-day period. It should be noted that the values plotted are percentages of the one-degree square covered with large floes as opposed to the ratio of large floes to the total amount of ice present. For example, if six oktas of ice were present and four oktas were large floes, 50 percent of the square would be covered with large floes and that is the statistic that was analyzed. Lines of equal large floe-size coverage, usually in 10% increments for each 15-day period, are given in figures C-2, C-4, C-6, C-8, C-10, C-12, and C-14.

c. Concentration Analysis

Half-monthly analyses from October through November indicate a slow decrease in pack concentrations; a rapid decrease commences 1 to 15 December.

14

During October (fig C-1 and C-3), little change is
apparent from mostly 7 to 8 okta concentrations that occur in the
shipping lanes between approximately 67°S and McMurdo Sound. Some small
6 okta areas develop temporarily, however, during late October to the
east of Cape Hallett. Very open and open pack from 2 to 3 degrees of
latitude wide lie to the north of the 7 to 8 okta pack. During November
(fig C-5 and C-7) the modal concentration in the approaches to McMurdo
Sound decreases slightly to 7 oktas, but significant areas of 4 to 6
okta concentrations form north of the Ross Ice Shelf during the latter
half of the month.

A rapid decrease in pack concentration begins during
1 to 15 December (fig C-9) in the area north of the Ross Ice Shelf;
however, 7 oktas of pack remain across the shipping lanes generally from
68°30'S to 70°30'S. A ship steaming along 176°E during 16 to 31 December
(fig C-11) generally will encounter an overall maximum pack concentration
of 4 oktas over approximately 1 to 2 degrees of latitude about 69°S.
However, some 6 and 7 okta pack probably would have to be transited south
of Franklin Island (76°05'S, 168°15'E) before reaching lighter concentrations
which extend northward from McMurdo Sound.

During 1 to 15 January (fig C-13), the pack band
extending across the northwest approaches to the Ross Sea narrows consider-
ably, but 4 okta concentrations probably still will be encountered over
small areas before reaching ice-free water north of the Ross Ice Shelf.
The northwest entrance to the Ross Sea becomes ice free during 16 to 31
January (fig C-15). However, 4 to 6 okta concentrations remain to the
south and west of Franklin Island the entire month. The apparent increase
in pack concentrations in the approaches to McMurdo Sound during January
may be attributed to compression of the pack due to westerly currents in
combination with increased dislodgment of fast ice from McMurdo Sound.

d. Floe-Size Analysis

During October (fig C-2 and C-4) high percentages (60% to
100%) of large floes occur in the northwestern approaches to the Ross Sea
and in the southwestern Ross Sea where 8 okta concentrations are prevalant.
However, a minimum area (30% to 50%) of large floe sizes off Victoria Land
north of 74°S is significant since·pack concentrations are 6 to 7 oktas.
This zone of low percentages of large floes and high pack concentrations
may occur in conjunction with accelerated growth of ice adjacent to the
coast. Breakup of relatively thin sea ice under pressure in a broad zone
along the outer edge of the thick coastal ice may account for this minimum
frequency area. The relatively thin sea ice may originate in the southern
Ross Sea and advect with a component against the thick coastal ice by pre-
vailing currents and drift to the left of mean surface winds.

During 1 to 15 November (fig C-6) this low percentage
area of large floes (along 174°E) extends northward to 68°S; maximum
percentages occur generally along a line from 69°S, 180° to 75°S, 170°E
and a zone of minimum percentages is located generally along 180° to
the south of 71°S. During 16 to 30 November (fig C-8), these three zones

15

appear to move 1 to 4 degrees of longitude westward with little decrease in percentage values.

A significant decrease of large floes occurs during 1 to 15 December (fig C-10). The decrease in percent of large floes south of approximately 72°S and east of 173°E is related to the rapid decrease in concentration in that sector. Between 172°E and 180° from 68°30'S to 72°S, however, large floe sizes occupy generally less than 30% of the surface although the pack concentration is 6 to 7 oktas. Continued rapid decreases of large floe percentages occur during 16 to 31 December (fig C-12) and 1 to 15 January (fig C-14) when few large floes are present east of 173°E.

e. Reliability of Analyses

Data from eight DEEP FREEZE seasons were used to determine mean ice concentrations and the distribution of large floe sizes over the western Ross Sea. However, data were not available for each one-degree square during each 15-day period. Therefore, the number of years of data that were used to compute the mean conditions were tabulated in order to indicate a degree of reliability to the analyses. Usually, no analysis was made without data. However, some areas were assumed to be ice free without data if the area was a considerable distance from any ice and there was no question that the area was ice-free before and after the period under study. This occurred in some one-degree quadrangles north of the north pack edge late in the season that were ice free earlier in the austral summer.

Areal distributions of the number of years of data used to prepare mean ice concentrations and large floe-size percentages were similar for analyses covering the same half-monthly period. During all periods except those in January, the most data were taken generally between 169°E and 174°E southward to 72°S and thence in a broad zone toward McMurdo Sound because most logistics/ice observation flights were conducted in that corridor. Excellent data reliability (7 or 8 years of data) occurred generally within a sector of that corridor from Cape Adare to McMurdo Sound approximately 50 to 100 nmi (93 to 185 km) wide during the latter half of October through November. Fair (3 or 4 years of data) and good (5 or 6 years of data) reliability extended northward over the corridor of maximum data and eastward of the excellent data sector to 180°. In other areas, the reliability of ice analyses generally was poor (1 or 2 years of data). During 1 to 15 October data reliability was generally good in the Cape Adare-McMurdo Sound sector; fair and poor in other regions.

During 1 to 15 December the northern extent of the area of excellent data reliability receded southward to 73°S; further recession to 76°30'S occurred during 16 to 31 December. During both periods data reliability was good over most of the remainder of the analysis area south of Cape Adare; fair and poor to the north. During January, good data reliability occurred over the entire analysis area south of approximately 71°S, whereas fair and poor reliability occurred northward.

16

5. Ice Thickness

Sea ice thicknesses, reported principally by icebreakers on north-south transits through the western Ross Sea, had a wide range of values. However, data indicate that the thickest drift ice encountered during the resupply season generally was found at locations between approximately 67°30'S and 72°30'S. As the austral summer progressed, ice thickness diminished, and the zone of maximum thickness narrowed and reached a central latitude of approximately 69°S. Most pack ice in the western Ross Sea is thin, medium, or thick first-year ice; that is, one winter's growth.

Accumulations of hummocky multi-year floes 8 to 12 ft (2.4 to 3.7 m) thick or more, which probably drift from the eastern Ross Sea, may be encountered in a zone eastward of a boundary generally extending from 67°30'S, 178°E to 72°30'S,178°E to 75°S,175°W; they probably can be found in this part of the western Ross Sea at almost anytime during the resupply season. On occasion, they also may be found in other sectors of the western Ross Sea or its approaches. Since they are thought to originate in the sector east of Cape Colbeck, the amount of multi-year floes present in the western Ross Sea during the austral summer probably is related to the availability of these floes and mean drift patterns and not directly to the severity of winter temperatures over the Ross Sea. Therefore, multi-year floes may be present or absent in the western Ross Sea during otherwise light or severe ice resupply seasons.

a. Western Ross Sea

Based on sparse icebreaker observations, first-year ice in the western Ross Sea and its approaches is estimated to have the following thicknesses at mid-months or periods. The ranges of ice thicknesses given probably will include most thicknesses encountered over the broad latitude zones given; however, some thicker or thinner ice may be encountered at specific locations within the zones.

November

Average conditions: 1 to 3 ft (0.3 to 0.9 m) from the northern pack edge* to the maximum thickness zone at approximately 67°30'S; 2 to 4 ft (0.6 to 1.2 m) with pressure ridges to 5 ft (1.5 m) in the maximum zone from 67°30'S to 72°30'S; 2 to 3 ft (0.6 to 0.9 m) with pressure ridges to 4 ft (1.2 m) south of 72°30'S to the eastern approaches to McMurdo Sound.

Severe conditions: 3 to 5 ft (0.9 to 1.5 m) with pressure ridges to 8 ft (2.4 m) from approximately 66°S to 72°30'S; 1 to 3 ft (0.3 to 0.9 m) northward to the pack edge and 2 to 4 ft (0.6 to 1.2 m) with pressure ridges to 6 ft (1.8 m) southward to the eastern approaches to McMurdo Sound.

Light conditions: 2 to 3 ft (0.6 to 0.9 m) with pressure ridges to 4 ft (1.2 m) over most of the maximum thickness zone from

_____
*See section II, para. F.1 and F.2

67°30'S to 72°30'S; 1 to 2 ft (0.3 to 0.6 m) north of 67°30'S to the pack edge and 2 to 3 ft (0.6 to 0.9 m) with a few pressure ridges to 4 ft (1.2 m) south of 72°30'S to the south pack edge.

December

Average conditions: 1 to 2 ft (0.3 to 0.6 m) with some floes to 3 ft (0.9 m) from the north pack edge to 68°S; 2 to 3 ft (0.6 to 0.9 m) with pressure ridges to 4 ft (1.2 m) from approximately 68°S to 71°30'S; 1 to 3 ft (0.3 to 0.9 m) from 71°30'S to the south pack edge.

Severe conditions: 2 to 5 ft (0.6 to 1.5 m) with pressure ridges to 6 ft (1.8 m) from 67°S to 71°30'S; 1 to 3 ft (0.3 to 0.9 m) from 67°S to the north pack edge; 1 to 4 ft (0.3 to 1.2 m) from 71°30'S to the south pack edge.

Light conditions: 2 to 3 ft (0.6 to 0.9 m) with a few pressure ridges to 4 ft (1.2 m) from approximately 68°S to 71°S;<1 to 2 ft (<0.3 to 0.6 m) from 68°S to the north pack edge; 1 to 3 ft (0.3 to 0.9 m) from 71°S to the south pack edge.

1 to 15 January

Average conditions: 2 to 3 ft (0.6 to 0.9 m) over the maximum thickness zone from 68°S to 70°S, floes 1 ft (0.3 m) thick or less generally extend 30 nmi (56 km) north and south of the maximum zone.

Severe conditions: 2 to 4 ft (0.6 to 1.2 m) with many floes up to 6 ft (1.8 m) thick from 68°S to 70°S, floes 1 to 2 ft (0.3 to 0.6 m) thick generally extend from 30 to 60 nmi (56 to 111 km) north and south of the maximum zone.

Light conditions: 1 to 3 ft (0.3 to 0.9 m) over the maximum thickness zone from 68°S to 69°30'S, essentially ice-free conditions to the north and south of the maximum zone.

16 to 31 January

Most of the remaining first-year floes in the western approaches to the Ross Sea finally melt during this period. Probably owing to the rapid disintegration of ice less than 1 ft (0.3 m) thick, floes that remain in the sector generally from 68°30'S to 69°30'S at mid-January are 2 to 3 ft (0.6 to 0.9 m) thick with some floes as much as 6 ft (1.8 m) thick. By 31 January essentially ice-free conditions prevail along some longitudes in the sector from 170°E to 180° but some isolated first-year floes 3 to 4 ft (0.9 to 1.2 m) thick and multi-year floes up to 8 ft (2.4 m) thick or more probably remain but are not observed because they are widely dispersed.

Severe ice conditions for 16 to 31 January are thought to be simmilar to average conditions for 1 to 15 January. Light ice conditions for 16 to 31 January are thought to be essentially ice free and probably commence at mid-January.

b. Approaches to McMurdo Sound

During the austral winter, drift ice accumulation along
Victoria Land varies from year-to-year. During November, the outer
edge of this mass of first-year ice extends generally northward from the
eastern extremity of Ross Island. The edge drifts westward and ice
thicknesses decrease during the austral summer, but these ice features
depend on the severity of the ice year. Based on sparse icebreaker
reports, this mass of first-year ice is estimated to have the following
thicknesses and outer edge positions at mid-months in the east and
northeast approaches to McMurdo Sound.

15 November

Average conditions: 3 to 5 ft (0.9 to 1.5 m) pack with some
floes and pressure ridges up to 7 ft (2.1 m) thick, extends eastward
approximately to 172°E where young ice is encountered north of the Ross
Ice Shelf.

Severe conditions: 3 to 6 ft (0.9 to 1.8 m) pack with some
floes and pressure ridges up to 10 ft (3 m) thick, extends eastward
approximately to 172°E, and fast ice covers the area from Beaufort Island
to the shelf ice in the southern end of McMurdo Sound.

Light conditions: 3 to 4 ft (0.9 to 1.2 m) pack with some
floes and pressure ridges up to 6 ft (1.8 m) thick, extends eastward
approximately to 169°E.

15 December

Average conditions: 2 to 5 ft (0.6 to 1.5 m) pack with
some floes and pressure ridges up to 6 ft (1.8 m) thick extends eastward
approximately to 169°E.

Severe conditions: 3 to 5 ft (0.9 to 1.5 m) pack with some
floes and pressure ridges up to 8 ft (2.4 m) thick, extends eastward
approximately to 170°E, and fast ice covers the area from Beaufort Island
to the shelf ice in the end of McMurdo Sound.

Light conditions: 2 to 4 ft (0.6 to 1.2 m) pack with some
floes and pressure ridges up to 5 ft (1.5 m) thick, extends eastward
approximately to 168°E.

15 January

Average conditions: 2 to 4 ft (0.6 to 1.2 m) pack with some
floes and pressure ridges up to 5 ft (1.5 m) thick, extends eastward
approximately to 168°E.

Severe conditions: 3 to 5 ft (0.9 to 1.5 m) pack with some
floes and pressure ridges up to 6 ft (1.8 m) thick, extends eastward
approximately to 169°E.

19

Light conditions: 2 to 3 ft (0.6 to 0.9 m) pack with some floes and pressure ridges up to 4 ft (1.2 m) thick, edge in the vicinity of Beaufort Island.

Near the end of January or during early February of light years, open water passages form between the southern Ross Sea and McMurdo Sound. During average or severe ice seasons, however, some first-year floes estimated up to 3 ft (0.9 m) thick probably remain in the eastern approaches to McMurdo Sound until freezeup.

G. Fast Ice in McMurdo Sound

1. Extent

Extent of fast ice often is related to geographical features; therefore, a place name chart for McMurdo Sound is given in figure 15. The extent of fast ice in the approaches to Hut Point during each season from DF I through DF 71 are presented on figures 16, 17, and 18. Observations were taken from icebreaker post-operational reports and from aerial reconnaissance and shipboard data contained in Operation DEEP FREEZE reports prepared by the Naval Oceanographic Office. Aerial photographs of fast-ice breakout, made by the U.S. Geological Survey, were used as well as observations made by Heine (1963).

The extent of fast ice was determined along a line from the southernmost latitude of the fast ice edge observed between 165°15'E and 165°45'E thence due south to a true bearing of 142° extending to Hut Point. This line coincides with the track taken by icebreakers in recent years in breaking a channel to Hut Point. After a channel was started, ice forming the outer eastern side of the channel often dislodged sooner than the ice forming the western side of the channel. When this occurred, the fast ice width was determined by the location of the outer eastern (shorter) side of the channel.

Fast ice widths were determined to the nearest nautical mile unless specific data permitted a determination to the nearest one-half mile. Observations plotted against time, were connected by straight lines. Ideally, a time-plot of the decrease of fast ice should be formed by only horizontal and vertical lines which may range down to very small increments. Sloping lines were usually drawn since observations of the fast ice usually were made less frequently than the occurrence of fast-ice dislodgments.

a. Individual DEEP FREEZE (DF) Seasons

Figures 16, 17, and 18 indicate that generally small dislodgments of fast ice of approximately 1 to 3 nmi (1.9 to 5.6 km) occurred from mid-October to early December, but may have occurred as late as late December. However, notable exceptions were observed during DF 61 and DF 68. Dislodgment of these small fast-ice sections may have been assisted by or completely the result of icebreaker operations. More frequent or larger breakouts, or both, generally occurred after early December. Accelerated fast-ice dislodgment occurred during many years from mid-December to mid-January. During this period, the slopes of many lines indicate an average decrease of approximately 1 nmi (1.9 km) of fast ice every 3 days.

20

The maximum extent of fast ice that was observed was 62 nmi (115 km) on 6 November 1962. Fast ice approximately 45 nmi (83 km) wide was observed during DF I, DF 61, and DF 69 while lesser amounts were observed during other DF seasons. Minimum amounts of fast ice were observed during periods in DF's II, 65, 67, and 68. During DF 68, a 14 nmi (26 km) section of fast ice was dislodged in late October but reattached a few days later. An additional large fast-ice dislodgment of 10 nmi (19 km) occurred on 8 December 1967 leaving only 5 nmi (9 km) of fast ice to the north of Hut Point.

The largest single observed dislodgment occurred on Christmas Day 1962 when the USCGC EASTWIND reported a breakout of 15 nmi (28 km) of channel. Larger fast-ice dislodgments may have occurred; for example, 19 nmi (35 km) of fast ice was dislodged between 14 and 24 October 1960. However, it is not known whether this dislodgment represents a single breakout or an accumulation of several smaller breakouts. In contrast to the largest breakout, the longest period of observed stable fast ice conditions occurred from 5 October to 24 November 1965 when the fast-ice edge was observed 26 nmi (48 km) north of Hut Point on 9 separate occasions.

During all years except DF I, the fast-ice edge receded to at least Hut Point. The latest data observed during each season indicate that fast ice broke out to the Ross Ice Shelf during approximately 8 of the 16 DEEP FREEZE seasons from DF I through DF 71. Some shelf ice also was dislodged in a number of years; therefore, the location of shelf ice varied from approximately 2.5 to 3 nmi (4.6 to 5.6 km) south of Hut Point. The largest remnant of fast ice occurred at the end of DF I when the edge was located 4 nmi (7.4 km) to the north of Hut Point.

b. Average, Median, and Extreme Values

Fast-ice widths on the 1st and 15th of each month from 15 October through 1 March were obtained from individual observations made during each DEEP FREEZE season (fig 16, 17, and 18). Values were interpolated between observations only when the 1st and 15th fell 10 days or less from an observation. An exception was made on 15 November 1956 because the extent of fast ice observed on 28 October and 2 December was almost identical. Extrapolation of data at the beginning and end of observations for each DEEP FREEZE season was limited to 6 days and 2 days, respectively.

Average, median, maximum, and minimum extents of fast ice at the beginning and at mid-months were calculated. Values are indicated in figure 19 with the number of years of data used in the calculations. Geographical features locate where fast-ice edges occur. Distances between these features and Hut Point were measured along the channel track. Fast ice widths for 1 February for DF's 70 and 71 were not used in the calculations because values were artifically small owing to icebreaker dislodgment of fast ice south of Erebus Ice Tongue.

The average extent of fast ice was almost always greater than median values owing to more years with an unusually large extent rather than to small areas of fast ice. Some indication of the latter shown in figure 19 by the larger area between the median and maximum lines than

21

between the median and minimum lines.

The median location of the fast-ice edge from mid-October to mid-November was adjacent to Cape Royds. Increased dislodgment of fast ice caused the edge to recede to the vicinity of Cape Barnes by 1 January and to Cape Evans by 15 January. The most rapid outflow of fast ice occurred from 15 January to 1 February during which the edge receded to 4 nmi (7.4 km) to the north of Hut Point. By 15 February virtually all fast ice forming the eastern side of the channel was dislodged from the coast north of Hut Point and by 1 March was located approximately 1 nmi (1.9 km) north of the Ross Ice Shelf.

2. Typical Fast Ice Dislodgment

When the fast-ice edge is located 5 to 10 nmi (9 to 19 km) west of Cape Royds during October and November, fast ice 1 to 2 nmi (1.9 to 3.7 km) wide often extends into Wohlschlag Bay. The latter fast ice is dislodged first, so that the fast-ice edge intersects the coast near Cape Royds by late November. After the channel is started, east to southeast winds break off fast ice along the eastern side of the channel and facilitate widening of the tidal crack along the coast from Cape Royds to Cape Evans. As a result, fast ice east of the channel and southward to Cape Evans dislodges ahead of the fast ice forming the outer edge west of the channel.

During DF 63, when the most extensive fast ice was observed, Captain B. R. Henry of the USCGC EASTWIND described this process. "During late January and all of February when the channel had been widened to a width of 200 to 300 yd (183 to 274 m) for a mile or two, light southerly winds would clear it of brash. Following east winds then broke off the adjacent ice east of the channel within a day or two. Within a few more days, the corresponding part of the fast ice west of the channel broke off. In this manner, the ice front was advanced southward."

Frozen or open cracks in the fast ice usually are observed between the Dellbridge Islands, as well as extending northwestward and southwestward from Erebus Ice Tongue. These cracks sometimes occur in the same location from year-to-year, as observed during DF III and DF IV by Captain J. A. Houston of the USS GLACIER. As a result, the fast-ice edge during late January usually breaks out to a line running from Cape Evans to Inaccessible Island, to Tent Island, and thence to the end of Erebus Ice Tongue. In some years these cracks were used by icebreakers to dislodge considerable amounts of fast ice. When the east side of the channel recedes to Erebus Ice Tongue, owing to icebreaker operations, the west side of the channel sometimes extends as much as 10 to 12 nmi (19 to 22 km) farther northwest (DF 70). During late January and all of February the latter ice gradually is dislodged. It is thought that long period swell entering McMurdo Sound, as well as wind action, are important factors for breakup of the ice west of the channel and southward of Winter Quarters Bay to the Ross Ice Shelf after the ice has become weakened by austral summer insolation.

After the east side of the channel receded to Erebus Ice Tongue,

a secondary or inner channel eastward of the original channel sometimes was broken due southward to Hut Point. The latter operation dislodged the last remaining ice forming the east side of the channel and reduced the threat of channel closure owing to natural fast-ice dislodgment. The last fast ice to dislodge north of Hut Point occurs during late February or early March, and probably comes from the inner area north and south of Erebus Ice Tongue between Turks Head and Turtle Rock. It is probable that in some years the latter ice remains to be frozen in by new ice.

By early March, at most only very narrow sections of fast ice generally remained attached to the Ross Ice Shelf. One very small segment of old sea ice that may remain, lies in the sector between Cape Armitage, Pram Point, and the Ross Ice Shelf. It is probable that any sea ice which has not been dislodged by mid-March will remain owing to hardening of the ice by rapidly decreasing temperatures.

3. Fast-Ice Thickness

Reports of fast-ice thickness in McMurdo Sound given in some of the icebreaker post-operational reports indicate that fast ice is least thick at its northern edge and increases in thickness southward somewhat irregularly. Thicknesses at the edge encountered by icebreakers at the start of channel cutting operations ranged from 2 to 5 ft (0.6 to 1.5 m); median and average thicknesses for 10 years of data were 3 to 4 ft (0.9 to 1.2 m). When the edge was encountered south of Cape Royds from late October to late December, the average thickness was 3 ft (0.9 m). Ice thicknesses at the edge generally were 4 to 5 ft (1.2 to 1.5 m) when the fast ice was more extensive.

Thicknesses increased usually to 4 to 6 ft (1.2 to 1.8 m) within a few miles of the edge. During light ice years, such as DF's 60 and 68, this thickness extended to Hut Point. Most often, thicknesses increased to 6 to 7 ft (1.8 to 2.1 m) with occasional 8-ft (2.4-m) areas in the sector from Hut Point and for approximately 10 nmi (19 km) northwest. One winter's growth (first-year ice) of fast ice south of Hut Point usually grew 9 to 10 ft (2.7 to 3.0 m) thick.

During severe ice years, fast ice 8 ft (2.4 m) thick and greater has extended far to the north of Hut Point. This occurred during DF I when 10-ft (3.0-m) fast ice was observed in the channel at 77°24'S or approximately 32 nmi (59 km) north of Hut Point; from 7- to 9-ft (2.1- to 2.7-m) fast ice extended from 77°30'S to 77°40'S. Farther southward, fast ice 8 to 10 ft (2.4 to 3.0 m) thick with pressure ridges to 12 ft (3.7 m) was encountered to 4 nmi (7.4 km) northwest of Hut Point.

Probably the thickest fast ice ever observed in the channel within 4 nmi (7.4 km) of Hut Point was subsequently broken by icebreakers during DF I. This ice probably had remained in place for two ice-growth seasons (second-year ice), or possibly longer, and was mostly 10 ft (3.0 m) thick, but in places reached 12 ft (3.7 m). Additionally, pressure ridges within and along the northern boundary were as thick as 15 ft (4.6 m). Fast ice up to 12 ft (3.7 m) thick with an additional layer of 3 to 4 ft (0.9 to 1.2 m) of compacted snow was observed in Winter Quarters Bay. West and

south of Hut Point, average fast-ice thicknesses were, respectively, 9 to 11 and 11 to 13 ft (2.7 to 3.4 and 3.4 to 4.0 m). During DF 63, when the most extensive fast ice was observed, ice up to 9 1/2 ft (2.9 m) thick was encountered in breaking the channel. The thickest fast ice reported during any DEEP FREEZE season was 21 ft (6.4 m) observed adjacent to Williams Field during DF 62. During DF IV, pressure ridges 20 ft (6.1 m) thick off Marble Point were reported by the USS GLACIER.

Icebreakers frequently have reported zones of ice thicker and thinner than surrounding ice during channel breaking operations. The thicker zones may form during the early ice growth months in McMurdo Sound owing to remnant first-year and second-year floes being frozen in rapidly growing new ice. Prevailing south winds may dislodge such floes from the southern end of the sound. The thinner ice zones may result from small northward displacements of fast ice, limited by coastal blockage, well into the ice growth season. The thickness attained by new ice formed in the openings would be related to the time of displacement during the ice growth season.

III. FORECASTING TECHNIQUES

Forecasts of the distribution of sea ice for summer resupply operations are made for several durations. For long-range periods, the forecaster should consider large-scale environmental factors such as mean wind velocities, storm tracks, and mean monthly air temperatures since they affect the overall disintegration and drift of the pack. Long-range forecasts of environmental conditions, however, generally are not available for Antarctic waters. Therefore, preparation of long-range ice forecasts for 30-days and longer rely to a large measure on an analog forecasting technique relating environmental and subsequent ice data observed during prior years to the present environmental conditions. For short-range ice forecasts, generally of 24 to 48 hours duration, the speed and direction of surface winds and currents are most often of primary importance. Short-range forecasts of the surface wind velocity over small or large areas required to prepare short-range ice forecasts are available on a routine basis. Current data input to short-range forecasts are taken from atlas presentations (fig 3).

This section describes the procedures and techniques used in preparing short-range ice forecasts and long-range ice estimates in support of the austral summer resupply operations. Information of a subjective nature based on forecasting experience also will be included.

A. Short-Range Ice Forecasts

1. Ross Sea

The preparation of short-range ice forecasts requires knowledge of the ice distribution at the beginning of the forecast period. Ice

24

observations taken from reconnaissance and logistics aircraft over the
Ross Sea are available to the ice forecaster generally once or perhaps
twice a week. These observations include information on many of the ice
features pertinent to ship operations such as pack edges, concentrations,
concentration boundaries, stages of development, floe size, topography,
and lead width and orientation. These data, however, often are limited
by undercast conditions and may be taken far distant from the shipping
lanes. The quantity of pertinent aerial reconnaissance data therefore
usually are not sufficient for preparing short-range forecasts. Satellite
imagery provide the required additional ice data.

a. Satellite Ice Data

The large advantage of a satellite over an aircraft as
a platform for obtaining ice data is its daily availability and broad
areal coverage over near and remote areas. Imagery taken in the visual
spectrum by scanning radiometer (SR) and very high resolution radiometer
(VHRR) sensors can be used for ice interpretation over the Ross Sea from
the first half of October until the start of the austral winter at approxi-
mately mid-March. Interpreted ice data, however, generally are limited to
large ice features of sufficient distinctness to be detected such as pack
edges and concentrations. The distribution of medium (100 to 500 m or
328 to 1640 ft) and smaller floes, new ice, or the amount and height of
ridges are ice features that cannot be detected by satellite at present.
SR and VHRR imagery in the infrared spectrum are available during the
entire year. Satellite imagery using an electronically scanning microwave
radiometer (ESMR) sensor provide data of low resolution on the location
of the ice edge during the austral winter. Large amounts of ice data
therefore are available from satellite imagery. The explicit data taken
from aircraft and ships during the austral summer serve as ground truth
for those ice features discernible concurrently by satellite.

The primary source of ice data available to the ice
forecaster is satellite imagery. A brief review of imagery interpretation
therefore is appropriate.

(1) Sea Ice Versus Clouds

Ice and clouds both have white images on SR and VHRR
satellite imagery and usually are distinguished by the rapid movement or
dissipation of clouds relative to the quasi-stationary location of ice
that is usually apparent on imagery from successive orbital passes. Another
distinguishing feature of ice is its irregular, and generally well defined
edge, in contrast to the relatively straight edge with gradual loss of
whiteness associated with cloud formations. Vast and giant floes or close
and very close belts of smaller floes within the pack also appear sharply
cornered with well defined edges. A gradual decrease from 8 okta ice
concentration to ice-free conditions along a straight or gradually curving
line presents an image similar to a cloud edge but persistence of the line
would identify it as an ice edge.

25

(2) Pack Concentration

Eight okta concentrations of first-year ice more
than 30 cm (1 ft) thick that generally occur in the western Ross Sea in
October appear white on SR and VHRR satellite imagery, and decreased
concentrations that occur later in the ice year appear as darker shades
of gray because of lower reflectivity from the larger percentage of
exposed water surface. Whiteness of the imagery is related subjectively
to eight pack concentrations which are given usually in overlapping
3-okta ranges. These ranges are: 0 to 2, 2 to 4, 3 to 5, 4 to 6, 5 to 7,
6 to 8, 7 to 8, and 8 oktas.

Pack concentrations less than approximately 2 oktas
presently are not discernible on SR and VHRR imagery because the ice
floes are widely separated and their dimensions generally are smaller than
the resolution of the satellite. A black image over a particular area
therefore indicates that as much as 2 oktas of ice may be present.
Historical ice data can indicate the probability of ice in that area.
Recent aerial reconnaissance or ship observations provide an increased
degree of reliability of the ice conditions that are present. Boundaries
between two given pack ice concentrations in the range from 2- to 8-oktas
appear as discontinuities between different shades of gray.

The ice feature most readily identified by satellite
probably is an extensive fast ice or shelf ice edge that lies adjacent
to an ice free area. The resolutions of SR and VHRR imagery are 2 and 0.5
nmi (3.7 and 0.9 km) respectively. Therefore vast, giant, and big floes
greater than 0.5 nmi (0.9 km) in extent and many tabular icebergs found in
Antarctic water surrounded by as much as 7 to 8 oktas concentrations can
be readily identified and tracked. Eight-okta belts consisting of floes less
than 0.5 nmi (0.9 km) across can be tracked but brightness of the image and
tracking ability will decrease as the concentration of the belt decreases
or the belt narrows to the width of strips ($<$1 km or 0.5 nmi).

(3) Stage of Development

The stage of development (thickness) of sea ice
can be estimated by satellite during only a small portion of its growth;
that is, for young ice which has a thickness of 10 to 30 cm (4 to 12 in).
Sea ice less than approximately 10 cm (4 in) thick is not discernible by
SR or VHRR satellites at present because of the low reflectivity from its
surface. Young ice (8 oktas) has a gray to gray-white color which gradually
becomes white as the thickness reaches 30 cm (12 in). The uniform white
color of ice more than 30 cm (12 in) thick (8 oktas) precludes differenti-
ation among ice thicknesses greater than young ice (30 cm or 12 in). Sea
ice in an advanced stage of deterioration may be more than 30 cm (12 in)
thick but is undetected by present satellites because of its large water
content and resultant low reflectivity. Aerial and shipboard observations
of rotten ice on the Ross Sea, however, are rare probably because it is
short-lived owing to disintegration by frequent high winds.

Young ice probably forms widely in the Ross Sea in late
March, April, and probably May, when decreased illumination precludes useful

26

imagery in the visual spectrum. Experience in interpreting infrared
imagery during the austral winter has been limited owing to the lack of
ground truth. After the sea ice has grown to first-year thickness, off-
shore ice drift often results in the formation of young ice-covered shore
and flaw leads. These leads are found on the leeside of islands or
adjacent to coastlines, ice shelves, or fast ice edges, and usually can
be identified on SR and VHRR satellite imagery. Snow cover on young ice
may mislead the forecaster by giving the surface a white color and the
appearance of first-year or older ice. Snow cover on young ice recently
formed along an ice edge (or between diverging first-year floes) can
indicate to the ice forecaster very cogently that young ice is present
when it was non-existent or normally undetected on previous satellite
imagery.

(4) Lead Orientation

The general direction of leads more than 0.5 nmi
(0.9 km) wide between first-year floes can be observed on VHRR imagery
over the Ross Sea. Under optimum observing and satellite operating
conditions, imagery of part of the ship channel through the fast ice in
advance of McMurdo Station has been observed on VHRR imagery. Leads may
contain small fragments of other ice stages of development and form with
strong winds of constant direction when sufficient water surface is avail-
able for their formation. Leads in pack ice tend to become aligned per-
pendicularly to the mean ice drift direction after a sufficient period
of time. Narrow passageways not navigable for long distances tend to occur
in the Ross Sea through 8- or nearly 8-okta concentrations and are not
discernible with the sensors presently used. Leads, that is, passageways
navigable by surface vessels, tend to form in 5 through 7 to 8 okta
concentrations. Ice concentrations of 1 through 4 oktas tend to form
into belts or strips. Strips also may form as a result of strong permanent
currents; therefore, the alignment of strips sometimes may have little relation
to the wind-induced drift direction.

Belts and strips tend to have approximate east-west
orientations in the shipping lanes between 176°E and 177°E during December
and January in response to permanent currents and dominant wind directions.
Pack concentration within the belts and strips is usually 6 to 8 oktas.
The belt of sea ice which usually forms the south pack edge in the western
Ross Sea tends to be 8 oktas concentration, contains smaller floes, and
often is wider than strips and belts northward of the edge owing to wind
and wave action.

(5) Location of Ice Data

Ice data must be located by geographic coordinates
or bearing and distance from prominent shore features to prepare an
ice summary message to shipping or to use the data in ice forecasting.
Occasionally the latitude and longitude grid lines are placed incorrectly
on SR satellite imagery. Grid errors can be detected by noting the
location of prominent large geographic features that are separated widely.
For example, the Bay of Whales is located near 78.5S,165°W; the center of
the large open water area that forms between Drygalski Ice Tongue and
Cape Washington is located near 75°S,165°E; and the 170°E meridian

27

extends from a small north-south orientation of the Ross Ice Shelf just eastward of Ross Island to near the east coast of Coulman Island (73°30'S, 169°45'E). A grid adjustment of one-half degree of latitude (30 nmi or 56 km) or more sometimes is required. Knowing the location of such permanent features also enables the forecaster to construct a grid when it is not provided on the satellite imagery.

The largest errors in positioning ice data occur along the edges of satellite imagery because of the distortion caused by curvature of the earth. Ice data therefore should be interpreted from the central portion of a satellite image whenever possible.

b. Estimating Surface Winds

Surface wind velocities can be estimated from isobar spacing and orientation on observed or forecasted surface pressure charts. Observed pressure distributions are used when hindcasting; that is, advecting previously observed ice conditions with past surface winds conditions. Winds reported by ships are very useful for hindcasting and should be used whenever the observations are close to and are representative of the surface winds at the hindcast area. When ship observations are not available, geostrophic winds (modified) found from the isobar spacing, are used to advect the ice fields. Together with mean currents, surface winds from observed charts are used to derive an updated ice distribution. Forecasted pressure distributions are used to project these updated ice conditions.

When shipboard winds are representative of wind conditions at the hindcast area, wind observations may be used with little or no change to predict ice drift at the hindcast area. Winds reported by shipboard observers are preferred to coastal station data because local terrain often affects observations on land. If the isobar spacing is slightly different at the hindcast location than at the ship location, the same ratio of reported wind speed to geostrophic wind speed can be used to estimate the surface wind speed at the hindcast location. The observed wind direction, as well as its angular difference from the isobar orientation, can be used to estimate the surface wind direction at the hindcast area. Additionally, wind velocities observed 6 or 12 hours prior to the time desired may be helpful in estimating wind conditions in the absence of more recent observations.

(1) Correction for Instability

When wind observations are not available and it is necessary to estimate the wind speed from the isobar spacing on observed or forecasted surface pressure charts, the surface wind speed can be estimated by taking 70% of the geostrophic wind speed. This correction, made for the degree of instability, results from air turbulence in the lowest air layer, caused over the oceans, by flow over a colder or warmer surface. A value of 70% is used generally over the ocean, and has been found to be most valid when the air is 5° to 10°F (2.8° to 5.6°C) colder than the water surface. Table 1 gives other factors when other temperature differences are thought to be present. For example, when the forecast or hindcast area is close to

28

land and the air is in the order of 16° to 20°F (9° to 11°C) colder than the water-ice surface, a 0.80 factor should be used. When the forecast area is far removed from land and there is little difference between the air and water-ice surface temperature, a factor smaller than 0.70 should be used.

Table 1

CORRECTION TO GEOSTROPHIC WIND FOR SEA SURFACE-AIR TEMPERATURE DIFFERENCE

Ts-Ta* (°F)	Ts-Ta* (°C)	Surface Wind Spd*/Geostrophic Wind Spd
< -7	< -3.9	0.55
-7 to 0	-3.9 to 0	0.60
1 to 4	0.6 to 2.2	0.65
5 to 10	2.8 to 5.6	0.70
11 to 15	6.1 to 8.3	0.75
16 to 20	8.9 to 11.1	0.80
> 20	>11.1	0.90

(2) Correction for Curvature of Air Trajectory

An additional correction to the geostrophic wind speed (which usually is applied before the correction for stability), can be made for curvature of the air trajectory in order to approximate the gradient wind. When isobars are straight or have small curvatures, the curvature of the path is negligible and the geostrophic wind speed is a good approximation of the wind speed above the frictional layer before correction is made for stability. Curvature of the path and isobars is the same for stationary pressure systems. When the pressure systems are not stationary or nearly so, the curvature of the path may differ considerably from the curvature of the isobars.

Petterssen (1940) calculated that gradient winds at 70°S were approximately 10% smaller than geostrophic winds for cyclonic flow when the radius of curvature of the path was 540 nmi (1000 km) and the wind speeds were less than approximately 40 kn (74 km/hr).** In addition, he found that for observed anticyclonic curvature, the wind speed was rarely very high and the radius of curvature was usually large. Thus, the difference between geostrophic wind and gradient wind for anti-cyclonic flow was found by observation to be small.

Since synoptic surface pressure charts over Antarctic waters are always drawn with extremely few data, and prognostic surface pressure charts are based to a large extent on the synoptic charts, the radii of curvature of isobars and trajectories can be only grossly estimated. Additionally, wind speeds found from the isobar spacing are probably 10% or more in error. Therefore, until many more observations are available,

---

*Taken aboard ship at approximately 20 ft (6 m) above the water-ice surface.

**At 70°S with 270 nmi (500 km) curvature, 10% reduction with 20 kn (37 km/hr), 20% with 40 kn (74 km/hr); with 108 nmi (200 km) curvature, 20% reduction with 20 kn (37 km/hr), 35% with 40 kn (74 km/hr).

29

correction to the geostrophic wind for curvature of air trajectories is almost always omitted over Antarctic water. However, if the forecaster is of the opinion that the radius of cyclonic curvature of a trajectory can be estimated to a fair degree, the percentages given or interpolated values between them may be applied before correction is made for stability.

(3)   Correction for Wind Direction

Friction between moving air and the earth causes surface winds to flow across the isobars toward low pressure. Over the ocean, the frictional force is small and the surface wind direction is nearly equal to the geostrophic wind direction; that is, along the isobars. Hewson and Longley (1944) have indicated a difference of approximately 20°; therefore, isobars on surface charts are drawn so that the surface wind blows at an angle of about 20° across the isobars toward low pressure. Accordingly, when wind directions are ascertained from the isobar orientation on surface pressure charts, 20° should be added to the geostrophic wind direction in the southern hemisphere for an estimate of the surface wind direction.

c.   Deviation Angle

The angle between the surface wind and the direction of ice drift, called the deviation angle, was found by Nansen (1902) while the FRAM drifted across the Arctic Ocean (1893-96) to average 28° to the right of the surface wind. This was substantiated by Zubov (1945) who found an average deviation angle of 29° from observations in the Arctic taken aboard the SEDOV (1938-39). These deviation angles pertain to the advection of close multi-year pack over the deep ocean far from the distorting influence of coastlines and exclude the effect of any steady current.

A plot of the SEDOV's drift superimposed on concurrent 10-day mean sea level pressure analyses led Zubov to empirically formulate the rule that close ice (6 to less than 7 oktas) drifts parallel to the isobars; that is, with the geostrophic wind. Subsequent examination of shipboard wind data not included in surface pressure analyses indicated that the surface wind deflected an average of 28° to the left of the isobars. Consequently, drift of close ice an average of 28° (Nansen) or 29° (Zubov) to the right of the surface wind direction virtually coincided with the isobar direction and confirmed his rule. Drift of close ice along the isobars has been used as a rule of thumb technique for ice advection because it is simple. Owing to the sparseness of wind observations in ice covered polar regions and contiguous seas, the ice forecaster invariably must rely on the sea level pressure distribution to infer wind conditions and resultant ice drift.

The forces governing the drift of close pack, however, are complex. Floes are in contact at various times, and random drift directions (and speeds) of individual floes under study may be not representative of the overall movement of the close ice field. Deviation angles also may be obscured because movement of an ice field can be modified from drift with local wind conditions by the remainder of prior windage or by contact with

adjacent pack concentrations. Large ice fields set in motion acquire great
inertia which may be transmitted from surrounding areas through collision
of floes or may be present at the observational point. Consequently, true
deviation angles are difficult to ascertain especially when winds are brief
or weak.

Although the wind and drift data indicated to Nansen and Zubov
the deviation angle for close ice was not dependent on wind speed, the range of
deviation angles from which the average values were computed varied quite
widely. Zubov found the largest and widest range of deviation angles occurred
with wind speeds under 8 kn (15 km/hr). Brennecke (1914) found the deviation
angle for the drift of very open (1 to less than 3 oktas) and open pack (3 to
less than 6 oktas) concentrations to vary with wind speed. Subsequent theoret-
ical study by Shuleikin has shown a similar dependence for the drift of consol-
idated pack (8 oktas). Therefore, it is apparent that intermediate close ice
concentrations also drift at various deviation angles which are dependent, in
part, on wind speed. As will be seen, Shuleikin (1953) indicates that drift
with a deviation angle of 28° pertains to a variety of ice thicknesses and
wind speeds; for multi-year pack 4 to 6 ft (1.2 to 1.8 m) thick, a deviation
angle of 28° occurs with wind speeds of 18 to 28 kn (33 to 52 km/hr). Further-
more, the cross-isobar deflection of the surface wind over the oceans has been
found by Hewson and Longley (1944) to be approximately 20° and by Karelin (1941)
to average 24° for Arctic stations. Drift of close pack ice along the sea
level isobars therefore can be considered at best only as a first approximation
in ice forecasting.

Drift of isolated floes presents a different problem than the
drift of close pack. Isolated floes move more erratically than close pack con-
centrations because the individual response of isolated floes to the wind as
well as wind generated surface currents is not restricted by surrounding floes.
Because the windage effect generally is stronger than the effect of surface
currents to advect ice, individual floes on the leeward side of a concentration
of sea ice often may be observed to disperse. Zubov has shown that the deviation
angle of isolated floes increases with latitude and increasing vertical dimen-
sion of the floe, and decreases as the speed of the floe increases. Since the
drift speed of a floe is related directly to wind speed, minimum deviation
angles are found for very thin floes and strong surface winds.

The wind drift of very open and open pack concentrations can
approximate the drift of close ice or isolated floes, or they may move in an
intermediate manner depending on the particular pack concentration and char-
acteristics. The resultant drift varies depending on the number of collisions
between floes, windage of the floes, as well as other forces common to the
drift of all sea ice. Drift observations of very open and open pack approx-
imately 3 ft (0.9 m) thick taken by Brennecke aboard the DEUTSCHLAND in the
Weddell Sea (1911-12) indicated that deviation angles ranged from 39° to the
left of the surface wind direction (direction reversed because of southern
hemispheric observation) with a wind speed of 4 kn (7 km/hr) to 26° with a
wind speed of 16 kn (30 km/hr). From drift measurements taken aboard the
MAUD in the East Siberian Sea (1922-24), Sverdrup (1928) also found the
deviation angle to vary. For winds that were sufficiently prolonged to
insure steady motion, the deviation angle varied from 26° to 47°; however,
no dependence on wind speed was given.

31

Combining the results of these studies into a unified relationship of the deviation angle to the environmental factors of ice concentration, ice thickness, and wind speed is a difficult task. The data sometimes are at variance which makes a solution impossible. Shuleikin, however, derived a theoretical solution for the drift of consolidated pack when equilibrum conditions are reached. From a balance of the forces for steady ice drift, various deviation angles were found for several sea ice thicknesses and a wide range of surface wind speeds. As can be seen in figure 20 deviation angles increase with increasing ice thickness and decreasing wind speed. An extrapolated minimum deviation angle of approximately 18° as the ice approaches zero thickness for wind speeds over 20 kn (37 km/hr) agrees well with the direction of observed wind-generated surface currents found by Hughes (1956). Realistic deviation angles are given. For example, an angle of 27° is indicated for a wind speed of 16 kn (30 km/hr) and an ice thickness of 3 ft (0.9 m) whereas Brennecke observed a deviation angle of 26° with these conditions but with very open and open pack concentrations instead of consolidated ice.

Many physical constants employed in theoretical ice drift formulations have been assumed owing to lack of basic theoretical knowledge. Therefore, empirical relationships sometimes are used when theory alone gives unrealistic results. In addition, theoretical relationships derived for a specific set of conditions which give realistic results sometimes are extended to other conditions because there is nothing better to use. Therefore, the deviation angles given in figure 20 are used for all ice concentrations even though the relationship was derived for 8 okta concentrations. Although values given are valid only at 68°30'S, the graph may be used without appreciable error at any location in the Ross Sea. Deviation angles differ from those given generally by 1° or less from 60°S to the Ross Ice Shelf for floes up to 16 ft (4.9 m) thick.

d. Drift Distance

Magnitude for the drift of close multi-year pack was calculated by Nansen from drift of the FRAM after excluding permanent currents to average 1.82% of the surface wind speeds observed on 76 drift segments. Small differences between average wind factors calculated for various wind speed categories supported his belief that the wind factor was not dependent on the wind speed; that is, a linear relationship existed between the drift speed of sea ice and the wind speed. Zubov similarly found the wind factor to be independent of the wind speed and calculated an average drift of the SEDOV of 1.5% of the wind speed measured 12.5 m (41 ft) above the ice surface. Observations taken by Efremov in the Arctic Basin, as quoted by Zubov (1945), indicated an increase of wind speed with elevation for all wind speed categories. At a height of 6 m (20 ft) the wind speed was 81.2% of the speed at 12.5 m (41 ft). The elevation at which Nansen took his wind data is not clear. The conclusions of Efremov, however, indicate the different wind factors found by Nansen and Zubov are compatible if Nansen took his wind data at a height of approximately 6 m (20 ft). The true drift speed of close pack is difficult to measure because of inertia of the floes at the observational point or forces transmitted to the floes under study

through contact with surrounding pack ice. Zubov therefore concluded that far from coastlines and over great depths, the drift speed of close multi-year pack is approximately 2% of prolonged surface wind speeds.

Sverdrup also found the wind factor is much higher during summer months than winter months which Zubov ascribed to a more uneven ice topography, thinner floes, and more freedom of floes to move owing to a large number of open water areas. Wind drift of typical open pack concentrations in summer had almost twice the drift distance of typical close pack concentrations observed in winter with a given wind speed.

A table of wind factors (Zubov, 1945) was compiled by Gordienko from many observations of ice drift taken by him and Shestiperov off Cape Schmidt in the Chukchi Sea. Drift measurements were taken with two theodolites mounted on the shore at a given distance from each other and from the drifting floes. Wind factors were compiled as a function of the pack concentration and amount of hummocking (surface topography) of the ice in tenths. Linear interpolation to derive wind factors for concentration in oktas (eighths) and multiplication by a factor of 24 to give percentages for daily drift were applied to Gordienko's values to derive table 2.

Table 2

RESPONSE FACTOR (PERCENT) TO OBTAIN WIND DRIFT OF SEA ICE (NMI/DAY) FROM WIND SPEED* (KN) FOR VARYING CONCENTRATION AND RIDGING (after Gordienko)

TOTAL CONCENTRATION OF ICE (OKTAS)

Extent of ridging and hummocking (Tenths)	0.5	1	2	3	4	5	6	7	7.5
1	23	21	18	15	12	9	8	6	6
2	45	42	36	30	25	20	16	13	11
3	67	63	56	49	42	35	27	20	17
4	89	85	75	64	55	45	35	26	21
5	112	106	94	82	70	58	46	34	28
6	134	127	112	98	84	71	56	41	34
7	156	148	131	115	98	82	65	49	41
8	179	169	150	133	114	95	76	57	47
9	201	190	169	146	125	104	84	63	53

*Height of observation assumed to be 20 ft (6 m).

Table 2 is used easily. For example, a 4-okta ice area with 3 tenths of its surface covered with ridges or hummocks will drift a distance in 24 hours equal to 42% of the magnitude of the surface wind speed; that is, 6.3 nmi (11.7 km) with a 15-kn (27.8 km/hr) wind, 10.5 nmi (19.4 km) with a 25-kn (46.3 km/hr) wind, etc. When the wind direction and speed change within the 24-hour period, a vector addition of the separate wind drift vectors proportioned to each duration is made.

From Gordienko's table, it is evident that ice with a concentration of 0.5 oktas drifts approximately four times faster than ice with a concentration of 7.5 oktas having the same extent of topography and that the drift speed increases rapidly with increasing ridging and/or hummocking. A maximum drift speed of approximately 8% of the surface wind speed is indicated. Zubov states that isolated floes may drift as fast as 10% to 12% of strong surface wind speeds. Additionally, it can be seen from Gordienko's table that sea ice of 6 to 7 oktas concentration and 6 tenths hummocking (close multi-year pack) will drift approximately 2% of the surface wind speed; this is in agreement with the conclusions of Nansen and Zubov. The response of 4 oktas ice concentration (open pack) is almost twice the response factor for 6 to 7 oktas which is in agreement with Sverdrup's observations. It should be noted that the factors given in table 2 are of surface wind speed. Therefore when sea level pressure charts are used in hindcasting or forecasting, conversion should be made from geostrophic wind speed to surface wind speed.

Gordienko's table is compiled for extents of surface topography up to 9 tenths. Very few observations of 8 or 9 tenths ridging and/or hummocking have been made over extensive ice areas in the open ocean. It is usual for such extreme amounts of surface topography to be observed in immediate coastal areas during winter or spring where consolidated pack has been subjected to strong onshore pressure or associated with the hummocky remains of melting floes during summer. Observations of 5 through 7 tenths ridging and hummocking are frequently made over the Arctic Ocean and other areas such as the Weddell Sea in the Antarctic where multi-year ice predominates over other stages of ice development. Ridges and hummocks observed on sea ice of one year's growth (first-year ice) that usually is found in the western Ross Sea probably range from 1 through 5 tenths.

e. Permanent Currents and Total Ice Drift

The magnitude and direction of prevailing surface currents must be vectorially added to the wind drift vector to obtain the total ice drift. This can be accomplished conveniently on a maneuvering board or on polar coordinate graph paper. A generalized distribution of surface currents in the Ross Sea is given in figure 3. Current directions and magnitudes in heavy print were taken directly from H.O. Pub. No. 705. Directions in lighter print and magnitudes in parenthesis have been estimated for use in ice forecasting.

34

f. Summary of Short-Range Ice Forecasting Procedures

(1) Estimate the surface wind speed or calculate it by taking 70% of geostrophic wind, or use table 1. Estimate the surface wind direction or add 20° to the geostrophic wind direction. Neglect curvature of the trajectory when calculating the wind speed.

(2) Enter figure 20, find the deviation angle using the surface wind speed and an average thickness of ice at the hindcast/forecast point or area.

(3) Add or subtract 180° from the surface wind direction and then subtract the deviation angle to get the direction toward which ice will drift.

(4) Enter table 2 with the ice concentration in oktas and the extent of ridging and/or hummocking in tenths and find the response factor.

(5) Multiply the surface wind speed with the response percentage to get the ice drift in nmi/day.

(6) Find the permanent current magnitude and direction set at the hindcast/forecast point or area from figure 3. Multiply the current magnitude by 24 to get the drift in nmi/day.

(7) Vectorially add the wind drift vector found in steps 3 and 5 to the permanent current vector found in step 6 on a maneuvering board to find the total ice drift direction and magnitude in nmi/day.

2. McMurdo Sound

Short-range ice forecasts for McMurdo Sound generally are concerned with pack concentrations north of the fast ice edge, dislodgment of fast ice, and efflux of brash and ice cakes from the shipping channel cut through the fast ice. The drift of icebergs, which occasionally enter the sound, also is pertinent because of their possible blockage of the channel.

a. Drift Ice

Pack ice north of the fast-ice edge drifts to the north or northwest with southerly component winds that usually dominate during the austral winter. The area north of the fast ice edge located near Cape Royds, therefore, is frequently covered with slush, ice rind, or young ice during October and November when air temperatures are well below freezing. With subsequent anomalous northerly winds, thick first-year pack, usually in combination with thinner ice, will be forecast to drift southward with the response factors given in table 2. Surface currents over the northeastern quadrant of the sound are mainly westerly and have only a small effect on the north-south drift speed of the ice. A return to normal south or southeast winds when pack ice lies adjacent to the fast ice edge indicates formation of the slush and ice rind flaw lead or area; lead formation occurs

35

with light to moderate south winds, an area extending to the latitude of Cape Bird forms with strong southerly winds.

Thick first-year pack usually lies adjacent to the fast-ice edge when the latter edge is located at the latitude of Cape Bird or farther north during October. Very close and consolidated pack north of the fast-ice edge do not permit flaw leads to form. Lead formation occurs during November with winds having a southerly component owing to northward compression of slightly decreased concentrations of the·thick first-year pack.

During the latter half of November pack concentrations to the north and west of Cape Bird normally become open pack. Strong southerly winds lasting 48 hours or more, during that period will widen the slush and ice rind area from Cape Royds well to the north of Beaufort Island by compression of the open pack area. During December when air temperatures increase to the freezing (melting) temperature of the water, open water with a few thick winter floes extending from the fast ice edge northward as far as 76°S would be forecast in response to strong southerly winds.

b. Fast-Ice Dislodgment

Short-range forecasts of the dislodgment of fast ice usually are based on the normal pattern of dislodgment outlined in Section II.G. The forecaster, however, should note the location of ridge lines in the fast ice because they often mark the location of old cracks along which the fast ice may separate during dislodgment. The location of open or refrozen cracks also should be noted. Any sudden increase in their widths during December or later indicate that dislodgment can occur. A forecast of dislodgment should be made when strong southerly winds are expected.

After mid-January the fast ice is weakened by austral summer insolation, the ice surface develops patchy gray areas (melt pools are virtually nonexistent) and dislodgment of large sections of fast ice occurs. Long period swell entering McMurdo Sound is thought to be an important factor in breaking the fast ice. The swells are not visible and breakup proceeds very quickly. During DF 68 breakup and northward drift of the fast ice approximately 200 yd (183 m) wide from Winter Quarters Bay to Cape Armitage on 5 February took a total of two hours. Ice drift from this sector is aided by a northward setting current.

Dislodgment of fast ice in late January or in February also may occur en masse from large coastal sectors. Such dislodgment is facilitated by development of a tidal crack between the fast ice and the shore line. The fast ice between Turtle Rock and Hut Point usually is dislodged in this manner in pieces 1 to 5 nmi (1.9 to 9.3 km) in extent and passage by resupply vessels to Winter Quarters Bay is temporarily blocked. In order to prevent such channel closure during ship entry, a large part of the fast ice in this sector often is broken off by icebreakers before natural dislodgment takes place.

c. Channel Clearing

        The channel through fast ice to Winter Quarters Bay should be forecasted to remain congested during the following 48 hours in the absence of expected strong (> 30 kn or 56 km/hr) south to southeast winds. The time required for channel clearing is related to the length of the channel and the strength and duration of the wind. The amount of ice left in the channel after it is broken by icebreakers and whether the ice is refrozen are added factors.

        Usually two icebreakers conduct channel breaking operations in a continuous ramming procedure. This technique leaves the channel congested with close to consolidated floes, which often refreeze into a large mass during November, and makes channel clearing difficult even with strong southerly winds. An alternate procedure is for the channel to be broken for a mile or two and then, in conjunction with light to moderate southerly winds, the icebreakers aid evacuation of the ice before possible refreezing occurs by use of their propellers in a technique called backwashing. Winter Quarters Bay usually is cleared in this manner. By setting the ice in motion, small discharges of floes from the channel entrance should be forecasted with light southerly winds, but the remainder of the channel will remain congested. Continued light southerly winds will gradually clear brash and ice cakes that are not frozen together from a channel 10 to 15 nmi (19 to 28 km) long in about 2 to 3 weeks. When outflow of ice has resulted in lowered concentrations in channels less than 15 nmi (28 km) long, south and southeast winds, deflected to the east by the south coast of Ross Island, clear the east side of the channel and cause congestion on the west side.

        Rapid clearing of a channel approximately 10 nmi (19 km) long should be forecasted with strong southerly winds lasting for at least 48 to 72 hours. Such rapid clearing of the channel occurred during DF 65. Channel breaking operations began on 21 November from the vicinity of Cape Royds, the channel was completed on 5 December, and subsequent strong southerly winds lasting approximately 72 hours established an open water channel 10 nmi (19 km) long by 10 December. In contrast, an extreme length of channel, as occurred during DF 63, or an abnormal amount of anomalous northerly winds, as observed during DF 66 and DF 67, can keep the channel congested until dislodgments cause the fast-ice edge to recede to Hut Point.

d. Currents and Iceberg Drift

        The westerly setting current along the Ross Ice Shelf continues around Ross Island at Cape Bird, and then turns south along the shore as far as Cape Royds (fig 15). Here the current turns west across the sound and then northwest and north along Victoria Land. At Cape Royds, the Cape Bird current is joined by a current from Hut Point which comes from under the ice shelf south of Cape Armitage and flows past Hut Point and Cape Evans. At certain phases of the tide and moon, the current may reverse flowing south past Hut Point.

        Observations of iceberg drift in McMurdo Sound are sparse. However, bergs entering the sound tend to drift with the current south to

Cape Royds with calm or light winds (<10 kn or 19 km/hr). Moderate south winds slow their southward drift and the icebergs may become stationary before reaching Cape Royds. Strong south winds (> 30 kn or 56 km/hr) probably will cause icebergs to reverse their direction and drift to the north. After a berg drifts to the vicinity of Cape Royds normal southerly winds and westerly current sets will move the berg west and northwest.

Iceberg drift south of Cape Royds can occur during periods of unusual strong north winds or current reversal over the sector to the south of Cape Royds. During mid-January 1970, a berg drifted approximately 11 nmi (20 km) south of Cape Royds where it impinged on the east side of the channel entrance. It remained near 77°44'S, 166°15'E for approximately six days and then drifted north and west.

Forecasts of iceberg movement may be made by vectorially adding the current set to the wind drift vector based on forecasted winds. The effect of wind on iceberg movement has been studied by Budinger (1960) both theoretically and empirically. Two equations relating the wind-induced movement for wind durations less than and equal to or greater than 24 hours for speeds from 10 to 50 kn (19 to 93 km/hr) are presented. The drift speed equations for blocky (tabular) and massive icebergs are:

$$V(iceberg) = 0.016 \ W(wind \ speed) \quad (< 24 \ hrs. \ duration)$$
$$V(iceberg) = 0.021 \ W(wind \ speed) \quad (\geqslant 24 \ hrs. \ duration)$$

(1)

The iceberg drift speed and the wind speed have the same units; the movement is directed 50° to the left of the surface wind direction. (These equations also may be applied to iceberg drift in the Ross Sea).

Tabular icebergs dislodged from the Ross Ice Shelf are estimated to have an exposed to submerged ratio of approximately 1:5. Measurements of the shelf ice thickness obtained by seismic means and above sea level elevations at a number of sites near Little America V indicated an average 1:5 height to depth ratio (Crary, 1961). Bender and Gow (1961) also found this ratio for a nearby hole drilled from the top to the bottom of the ice shelf 256 m (840 ft) thick. The ratio probably varies slightly for tabular bergs and may be as low as 1:4.5 because of considerable melting of high density ice from the bottom of the ice front and of bergs, which lowers the average density. Smith (1928) has tabulated values for various shaped bergs found in the Arctic; a ratio of 1:5 is given for blocky bergs, 1:4 is given for rounded bergs. Measurements of the height of tabular bergs drifting into McMurdo Sound therefore can indicate their approximate grounding depth.

B. Long-Range Ice Estimates

Analog (impirical) techniques are employed in preparing long-range ice estimates because long-range environmental forecasts generally are not available for Antarctic areas. One analog technique is to establish a relation between historical observations of an environmental factor and data on the particular ice feature under investigation. The environmental factor used to establish the relationship may be observed concurrently with or prior to the occurrence of the ice feature. A forecast of the environmental

factor is required to estimate the ice feature when concurrent data are used to derive the relationship. However, environmental observations may be used for preparing the ice estimate when the derived relation is between the ice feature and prior environmental observations.

1. Ross Sea

a. Mid-November North Pack Edge and Pack Thickness

Two large scale ice features in the Ross Sea which affect mid-November ship operations are the location of the northern edge of pack ice and the overall thickness of sea ice. The average 15-day wind velocity at 70°S, 175°E computed from the four 15-day means from mid-July to mid-September has been found to be a good indicator of the location of the north pack edge on 15 November along 176°E. Southerly winds advect the north pack edge northward and conversely, northerly winds tend to retard movement the edge to the north. An average 15-day geostrophic wind with a south component of +6 kn (11 km/hr) was found to be related to a north pack edge at 64°30'S on 15 November; a north-component wind of -4 kn (7 km/hr) was related to a position of the edge at approximately 65°30'S. This relation, based on observations taken during four years and normal data, is shown in figure 21. The normal north-south component of the geostrophic wind (+6.6 kn or 12 km/hr) was computed from figures A-7, A-8, and A-9 (weighting August twice as heavily as July and September); the normal position of the north pack edge at 64°25'S on 15 November was taken from figure 6. The regression line (visually determined) was drawn through the normal position because it is based on ice observations taken during twelve DF seasons and long-term surface pressure data. The relation is shown north to 63°S because the north pack edge was located farthest northward at 63°S along 176°E on 15 November (DF 61).

Drift of pack ice to the north during the austral winter results in dispersal of the pack, the formation of new ice between ice floes, and a decrease in the average ice thickness.* Geostrophic winds having a southerly component greater than approximately +12 kn (22km/hr) are estimated to be associated with light thickness conditions* over the western Ross Sea. Conversely, average geostrophic wind components that are negative indicate resultant winds with northerly components which are estimated to be associated with severe thickness conditions.* Geostrophic winds with a south component of zero to +12 kn (22 km/hr) are associated with average thickness conditions.*

b. Warming Degree Days

Figures 22, 23, and 24 indicate the accumulation of warming degree days (Wdd's) at McMurdo Station at the end of each day from 1 November through 28 February for DF II through DF 71. The curves were constructed using daily mean temperatures and an arbitrarily chosen 18°F base and starting date of 1 November. For example, a daily mean temperature of 15°F gives a -3 value; a daily mean temperature of 26°F contributes a +8 to the cumulative total. Average and median values computed at 5-day intervals and envelopes of extreme values are presented in figure 25.

_____
*See section II, para. F.5.

The degree-day curves for individual resupply seasons indicate a wide year-to-year variance of austral summer heating. During all years, daily mean temperatures were colder than 18°F (-7.8°C) at the start of November as indicated by the downward slope of the curves. The earliest rise of daily mean temperatures above 18°F (-7.8°C) (upward sloping curves) was in DF 65 (7 November) and latest during DF IV (11 December). The average and median values were 20 November. The coldest temperatures were recorded during November 1959 (-240 Wdd's) while the warmest November occurred during DF 65 (-48 Wdd's). An average total of approximately -121 Wdd's was accumulated before seasonal heating caused the curves to slope upward from their lowest points.

Warming degree-day totals became positive from 27 November to 29 December; an average value of 14 December was calculated. The slopes of the curves increased steadily after mid-December at a rate of approximately 10 Wdd's/day except during DF 60 which had an unusual cold period in mid-January. Positive Wdd's were accumulated to an average date of 14 February. However, ensuing downward slopes of the curves associated with seasonal cooling started as early as 3 February (DF 60) and as late as 27 February (DF 68).

A maximum of almost 700 Wdd's was accumulated during DF III and slightly less during DF 67 making them the warmest summers. A minimum of slightly less than 200 Wdd's was accumulated during DF 60 making it the coldest summer. Average and median values for all years were respectively, 462 Wdd's and 434 Wdd's. When total seasonal warming is considered, that is, positive Wdd's accumulated between the lowest and highest points on each curve, three years had equally low warming amounts. They were DF IV, DF 60, and DF 63 with warming totals of approximately 440 Wdd's. Using this same measuring technique, DF III remained as the season with the greatest total warming.

(1) Mid-December South Pack Edge

Location of the south pack edge in the western Ross Sea is a large scale ice feature important to ship transit to and from McMurdo Sound. Northward recession of the edge is related to surface currents, wind velocity, and the rate of pack disintegration. These factors are not mutually independent and involve processes which are quite complex.

The minimum Wdd total computed from daily temperature data taken at McMurdo Station is useful for indicating the location of the south pack edge (at 178°E) on 15 December. Minimum Wdd's generally occur during the latter half of November; therefore, observed Wdd totals can be used directly for estimating the mid-December location of the edge. Low minimum Wdd totals are related to southern locations and high Wdd totals to northern locations of the south pack edge. A plot of 9 years of observed Wdd data and corresponding edge locations indicates a linear relation; a linear correlation coefficient of -.87 was calculated. The slope of a manually prepared regression line passes through zero Wdd's and 68°30'S and increases 1° of latitude for each additional -40 Wdd's. Written as an equation,

$$\text{Latitude (15 Dec south pack edge)} = 68.5 - \left(\frac{\text{min. Wdd total}}{40}\right)$$

The relation between minimum Wdd's and location of the south pack edge is substantiated by environmental factors. Low surface

temperatures and low minimum Wdd's are related to the advection of cold air from the continent, which retards ice disintegration in the southwestern Ross Sea. Wind speeds are low, which inhibits vertical mixing of the lower atmosphere and resultant increases in the surface air temperature owing to the strong temperature inversion present in Antarctica. Low wind speeds also result in small wind drift of the ice.

High (relative) temperatures and high minimum Wdd's are related to moderate and strong surface winds and resultant vertical mixing of the warm air aloft. Storms migrating into the south central Ross Sea produce strong southeast to southerly winds over the western Ross Sea that advect the south ice edge northward. The strongest surface winds and the most rapid northward advection of ice occur when a deep surface low pressure center is located over the southern Ross Sea. Retrograde type storms that move westward over the Ross Ice Shelf generally result in less severe winds and smaller northward advection of the south pack edge than is associated with severe storms, but the northward recession undoubtedly will be greater than normal.

c. Historical Ice Data

The analog (empirical) technique frequently used to prepare 15- and 30-day ice estimates is to find past ice conditions similar to the current areal ice distribution and follow the same historical progression of pack disintergration. This technique assumes that environmental conditions affecting ice drift and disintegration such as mean surface wind velocity, pack concentration, mean ice thickness, and stage of deterioration are approximately the same during the past and future period covered by the ice estimate. Usually, initial ice conditions for the two years will not be identical. In that case the long-range ice estimate is developed by modifying the latest ice conditions by the change of conditions that occurred during the prior year.

Thirty-day ice estimates are prepared initially; 15-day estimates are interpolations between the observed and 30-day estimated conditions. Linear interpolations usually are made within any 30-day period for pack edge and concentration data, although historical changes in these ice features may have an accelerating seasonal trend. The third major ice feature given in long-range ice estimates is the stage of development (age) of the pack. By convention, the age category of the maximum seasonal growth is retained through its disintegrating stages even though the ice thickness is equivalent to a thinner ice category. During the melt season, the primary age of the pack at a particular location, however, may change owing to advection, or it may increase owing to the final disintegration of a predominant thinner ice age ahead of thicker ages. An increase of the average thickness of the remaining pack therefore may occur although the areal extent and concentration is much less. This often occurs in the northern Ross Sea owing to final disintegration of the predominant thin and medium first-year pack and the accumulation of thick first-year and remnant multi-year floes. The dominant floe size of the pack is estimated using the normal floe-size analyses or applying the changes between analyses to recent aerial reconnaissance data.

In order to make a proper assessment of the comparability between the present pack conditions and the similar historical data, it

41

may be necessary to account for the difference in the dates of observation. Comparability of ice edges can be made using figures 9 and 14. For example, if the north pack edge was observed by satellite at 64°30'S between 174°E and 180° on 9 November, the seasonal recession rate of 10 nmi (19 km) per 3 days (fig 9) indicates a comparable location of the edge at 64°50'S on 15 November. If the north pack edge associated with similar past data was observed at 65°00'S on 17 November, that location adjusted to 64°53'S at 15 November is nearly identical to the 9 November edge adjusted to 64°50'S. In this example, subsequent location of the past edge is used as the forecasted location. If for example, the adjusted edges were 30 nmi (56 km) apart, recession of the edge from the past data would be added to the present location to get the forecasted location of the north pack edge. Comparison usually is made to the 1st or 15th of the month because long-range ice estimates are prepared for those periods. Comparison of the adjusted edge at 64°50'S to the mean position of 64°25'S on the 15 November (fig 9) indicates the edge is 25 nmi (46 km) south of normal. Similar comparisons of the south pack edge data using figure 14 can be made. If the ice data are observed from shipboard along a particular longitude, the median positions indicated in figures 4 and 10 may be used for determining the anomaly of the edge position.

A comparison of observed pack concentrations to normal and past conditions is accomplished by the same technique used with pack edges. Areas with the highest pack concentrations are considered first because that ice will have the greatest adverse effect on shipping. In preparing ice estimates for periods from November through mid-December, the forecaster should note the location of the northern edge of the 7- and 8-okta pack in the western Ross Sea. Historical ice data should be searched for an edge having a similar latitude as well as a comparable position of the north pack edge. When similar historical data are found, the southward recession of the 7- and 8-okta edge should be added to the latest location of the edge for the pertinent time interval. For areas with lesser pack concentrations, the decrease in the pack concentration indicated by the similar historical observation should be used to decrease the concentrations associated with the latest observed data.

Therefore, average movements of ice edges and other background mean ice data are useful, but the ice forecaster also needs data on the progression of ice conditions that occurred during previous resupply seasons. If these data are not available, statistics given on the recession of pack edges given in sections II.F.1.c. and II.F.2.b. may be used together with the mean-concentration and floe-size analyses. Occasionally, a series of ice observations taken during the current and a prior year are very similar. For this special case, the prior year is called the analog ice year.

d. Optimum Ice Routes

The average concentration and frequency of large floe size analyses in Appendix C may be used as partial inputs to estimate an optimum route through the pack in the absence of ice reconnaissance data. These ice parameters, however, cannot be used alone to determine a route because in addition to the amount of surface water between floes (pack concentrations over small areas), the ability of a ship to break ice is dependent on

42

other factors such as ice thickness (including the extent of ridging and hummocking), ship's characteristics such as weight, power, plate thickness, and shape, and depth of snow cover.

New and young ice (up to 30 cm or 1 ft thick) may tend to slow an icebreaker, but the ice does not prevent her from maintaining a course. Change in concentration in new and young pack areas is rarely a factor in altering a route through these stages of ice developr.c. As sea ice gets thicker, concentration of the pack becomes more important in choosing a particular route. For thicknesses greater than approximately 5 ft (1.5 m), pack concentration becomes the deciding factor in choosing a route, because the amount of open water between floes into which the icebreaker-broken ice can move, is of prime importance.

Floe-size probably is less important than ice concentration or thickness in choosing an optimum route. When a ship hits ice floes, cracks radiate from the point of impact, forming paths of least resistance along which the ship is likely to move making it extremely difficult to return to the proper heading. When large floes are broken the icebreaker may go contrary to the desired course for a considerable distance. Small floes are less of an obstacle to maintaining a constant heading.

Other factors such as snow cover, convergence and divergence of the pack, and orientation of leads also are important. Snow 24 in (61 cm) or deeper, if the temperature is not too low, forms a cushion absorbing a large part of the breaking force so that ice breaking is less effective. These factors can best be used for track selection on a real-time basis; that is, based on aircraft or satellite observation and meteorological conditions just prior to entry into the pack.

In locations where pack is subject to strong drift, rapidly changing concentrations and advection of different ice thicknesses (ages) into the area indicate that an optimum route can be determined best by ship-based helicopter observations.

The normal pack-concentration and floe-size analyses and the estimated thickness of ice in the western Ross Sea indicate that during October and November of a normal ice year, the optimum route through the pack south to 75°S usually lies east of 177°E. During December, a track varying between 175°E and 176°E appears superior to other routes. During 1 to 15 January variable pack concentrations indicate that the track should be determined on a real-time basis and probably would lie near 175°E. By late January, a track generally along 173°E normally may be taken. Pack concentration and thickness, and floe size, however, rarely are normally distributed over extensive areas. Therefore operational tracks should be determined from real-time data. The normal ice data indicate, however, that optimum ice tracks through the western Ross Sea generally shift progressively westward during the resupply season.

Surface winds over the southwest sector of the Ross Sea prevail from the southeast. Probably owing to the elevation of Ross Island, sea ice has a tendency to remain in the lee of its north coast. Westerly surface currents are present there but partial blockage of drift ice by

Cape Bird peninsula often keeps the area between Beaufort Island and Cape Bird peninsula during November covered with very close pack; fast ice also may extend across this passageway. However, leads and areas of lesser concentration tend to form for short durations northward of Beaufort Island to 76°30'S and may explain why many icebreaker tracks into McMurdo Sound during November lie in that sector.

2. McMurdo Sound

a. Frost-Degree Days and Ice Growth

Frost-degree days (Fdd) are used to indicate the onset and severity of cold air temperatures. Fdd accumulations made after ice first forms can be related empirically to the undisturbed growth of sea ice at coastal locations; that is, where the ice has remained in place after initial formation. Seasonal Fdd totals are usually computed from daily mean temperatures. However, Fdd's also may be computed from monthly mean temperatures without differing appreciably from monthly accumulations using daily temperatures.

A frost-degree day is defined as a day with a mean temperature 1°F or 1°C below a particular base. The base temperature used usually is 32°F or 0°C. Occasionally the base temperature chosen is the freezing temperature of the water; for example, 28.6°F or -1.9°C with salinities of 35°/$_{oo}$. Using a 32°F base, 7 Fdd's are accumulated when the daily mean temperature (midway between the daily high and low temperature) is 25°F; a monthly mean temperature of -10.8°F indicates that 1327 Fdd's are accumulated during a 31-day month.

Many studies relating sea ice growth in the Arctic to Fdd's have used a 0°C or 32°F base. Zubov (1945) found the regression equation

$$I^2 + 50I = 8R$$

best fitted the average rate of sea ice growth after ice has formed in the seas bordering the Soviet Arctic, where I is the ice thickness in centimeters and R is the total of Fdd's (0°C base). Application of this equation in the form of

$$I = \sqrt{625 + 8R} - 25$$

or using inches and a 32°F base

$$I = \sqrt{97 + .69 \, \Sigma Fdd} - 9.8 \qquad (2)$$

to mean monthly temperatures recorded at McMurdo Station from March through November indicates that normal undisturbed growth of sea ice in the immediate area (Winter Quarters Bay) amounts to about 193 cm (76 in). Fdd's accumulated in March and November are included because freezeup of Winter Quarters Bay usually occurs by early March and thickness data indicate that ice growth continues at a slow rate through November. A simplified incremental form of equation (2),

44

$$\Delta I = \frac{0.69 \Delta \Sigma Fdd}{2I_0 + 19.69}$$

may be applied to June and following mean temperature data with negligible error in total ice thickness for undisturbed growth where ΔI is the increase in ice thickness with an increase of frost-degree days $\Delta \Sigma Fdd$ and I_0 is the thickness of the ice already formed.

In addition to air temperature, however, ice growth is related to other local meteorological and oceanographic factors such as vertical distribution of temperature and salinity, snow thickness and density, and wind speed. The rate of ice accretion during any period also is a function of the ice thickness at the start of the period; the thicker the ice, the slower is further growth. Of all the factors, snow depth probably has the greatest effect on ice growth and is especially significant shortly after ice growth begins when a large snow accumulation retards ice growth more than late season accumulations of the same depth. The constants in Zubov's equation were derived empirically and consider the combined effect of normal values of all these additional factors observed in the Soviet Arctic.

It is not surprising that, for a few ice growth seasons tested, Zubov's equation when applied to monthly mean temperatures recorded at McMurdo Station gives thicknesses which are generally 10% to 15% smaller than measurements taken in Winter Quarters Bay. Atlas data indicate that much of the seas bordering the Soviet Arctic have annual snow accumulations of 4 to 6 in (10 to 15 cm). Similar depths were observed during test years in Winter Quarters Bay. Therefore, the difference in ice growth may be related to probable, but unknown, dissimilarities between the other meteorological and oceanographic factors.

The undisturbed thickness of first-year ice in Winter Quarters Bay at the end of November may be estimated by the application of Zubov's equation to Fdd's accumulated from monthly mean temperatures for March through November recorded at McMurdo Station. If snow depths throughout the winter are 6 in (15 cm) or less or are unknown, add 10% to 15% to the calculated ice thickness. For snow depths which accumulate to greater than 6 in (15 cm), an equation derived by Kolesnikov (1946) may be used to estimate the ice growth. The equation takes into account many meteorological factors. For practical calculation of ice growth with the degree of accuracy required for ice forecasts, Kolesnikov's equation may be simplified to

$$(\Delta I)^2 + (12.1d + \frac{90}{1.75V_0 \ EXP \ 0 \ 656} + 2I_0) \Delta I = 10.8 \sum_D \frac{-(1.9 + \Theta)}{1 - 0.005(1.9 + \Theta)}$$

where ΔI = increase in ice thickness (cm)*

   d = snow depth (cm)

   V_0 = surface wind speed (m/sec)

   I_0 = initial ice thickness (cm)

   D = number of days over which ΔI is calculated

   Θ = equivalent air temperature (°C)

* 1 inch = 2.54 cm

45

The equivalent air temperature, θ is the surface air temperature that is modified to take into account the net effect of various meteorological factors which are present in polar latitudes. Values of θ, in effect, are summed below the freezing temperature of the sea water; -1.9°C (28.6°F) for salinities near 35°/oo. Near Hut Point Peninsula salinities generally range from 34.1°/oo at the surface to 34.8°/oo at 500 m (1640 ft).

Kolesnikov's equation may be modified to use Fdd values using a 32°F base, a surface wind term W, the snow depth and initial ice thickness in inches, and a temperature adjustment term, K, which combines the net effect of the meteorological factors with the freezing temperature of the water for calculation of ice growth in centimeters. Values of the temperature adjustment K are given in table 3.

Table 3

Temperature Adjustment for Winter Months in the Antarctic

	K (°C)
March	+3.4
April	+0.1
May	-3.1
June	-3.3
July	-3.5
August	-2.3
September	+1.3
October	+4.9
November	+7.4

With these modifications, Kolesnikov's equation becomes

$$(\Delta I)^2 + (30.7d^* + W + 5.1I_0^*)\Delta I = \frac{6(\Delta \Sigma Fdd - 1.8DK)}{1 + \frac{0.003}{D}(\Delta \Sigma Fdd - 1.8DK)} \quad (3)$$

where d* and I_0^* are the snow depth and initial ice thickness in inches.

Although this equation looks complicated, it can be evaluated easily. For convenience, figure 26 is given from which the wind term (W) may be found directly from the wind speed in knots averaged over the period in days (D) of uniform snow depth. Wind speed is measured at the site of ice growth; wind direction is not considered in calculating the average speed.

For example, with an initial ice thickness of 24 in, snow depth of 7 in, average wind speed of 13 kn and an average temperature of -8.2°F for April, the equation becomes

$$(\Delta I)^2 + [30.7(7) + 15 + 5.1(24)]\Delta I = 6 \frac{[1206 - 1.8(30)(0.1)]}{1 + \frac{0.003}{30}[1206 - 1.8(30)(0.1)]}$$

Solving this quadratic equation yields

$$\Delta I = 16.5 \text{ cm or } 6.5 \text{ in.}$$

or the ice will grow to approximately 30.5 in (77 cm) at the end of April. For periods not equal to a calendar month, the Fdd total computed from daily mean temperatures (°F), may be substituted in equation (3). An average value of K should be found from figure 27 for the time interval involved. Since snow depth has a pronounced effect on ice growth, the occurrence and amounts of significant increases or decreases in snow accumulation (>4 in or 10 cm) should be noted in order to facilitate construction of a step-line graph of uniform snow depths in application of Kolesnikov's equation.

The occurrence of severe storms at McMurdo Station during the austral winter may be used to estimate the character of the fast ice thickness over McMurdo Sound for icebreaker operations conducted during the followin DF season. Frequent dislodgment of newly formed ice during March is common. When repeated strong southerly winds, estimated to be storm force or higher (≥48 kn or 89 km/hr) occur well into June with a subsequent absence of severe storms, concurrent refreezing of extensive portions of the sound is probable. Therefore, relatively thin fast ice of approximate uniform thickness may be expected during November over most of the channel to Hut Point, as was observed during DF 68. Frost-degree-day data accumulated after the final storm may be used to estimate the ice thickness. On the other hand, when storms are not severe and occur at infrequent intervals during the ice growth season, thickness of the fast ice can be expected to be relatively large and to decrease to the north in irregularly wide zones of approximate uniform thickness. Icebreaker observations during November and December indicate the latter decreasing thickness distribution often is present. Therefore, it is probable that zones of fast-ice dislodge periodically from the edge during the ice growth season separated by periods during which the fast-ice edge advances northward.

Repeated dislodgment of newly formed ice from Winter Quarters Bay during the initial ice growth months with no later dislodgments results only in a slightly thinner thickness at the end of the ice growth period than if the growth was undisturbed. The small difference in thickness can be attributed to the rapid regrowth of ice and the large remaining period of the ice growth season. For example, during the winter of 1968, 9908 Fdd's accumulated from 1 March through 30 November indicated (by Zubov's equation plus 10%) ice growth to 81 in (206 cm). If dislodgment of all ice occurred on 1 May and no later dislodgments occurred, regrowth of ice would have reached 73 in (185 cm) by 30 November.

Data on the wind force and duration required to dislodge various amounts and thicknesses of fast ice from McMurdo Sound during the austral winter are not available. Knowledge of the occurrence of severe storms at

McMurdo Station during the austral winter, however, can be useful in estimating the qualitative distribution of fast-ice thickness in McMurdo Sound.

b. Warming Degree Days and Ice Melt

Warming degree day (Wdd) totals can be used to estimate the commencement of melting and decreases in ice thickness. Wdd and thickness data from several years indicate that the annual ice runway at Williams Field starts to decrease in thickness when total warming of approximately 100 Wdd's are accumulated; that is, after the Wdd minimum is reached. For example, during DF 65 the Wdd minimum of -48 occurred on 7 November and the ice thickness started to decrease on 5 December when the Wdd total was +50, or a gain of 98. During DF 70 the Wdd minimum was -115 and the annual ice started to decrease on 11 December when the Wdd totaled -10 or a gain of 105.

Based on limited data, the ratios of Wdd's accumulated after the ice thickness starts to diminish appear to be well related to decrease in ice thickness in inches. The number of Wdd's effective for melting can be found by adding the above-zero total indicated on the positive ordinate scale to the absolute value of the Wdd minimum and then subtract 100 Wdd's. The data also indicate the ratios of "melting" Wdd totals to decreases in ice thickness tend to decrease with time. The following median ratios were found at the given dates:

1 January - 17

15 January - 15

25 January - 12

To use these ratios in forecasting decreases in ice thickness of the runway at Williams Field for a period during 1 to 25 January, divide the "melting" Wdd's by the proper factor. Thus during DF 67, 220 above-zero Wdd's were accumulated on 1 January and the Wdd minimum was -50 which yields a "melting" Wdd total of 170 (220 + 50 - 100). The forecasted decrease in ice thickness on 1 January is 10 inches (170 divided by 17) or 25 cm. On 25 January, the 430 "melting" Wdd's accumulated relates to a 36-in (107 cm) decrease in ice thickness (430 divided by 12). Interpolated ratios can be used for other dates; for example, a 13.5 ratio for "melting" Wdd's totaled to 20 January.

The ratios given for diminishing ice thickness are in general agreement with Assur (1956) who found a factor of 30 using a base temperature of 10°F for accumulation of Wdd's and the study of Karelin, as quoted by Bilello (1960), who found a comparable number of Wdd's must be accumulated before ice thicknesses diminish.

Wdd curves therefore can be used to indicate the start and amount of decreasing thickness of sea ice in the absence of thickness measurements. A projected Wdd curve based on large scale weather trends similarly can be used to forecast decreasing thickness of the ice at Williams Field.

48

c. Austral Winter Temperatures and Fast Ice Width

An analysis of monthly mean temperature data and the extent of fast ice in McMurdo Sound indicates that a sum of the mean temperatures for September and October less than -30°F (-34.4°C) is related to fast-ice widths of approximately 45 to 60 nmi (83 to 111 km) to the north of Hut Point on 15 November. Temperature totals usually ranged, however, from -7° to -17°F (-21.7° to -27.2°C). Although the relation of temperature data in that range to fast-ice observations is not precise, -7°F (-21.7°C) totals were associated with fast-ice extents which averaged 20 nmi (37 km) and -17°F (-27.2°C) totals were associated with fast ice extents which averaged 24 nmi (44 km). Observations of temperature sums between -17° and -30°F (-27.2° and -34.4°C) and fast-ice extents between 27 and 43 nmi (50 and 80 km) on 15 November were not recorded.

IV. FORECASTING EXAMPLES

Examples of short-range forecasts and long-range ice estimates are given in order to relate the working procedures and summarized historical data to operational situations. The short-range (24- and 48-hour) examples assume that all pertinent ice parameters are known and perfect wind forecasts are made. Often in practice, it is necessary to estimate various factors from historical data, such as ice thickness, in order to make a forecast. At other times, ranges of ice parameters such as ice concentration or the forecasted wind velocity, or both, must be used to develop a forecast which indicates the maximum and minimum extents of ice drift.

A number of locations with different ice concentrations, extents of ridging, and expected surface winds should be chosen when preparing a short-range forecast for an area. Locations may be chosen on ice boundaries; that is, between areas of different ice concentrations, or on ice edges in order to forecast drift of these ice discontinuities. In this manner, a chart of the overall distribution of forecasted pack concentrations can be prepared from which a word forecast can be written.

Disintegration of the pack is often considered to be negligible during a 24- to 48-hour period. This may not be true with strong winds and ice that is in an advanced state of disintegration. Pack disintegration, however, must be taken into account in a continuous series of short-range forecasts.

Long-range ice estimates (15- and 30-day) are based on historical ice data which combine average disintergration rates as well as average wind and current drift. Long-range wind forecasts are presently not made for Antarctic waters. Therefore long-range ice estimated most often are based on the relation of environmental data and synoptic ice observations to similar historical data. In the absence of environmental and synoptic ice conditions, long-range estimates may be made utilizing only historical data.

A. Short-Range Ice Forecasts

Example 1

Given: Ice: 6 oktas, 0.3 ridging, 8 ft* thick

        Wind: NW 25 kn

----
*1 ft = 30.48 cm

49

Find:

    a) 24-hour response factor

    b) 24-hour drift distance

    c) deviation angle

    d) wind drift direction

Solution:

    a) From table 2, response factor is 0.27

    b) (0.27) (25 kn) = 6.75 nmi*

    c) From figure 20, deviation angle = 32°

    d) Drift is toward 315° -180° = 135° - 32° = 102°

Example 2

Given: Ice: 2 oktas, 0.4 ridging, 2-4 ft thick

       Wind: Geostrophic NE 20 kn

       Location: 70°S 175°E

Find:

    a) Surface wind velocity

    b) 24-hour wind drift vector

    c) 24-hour current drift vector

    d) Resultant 48-hour ice drift vector

Solution:

    a) Surface wind speed = 0.70(20) = 14.0 kn

         Surface wind direction = 045° + 20° = 065°

    b) Distance: (0.75) (14.0) = 10.5 nmi

         Direction: 065° + 180° = 245° - 28° = 217°

---

*1 kn = 1.852 km/hr
1 nmi ≈ 1.852 km

c) From figure 3, direction = 320°

Distance: 24 x 0.3 = 7.2 nmi

d) Vector addition of 219° @ 10.5 nmi

and 320° @ 7.2 nmi = 257° @ 11.5 nmi

48-hour drift = 257° @ 23.0 nmi

Example 3

A ship is operating in a 20 nmi wide band of evenly distributed remnant first-year floes of 2 oktas concentration and 0.4 ridging. This very open pack band lies adjacent to an east-west oriented fast ice edge where a north 0.3 kn current has been measured. Ice drift is observed by shipboard personnel due southward with a 20-kn wind. Assuming no ice disintegration, how long will it take the 2 okta belt to compact along the fast ice edge?

Solution: The 2 okta band of ice will become compact when it is compressed to a 5 nmi width because only one-fourth of the 20 nmi wide band is composed of ice. The 75% response factor from table 2 and the 0.3 kn current indicate a net southward ice drift of 7.8 nmi/day. Therefore it will take approximately 46 hours for the ice edge to drift 15 nmi southward and for the belt to become compact.

Example 4

An open water area of 0.4 hummocky floes estimated by shipboard observers to be from 8 to 12 ft thick was skirted to the west near 70°S, 180° on 21 January at 0600Z. The surface wind is forecasted to be E @ 20 kn for the next 2 days. Where can this ice area be expected to drift in 48 hours? Along what longitude would another vessel be advised to steam in order to avoid the western portion of this ice area in 48 hours?

Solution: From table 2, 24 hour response factor is 0.89 indicating a wind drift of 17.8 nmi in 24 hours. From figure 20, the deviation angle is -38°. From figure 3 the surface current is 290° at 0.2 kn. A vector addition (232° @ 17.8 nmi and 290° @ 4.8 nmi) yields a total ice drift toward 243° @ 20.8 nmi or 41.6 nmi for 48 hours. The components of the ice drift are 37.0 nmi westward and 18.8 nmi southward. Therefore, the ice will drift southward to approximately 70.3°S (60 nmi per one degree of latitude). Since one degree of longitude at 70.0°S is approximately 20.5 nmi wide*, the western edge of the ice will drift to approximately 70.3°S, 178.0°E using a mean longitudinal width over the drift path. If all ice is to be avoided, a track no farther east than 175°E will be advised to avoid isolated floes drifting up to 10% of the wind speed or to allow for stronger winds than were forecasted.

___

*With an error smaller than ± 0.15 nmi (0.28 km) the length of one degree of longitude in nautical miles and tenths at any latitude south of 63°S is numerically equal to the latitude in degrees and tenths subtracted from 90.5 (Bowditch, 1966).

Example 5

A 4-okta area of sea ice with 0.3 ridges was observed by aerial
reconnaissance at 72°30'S, 175°E at 0400Z on 5 December. It was estimated to
be 4 ft thick from previous reports of ships steaming through the area.
Owing to flight time in returning to base, this observation was available to
the forecaster 8 hours later. Geostrophic winds on the 5 December 0000Z and
1200Z surface pressure charts were SE @ 30 kn. Forecasted surface winds for
the area are S to SW @ 30 kn for 24 hours after 5 December 1200Z and then W @
5 to 10 kn for an additional 24 hours. Where will the ice drift by
7 December 1200Z?

Solution: Drift of the ice must be hindcasted to the start of
the forecast period and then drifted with the forecasted winds.

a) Hindcast wind drift

Geostrophic wind to surface wind: 0.70(30) = 21.0 kn
135° + 20° = 155°

Drift distance: 0.42(21.0) = 8.8 nmi/day; drift for
8 hours = $\frac{8.8}{3}$ = 2.9 nmi

Deviation angle: -27°; drift is toward 155° + 180°
= 335° - 27° = 308°

b) Forecast wind drift for 1st 24 hours:

Drift distance: 0.42(30) = 12.6 nmi

Deviation angle: -24°; drift is toward 203° - 180° =
23° - 24° = 359°

c) Forecast wind drift for 2nd 24 hours:

Drift distance: 0.42(7.5) = 3.2 nmi

Deviation angle: -40°; drift is toward 270° - 180° =
90° - 40° = 050°

d) Current drift

From figure 3, the surface current is 330° @ 0.3 kn or a
vector of 330° @ 16.8 nmi for 56 hours from the time of ice observation to
the forecast time.

e) Vector addition for total drift

Total wind drift vector:

308° @ 2.9 nmi (a), plus 359° @ 12.6 nmi (b), plus 050°
@ 3.2 nmi (c) = 000° @ 16.4 nmi,

Total wind drift added to current drift:

000° @ 16.4 nmi plus 330° @ 16.8 nmi gives a total drift toward 345° @ 32.0 nmi which has a north component of approximately 30 nmi and a westward component of 8 nmi or 0.5° latitude and 0.5° longitude. Subtracting both of these values from the observed location gives the forecasted position of 72.0°S, 174.5°E.

Example 6

The north pack edge is observed at 67°S, 177°E, sea-ice conditions southward are 2 to 3 oktas for 50 nmi then 7 to 8 oktas for an additional 250 nmi. All ice has 2 tenths ridging and is estimated to be from 2 to 4 ft thick. The surface wind is forecasted to be N @ 30 kn for the next 48 hours.

Find:

   a) How far south will the north pack edge drift?

   b) What drift will the 7 to 8 okta area experience?

   c) To what width will the original 2 to 3 okta area be compressed (assume no pack disintegration)?

   d) Assuming the 2 to 3 okta area compresses to 7 to 8 oktas and no disintegration occurs, what effective movement of the boundary between the 2 to 3 and 7 to 8 okta areas would be observed at the verifying time?

Solution:

   a) From table 2, the 2 to 3 okta area has a .33 wind response factor or a drift of 19.8 nmi in 48 hours. The direction of drift is 23° to the left of 180° or toward 157°. The prevailing current is 285° @ 0.2 kn, which produces a drift of 9.6 nmi in 48 hours. A vector addition yields a resultant drift toward 185°, a distance of 15.8 nmi that has a due southward component of 15.7 nmi. The north pack edge therefore recedes southward to approximately 67°16'S.

   b) Using the same techniques, the 7 to 8 okta area drifts toward 242° a distance of 7.6 nmi (vector addition of wind drift of 157° @ 6.6 nmi and current of 285° @ 9.6 nmi).

   c) The 7 to 8 okta area moves due southward, a distance of 3.5 nmi, while the north pack edge moves southward 15.7 nmi. The original 2 to 3 okta area therefore undergoes an approximate 12 nmi compression that reduces its width to 38 nmi.

   d) The 2 to 3 okta area drifts southward against the original 7 to 8 okta area and a portion of it compresses to 7 to 8 oktas. Since the total amount of ice in the original 2 to 3 okta area and its new configuration remains the same, the products of concentrations and widths at the verifying time must equal the amount of ice at the time of observation. Letting X equal the new width of the 2.5 okta band, Y equal the width of new 7 to 8 okta area formed, and knowing the total new width is 38 nmi we get the simultaneous equations,

$$2.5X + 7.5Y = 2.5 \ (50)$$

$$X + Y = 38$$

Solving, we get X = 32 and Y = 6. Therefore, at the verifying time the original 2 to 3 okta band will be reduced from 50 nmi to 32 nmi and the 7 to 8 okta combined area will extend 2.5 nmi farther north although the ice drift has been to the south. The northward movement results from a 6 nmi wide formation added on to a 3.5 nmi southward movement of the original 7 to 8 okta area.

B. Long-Range Ice Estimates

Example 1

An early transit of the western Ross Sea and entry into McMurdo Sound in planned. Two icebreakers are expected to leave Port Lyttelton, N.Z., during late October and no reconnaissance or environmental data from the Ross Sea or McMurdo Sound are available. Estimate:

a) At what latitude could the north pack edge be encountered?

b) Where may the south pack edge be expected?

c) What pack concentration and percentage of larger floes can be expected?

d) Where and what is the thickest ice to be expected in the Ross Sea?

e) Where can the fast-ice edge be expected in McMurdo Sound?

Answer:

Estimates of all ice conditions are based on the analyses of historical ice data given in sections II.F. and II.G.

a) Steaming at 10 kn, the breakers will take approximately 5 days to steam to 63°S. Therefore, the north pack edge could be encountered at an average latitude of 63°40'S on 1 November (fig 9). For each 10 days of early or late departure from port, the north pack edge can be expected to be approximately 30 nmi north or south of 63°40'S respective to early or late departure (fig 9). The edge may be located slightly farther south along 178°E or 180° than westward (fig 4). The range of observed latitudes of the north pack edge on 1 November is smallest along 176°E where, over an 8 year period, it has been located as far north as 62°45'S or as far south as 64°05'S (fig 6).

b) The south pack edge on 1 November probably is located adjacent to the Ross Ice Shelf. Assuming a speed of 5 kn through the pack and noting that the overall position of the south pack edge is at 76°25'S on 15 November (fig 14), the icebreakers could steam to 77°S by 7 November where a linear interpolation indicates the south pack edge may be expected.

If departure from Port Lyttelton is delayed one week, transit may be made toward 76°S, 178°E where the edge can be expected by 15 November (fig 10), or toward 74°20'S, 176°E where the edge was observed farthest north by 15 November (fig 11).

c) During 1 to 15 November, 3 to 5 oktas of ice concentration could be expected from the north pack edge to approximately 66°30'S, then 7 oktas southward to the south pack edge. An area of lesser concentration (5 to 6 oktas) may be located near 74°30'S, 178°W (fig C-5). Large floes can be expected to cover 50% or more of the surface from 67°S to 72°S generally east of 176°E with lower percentages westward. South of 72°S,180°, an area of lower percentage of large floes has been found (fig C-6).

d) The thickest ice for average conditions during November extends from 67°30'S to 72°30'S; the ice will average 2 to 4 ft thick with pressure ridges to 5 ft. Multi-year floes 8 to 12 ft thick or more may be encountered eastward of a boundary generally extending from 67°30'S,178°E to 72°30'S,178°E to 75°S,175°W; occasionally they also may be encountered westward of this boundary owing to advection by mean currents (fig 3) and mean winds (fig A-11).

e) Fast ice in McMurdo Sound on 8 November can be expected most often near Cape Royds or about 22 to 23 nmi northwest of Hut Point (fig 19). The average width will be about 28 nmi with a maximum width of 61 NM and a minimum width of only 18 nmi (fig 19). Thickness of the fast ice will most probably be 3 to 4 ft along the north edge increasing to 6 ft (1.8 m) 2 to 3 nmi south of the edge. Thickness of the ice will gradually increase to 6 to 7 ft from Tent Island to Hut Point; occasional 8-ft thick zones also could be expected.

Example 2

The geostrophic wind velocity at 70°S, 175°E during 16 to 31 July, 1 to 15 August, 16 to 31 August and 1 to 15 September was estimated to be 180° at 18 kn, 135° at 12 kn, 210° at 17 kn, and 240° at 14 kn, respectively. At what latitude would the north pack edge in the western Ross Sea on 15 November be estimated? What overall ice thickness can be expected?

Answer:

A tip-to-tail summation of the four wind vectors indicates an average 15-day south component of the geostrophic wind of approximately +12.0 knots. From figure 21 the north pack edge is estimated at approximately 63°50'S on 15 November. The southerly wind component of 12.0 knots indicates light to average in thicknesses can be expected. From section II.F.5. the overall ice thickness is estimated at 1 to 2 1/2 feet from the north pack edge to 67°30'S, thence from 2 to 3 1/2 feet with pressure ridges 4 to 5 feet thick to 72°30'S, thence 1 to 3 feet thick to the south pack edge.

Example 3

Warming degree day (Wdd) accumulations indicate a minimum total of -140 Wdd's occurred before seasonal heating resulted in an upward slope of the Wdd curve. Estimate the latitude at which the south pack

edge could be expected on 15 December.

Solution: From section B.1.b.(1)

$$\text{Latitude} = 68.5 - \frac{\text{min. Wdd total}}{40}$$

$$= 68.5 - (\frac{-140}{40}) = 68.5 + 3.5$$

$$= 72.0 \text{ or } 72.0°S$$

Example 4

The north pack edge is observed at 64°30'S on 15 November with 4 oktas of ice concentration in a 60 nmi wide band adjacent to the edge and 7 to 8 oktas southward to the south pack edge at 76°30'S. Ice data from prior years is searched for similar conditions and during a particular year the north pack edge was observed at 63°50'S, 176°E on 12 November, the pack band along the edge was 3 to 4 oktas and only 30 nmi wide, and the ice southward was 7 oktas concentration. On 15 December of that prior year the edge receded to 65°30'S, the 3 to 4 okta concentration band became 2 to 3 oktas and 60 nmi wide and the pack southward became 4 to 5 oktas. Make a 15 and 30-day estimate of pack conditions valid 1 December and 15 December respectively.

Answer:

The present north pack edge is 30 nmi south of the past edge which is adjusted to 64°S for 15 November (fig 9). Since the past edge receded 90 nmi by 15 December, the 30-day forecast is for the edge to recede by 90 nmi to 66°S. The pack band decreased 1 okta from 3 to 4 oktas to 2 to 3 oktas; therefore, the forecast is for the 4 okta band to decrease to 3 oktas. The increase of 30 nmi in width results in a forecasted width of 90 nmi. Since the pack southward decreased 2 to 3 oktas, the 30-day forecast is for the 7 to 8 okta area to become 4 to 6 oktas. No south pack edge was observed during the prior year, therefore, the fore-casted location is made with respect to its normal position. Because 76°30'S is very close to the normal position of the south pack edge on 15 November (fig 14), a normal position of 72°S is forecast for 15 December.

The 15-day ice estimate valid 1 December will be a linear inter-polation between the latest conditions and the 30-day estimate. The north pack edge will recede 45 nmi to 65°15'S, the 4-okta concentration band will become 3 to 4 oktas and 75 nmi wide, the pack concentration southward of 66°30'S will become 5 to 7 oktas to a normal position of the south pack edge at 73°15'S.

Example 5

Monthly mean temperatures at McMurdo Station for March through November are respectively +2.0°F, -7.5°F, -13.2°F, -12.4°F, -16.8°F, -21.3°F, -10.6°F, -4.1°F, and +17.0°F. No ice thickness or snow depth data are available. Estimate the sea ice thickness in Winter Quarters Bay on 1 December.

Solution:

Zubov's English unit equation relating frost degree days (32°F base) to ice thickness (in inches) is used because no snow depth data are given; add 10% and 15% and round to the nearest inch.

Month	Temp (°F)	32°F base	No. of days	Fdd's
March	+2.0	30.0	31	930
April	-7.5	39.5	30	1185
May	-13.2	45.2	31	1401
June	-12.4	44.4	30	1332
July	-16.8	48.8	31	1513
August	-21.3	53.3	31	1652
September	-10.6	42.6	30	1278
October	-4.1	36.1	31	1119
November	+17.0	15.0	30	450

$$\Sigma \text{ Fdd's} = 10860$$

substituting in Zubov's English unit equation (2),

$$I = \sqrt{97 + .69\ (10860)} - 9.8$$

or $\quad I = \sqrt{7590} - 9.8; \quad I = 77.3$ inches

Adding 10% and 15% and rounding to the nearest inch yields a thickness range of 85 to 89 in.

Example 6

Thickness of the annual ice runway at Williams Field was measured on 15 July as 52 in with a snow cover of 12 inches. During the remainder of July the snow depth remained constant, 912 frost degree days were accumulated, and the average wind speed was 16 kn. What is the estimated ice thickness on 1 August?

Solution:

Finding a value of W from figure 26, a value of K from figure 27, and substituting in Kolesnikov's equation (3), we have

$$(\Delta I)^2 + [(30.7)(12) + 13 + (5.1)(52)]\,\Delta I = \frac{6\,[912-(1.8)(16)(-3.3)]}{1 + \dfrac{0.003[912-(1.8)(16)(-3.3)]}{16}}$$

$$(\Delta I)^2 + 646.6 \Delta I - 5077 = 0$$

substituting in the quadratic equation

$$\Delta I = \frac{-b + \sqrt{b^2 - 4ac}}{2a}$$

where a = 1, b = 646.6 and c = -5077 we have

$$\Delta I = \frac{-646.6 + \sqrt{418092 - 4\ (-5077)}}{2} = \frac{-646.6 + 662.1}{2}$$

$$\Delta I = \frac{15.5}{2} = 7.8 \text{ cm or } 3.1 \text{ in}$$

The ice thickness on 1 August therefore is estimated to be 55.1 in.

Example 7

The Wdd curve has reached a minimum value of -75 on 25 November and is forecast to reach "zero" on 15 December, and increase linearly to +250 on 8 January and reach +450 on 25 January. When will the ice thickness at Williams Field start to decrease and what is the estimated ice thickness on 8 January and on 25 January?

Solution:

From section III.B.2b. the ice thickness on the annual ice runway will start to decrease when approximately 100 Wdd's have occurred after the Wdd minimum has been reached. That accumulation is expected on 18 December assuming the linear Wdd increase after 15 December. Thickness of the ice runway is estimated to decrease approximately 14 in by 8 January (250 + 75 - 100) ÷ (16) and approximately 35 in (450 + 75 - 100) ÷ (12) by 25 January.

Example 8

At McMurdo Station the monthly mean temperatures for September and October are -23.0°F and -8.5°F, respectively. Where can the fast ice edge in McMurdo Sound be expected on 15 November?

Solution:

The sum of the mean monthly temperatures for September and October is less than -30° which is related to the fast ice edge lying 40 to 60 nmi north of Hut Point (section III.B.2.c). A qualitative forecast of "extensive fast ice" or "wider than normal fast ice" would be given. A quantitative estimate of the edge located approximately 50 nmi north of Hut Point would be made.

REFERENCES

Assur, A., Airfields on floating ice sheets, Snow, Ice and Permafrost Research Establishment, Rep 36, 1956.

Ball, F.K., Winds on the ice slopes of Antarctica, Proc. Symposium Antarctic Meteorology, 9, Pergamon Press, 1960.

Bender, J.A., and A.J. Gow, Deep drilling in the Antarctic, Assn. Intern. Hydrol. Sci. Assemblée Générale de Helsinki, Colloque Glaciologie Antarctique, 132, 1961.

Bentley, C.R., Glacial and subglacial geography of Antarctica, Am. Geophys. Union, Geophys. Monograph 7, 11, 1962.

Bilello, M.A., Formation, growth, and decay of sea ice in the Canadian Arctic Archipelago. Snow, Ice, and Permafrost Research Establishment, Research Rep. 65, 1960.

Bowditch, N., American practical navigator, U.S. Naval Oceanographic Office, H.O. Pub. 9, reprinted 1966.

Brennecke, W., Deutsche Antarktische Expedition 1911-1913: Die ozeanographischen arbeiten in Weddell-Meer, Gesellschaft Erdkunda Berline, 2, 119, 1914.

Budinger, T.F., Wind effect on icebergs, Rep International Ice Patrol Service in the North Atlantic Ocean, U.S. Coast Guard, Washington, D.C., 1960.

Crary, A.P., and F.G. Van der Hoeven, Sub-ice topography of Antarctica, Assn. Intern. Hydrol. Sci. Assemblée Générale de Helsinki, Colloque Glaciologie Antarctique, 125, 1961.

Debenham, F., Report on the maps and surveys, British (Terra Nova) Antarctic Expedition 1910-13, Harrison and Sons, London, 1923.

Heine, A.J., Ice breakout around the southern end of Ross Island, Antarctica, New Zealand J. of Geol. Geophys., 6, June 1963.

Hewson, E.W., and R.W. Longley, Meteorology theoretical and applied, John Wiley & Sons, New York, 1944.

Hughes, P., A determination of the relation between wind and sea surface drift, Quart. J. R. Met. Soc., 82, 494, 1956.

Karelin, D.B., O sviazi vetra s gradientom davleniia arkticheskikh moriakh. (On the relationship of the wind to the pressure gradient in the arctic seas). Problemy Arktiki, 2, Bureau of the Northern Sea Route, Leningrad, 1941.

Kolesnikov, A.G., On the theory of ice accretion on the sea surface, Problems of Marine Hydrological Forecasts, Leningrad, 1946.

Nansen, F., The oceanography of the North Polar basin, Scientific Results Norwegian North Polar Expedition, 1893-1896, 1902.

Petterssen, S, Weather analysis and forecasting, McGraw-Hill, N.Y., 1940.

Shuleikin, V.V., Fizika moria, izdanie tret'e. (Physics of the Sea, 3rd. ed.) Press of the Academy of Sciences of the USSR, Moscow, 1953. Par 16, Drift of Ice Fields, p. 113-129, translation, U.S. Naval Oceanographic Office.

Smith, E.H., The Marian expedition to Davis Strait and Baffin Bay, scientific results pt. 3, Rep. International Ice obs. and Ice Patrol Service in the North Atlantic Ocean, 19, U.S. Coast Guard, Washington, D.C., 1928.

Sverdrup, H.U., The wind drift of the ice on the North Siberian shelf, Norwegian North Polar Expedition with the Maud 1918-1925, Scientific Results, 4, 46 pp., 1928.

Taljaard, J.J., H. van Loon, H.L. Crutcher, and R.L. Jenne, Climate of the upper air, Part I, Vol. I, National Center for Atmospheric Research, NAVAIR 50-1C-55, September 1969.

Thiel, E.C., The amount of ice on planet Earth, Am. Geophys. Union, Geophys. Monograph, 7, 172, 1962.

U.S. Coast Guard, Icebreaker post operation reports for Antarctic cruises - Series, Operation DEEP FREEZE I through DEEP FREEZE 71, U.S. Coast Guard, Washington, D.C.

U.S. Geological Survey, Antarctic map and aerial photographic library. Various Photographs, unpublished.

U.S. Navy, Icebreaker post operation reports for Antarctic cruises - Series, Operation DEEP FREEZE I through DEEP FREEZE 65, U.S. Navy, Washington, D.C.

U.S. Navy Hydrographic Office:

U.S. Navy Hydrographic Office report on operation DEEP FREEZE I, Tech. Rep. TR-33, 182pp., U.S. Naval Oceanographic Office, Washington, D.C., 1956.

Operation DEEP FREEZE II (1956-1957) oceanographic survey results, Tech. Rep. TR-29, 156pp., U.S. Naval Oceanographic Office, Washington, D.C., 1957.

Oceanographic atlas of the polar seas, Part I, Antarctica, H.O. Pub. 705, 70pp., U.S. Naval Oceanographic Office, Washington, D.C. 1957.

Operation DEEP FREEZE III (1957-1958) oceanographic survey results, Unpublished manuscript, U.S. Naval Oceanographic Office, Washington, D.C., 1961.

Operation DEEP FREEZE 60 (1959-1960) Oceanographic survey results, Tech. Rep. TR-82, 231pp., U.S. Naval Oceanographic Office, Washington, D.C., 1961.

Antarctic ice reconnaissance operation DEEP FREEZE 61, Unpublished manuscript, U.S. Naval Oceanographic Office, Washington, D.C., 1961.

Operation DEEP FREEZE 61 (1960-1961) marine geophysical investigations, Tech. Rep. TR-105, 217pp., U.S. Naval Oceanographic Office, Washington, D.C., 1962.

Antarctic aerial ice observations October-December 1961, Informal Manuscript Rep. IMR. 0-29-62, U.S. Naval Oceanographic Office, Washington, D.C., Unpublished manuscript, 1962.

U.S. Naval Oceanographic Office:

Antarctic ice observations (October 1962-March 1963), Spec. Pub. SP-80 (62), 58pp., U.S. Naval Oceanographic Office, Washington, D.C., 1963.

Antarctic ice observations (October 1963-January 1964), Spec. Pub. SP-80 (63), 27pp., U.S. Naval Oceanographic Office, Washington, D.C., 1965.

Report of the Antarctic ice observing and forecasting program (1964), Spec. Pub. SP-80 (64), 31pp., U.S. Naval Oceanographic Office, Washington, D.C., 1966.

Report of the Antarctic ice observing and forecasting program (1965), Spec. Pub. SP-80 (65), 26pp., U.S. Naval Oceanographic Office, Washington, D.C., 1967.

Report of the Antarctic ice observing and forecasting program (1966), Spec. Pub. SP-80 (66), 28pp., U.S. Naval Oceanographic Office, Washington, D.C., 1967.

Perchal, R.J., Report of the Antarctic ice observing and forecasting program (1967), Spec. Pub. SP-80 (67), 36pp., U.S. Naval Oceanographic Office, Washington, D.C., 1969.

Potocsky, G.J., Report of the Antarctic ice observing and forecasting program (1968), Spec. Pub. SP-80 (68), 28pp., U.S. Naval Oceanographic Office, Washington, D.C., 1969.

Perchal, R.J., Report of the Antarctic ice observing and forecasting program (1969), Spec. Pub. SP-80 (69), 125pp., U.S. Naval Oceanographic Office, Washington, D.C., 1971.

U.S. Naval Weather Research Facility, Notes on Antarctic weather analysis and forecasting, NWRF-16-1260-038, 71pp., December 1960.

Wexler, H., Heating and melting of floating ice shelves, J. of Glac., 3, 626,1960.

Wittmann, W.I. and G.P. MacDowell, Manual of short-term sea ice forecasting, Spec. Pub. SP-82, 142 pp., U.S. Naval Oceanographic Office, Washington, D.C., 1964.

Zubov, N.N., L'dy Arktiki (Arctic Ice). Northern Sea Route Directorate Press, Moscow 1945, Translation, 491pp., U.S. Naval Oceanographic Office, Washington, D.C.

Zumberge, J.H. and C. Swithinbank, The dynamics of ice shelves, Am. Geophys. Union, Geophys. Monograph 7, 197, 1962.
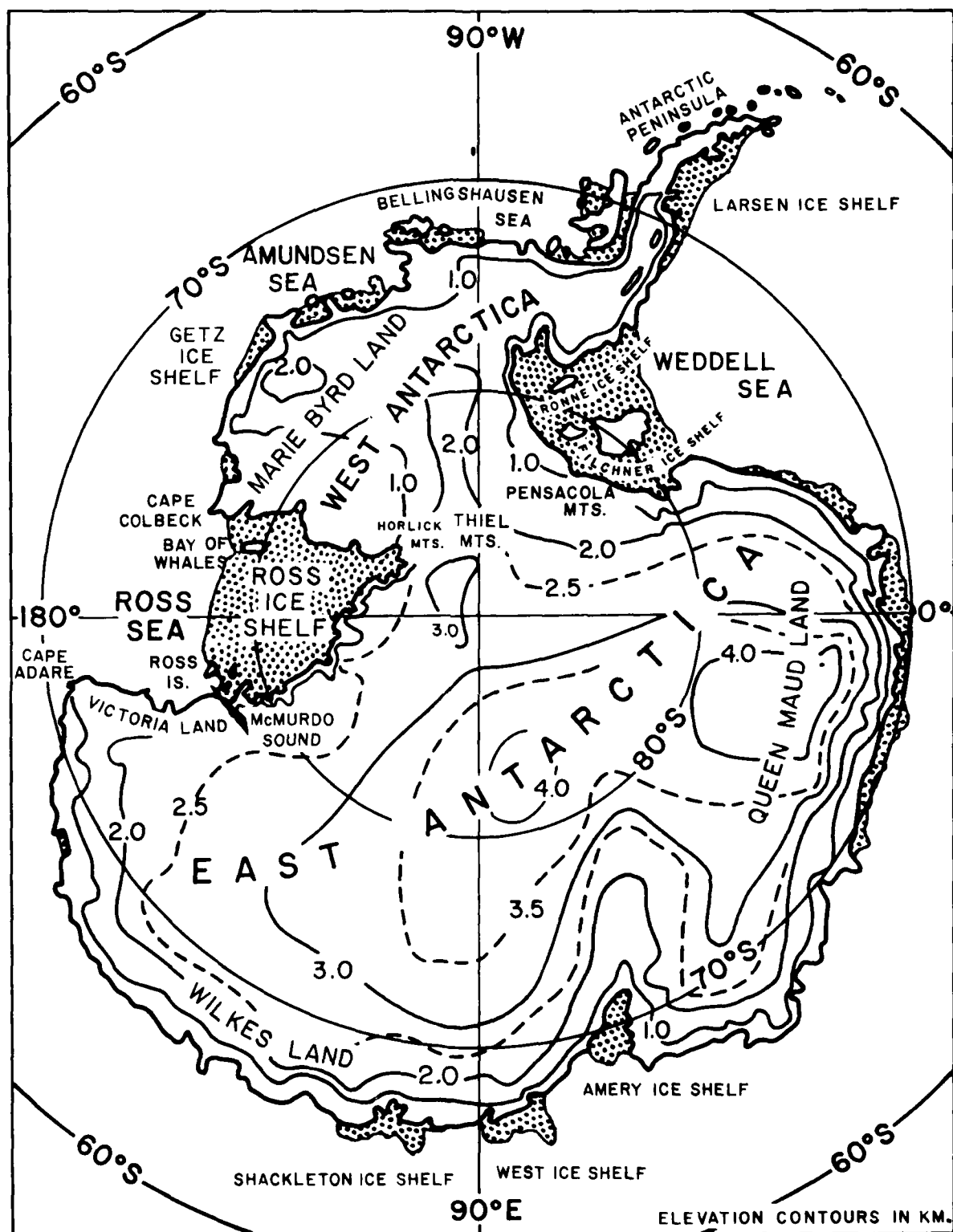
FIGURE I. ANTARCTIC PLACE NAMES
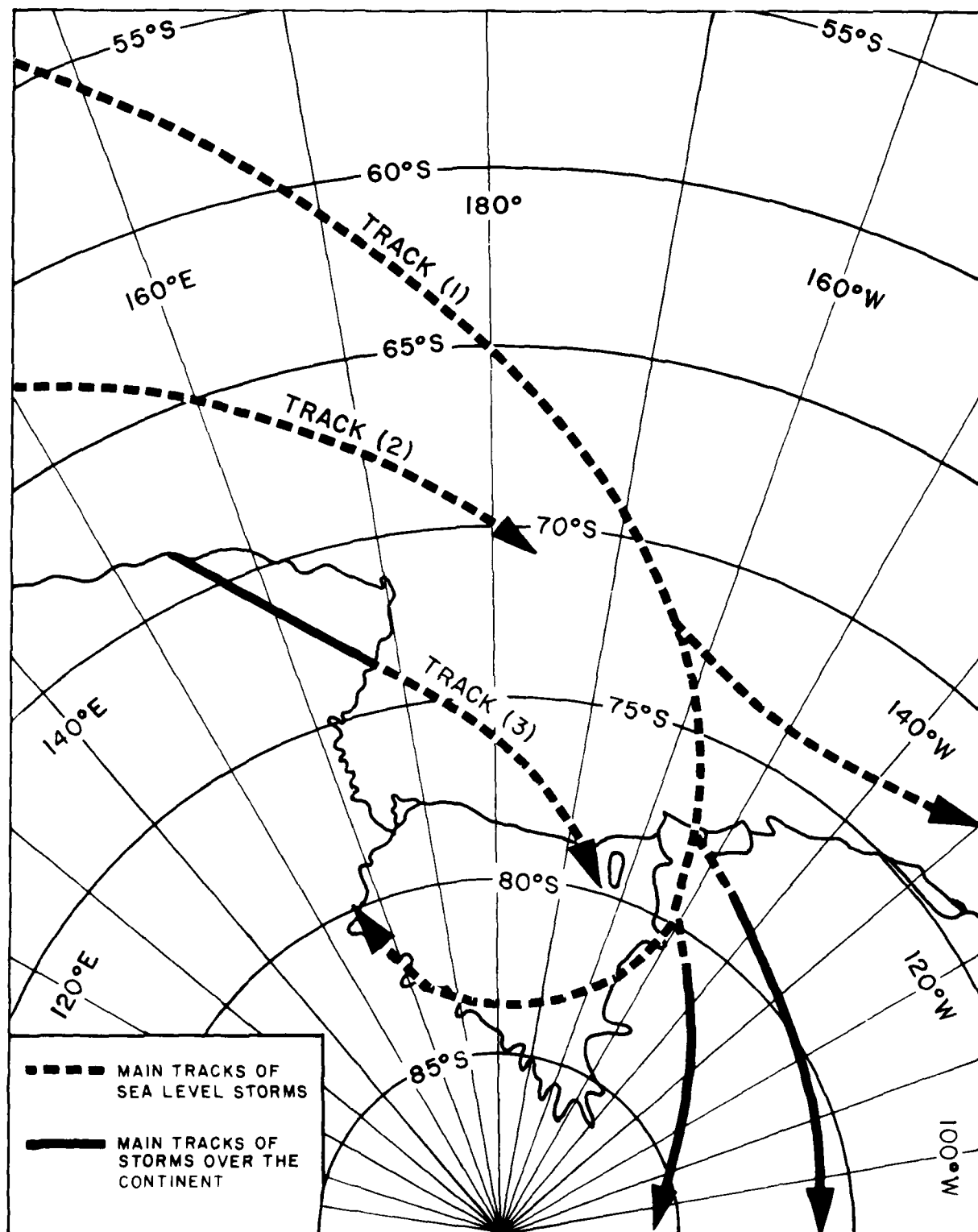
FIGURE 2. PRINCIPAL STORM TRACKS IN THE ROSS SEA
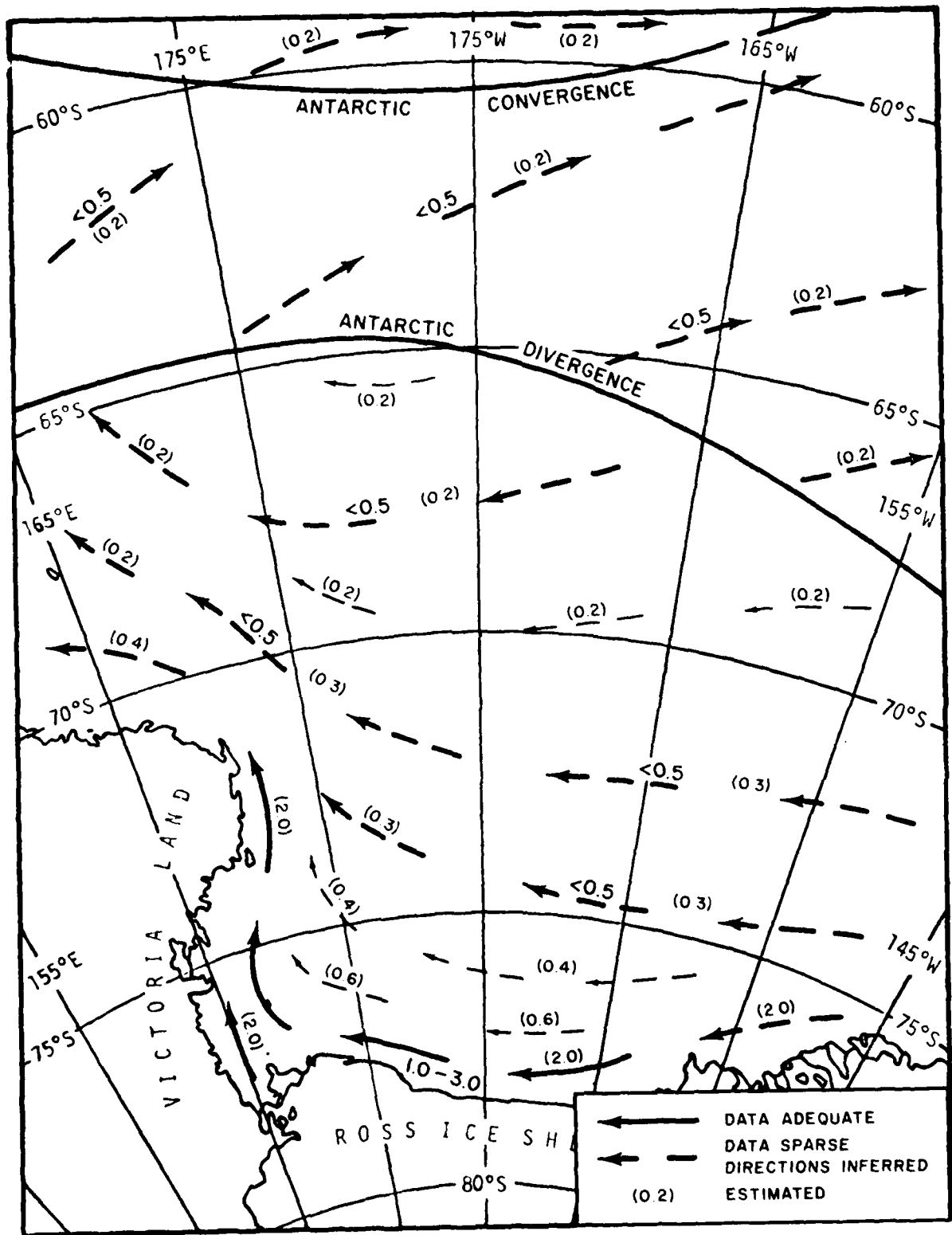
FIGURE 3. GENERAL SURFACE CURRENTS (KN)
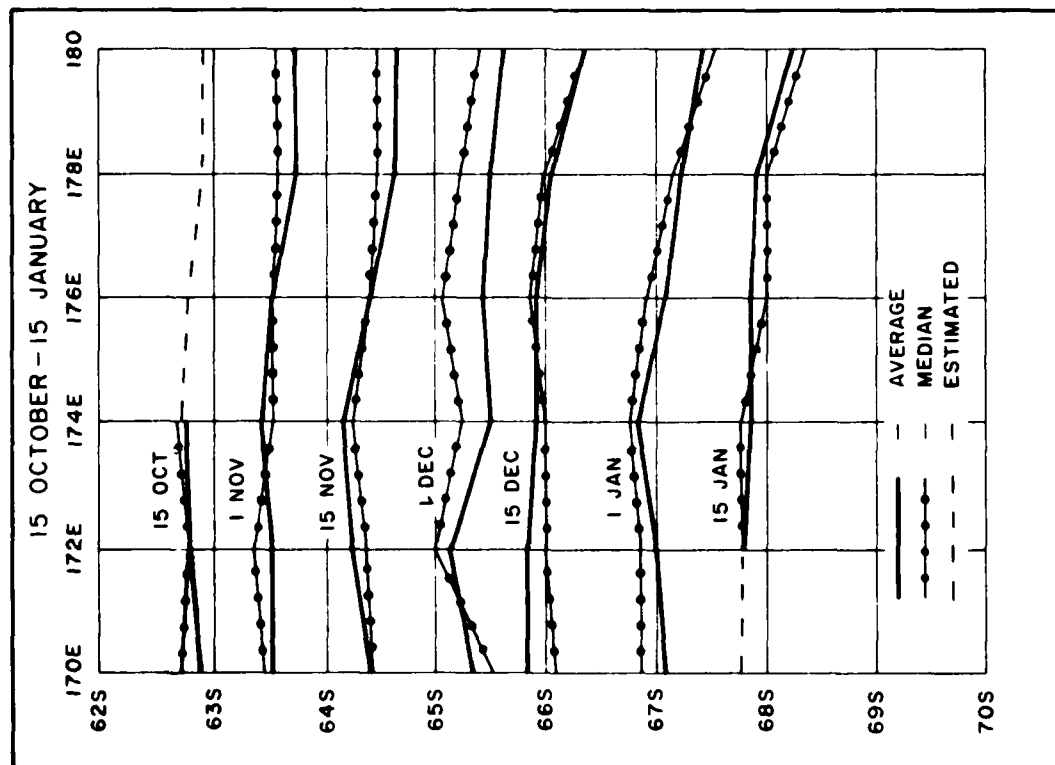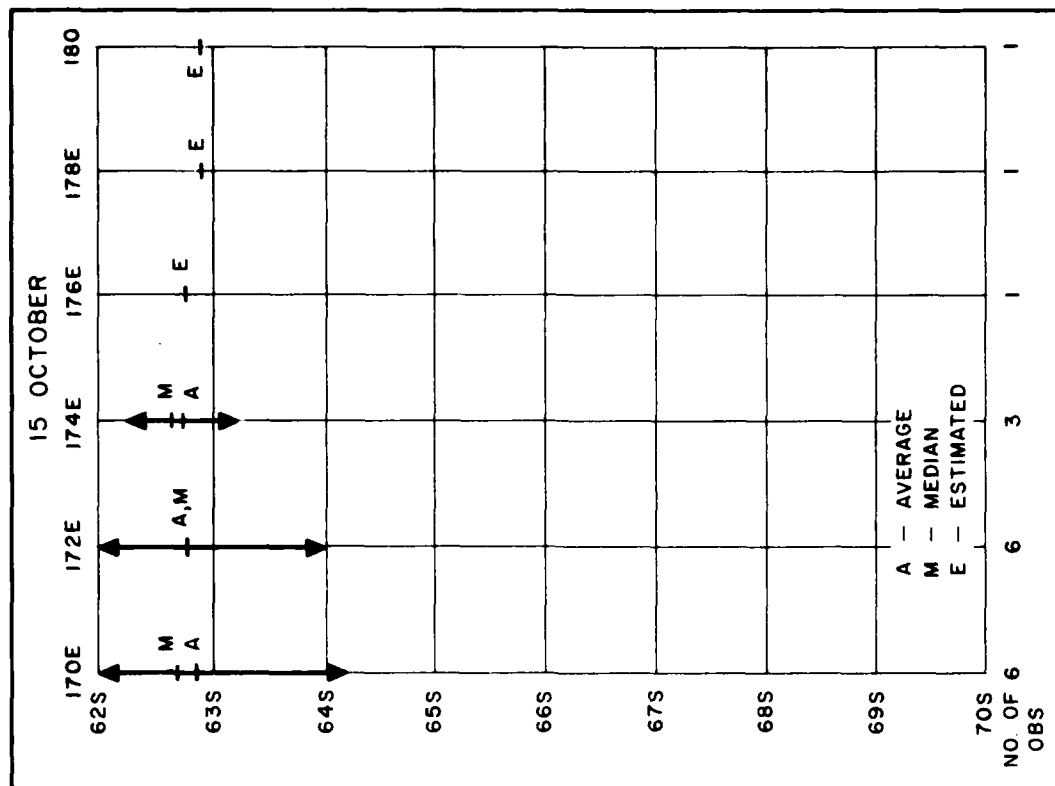
FIGURE 5. AVERAGE, MEDIAN, AND LATITUDE RANGES OF THE NORTH PACK EDGE, WESTERN ROSS SEA, 15 OCTOBER (DF I – DF 71).

FIGURE 4. AVERAGE AND MEDIAN LATITUDES OF THE NORTH PACK EDGE, WESTERN ROSS SEA, 15 OCTOBER – 15 JANUARY (DF I – DF 71).

66
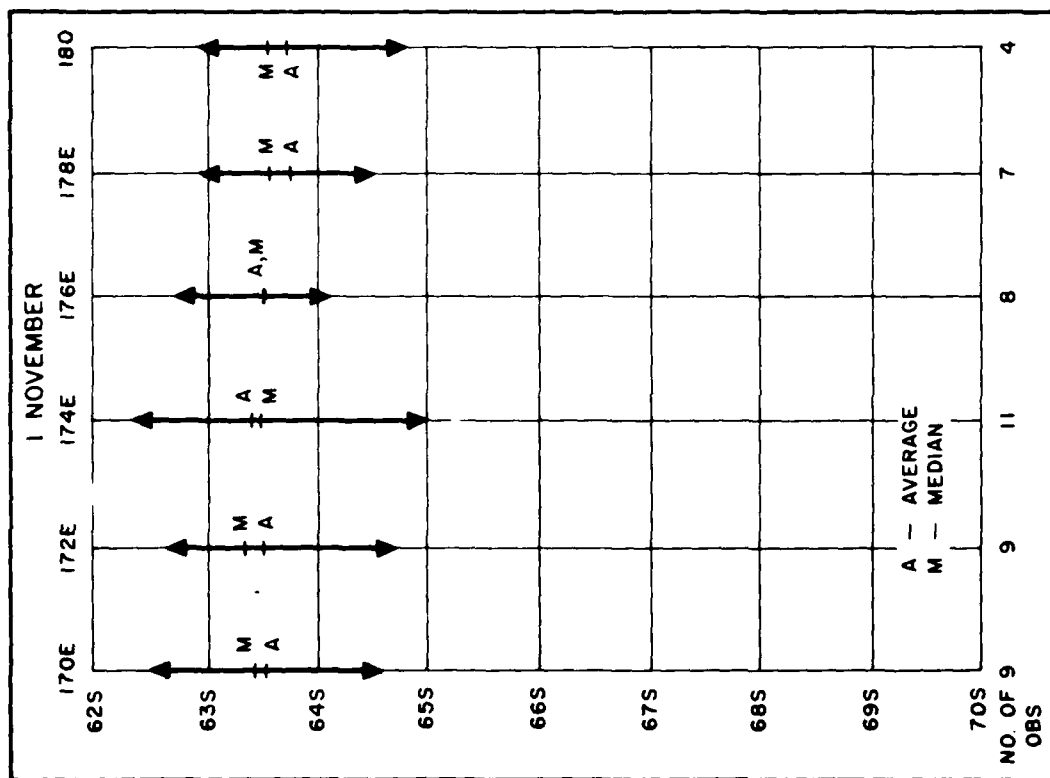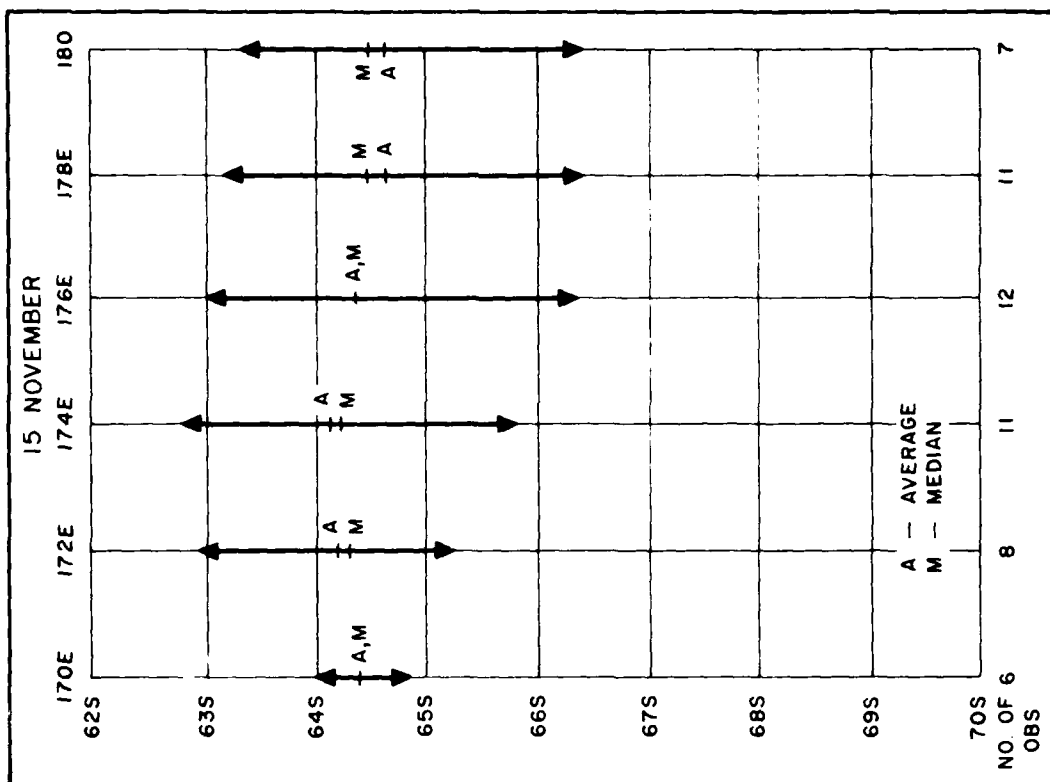
FIGURE 6. AVERAGE, MEDIAN, AND LATITUDE RANGES OF THE NORTH PACK EDGE, WESTERN ROSS SEA, 1 NOVEMBER, 15 NOVEMBER (DF I – DF 71).
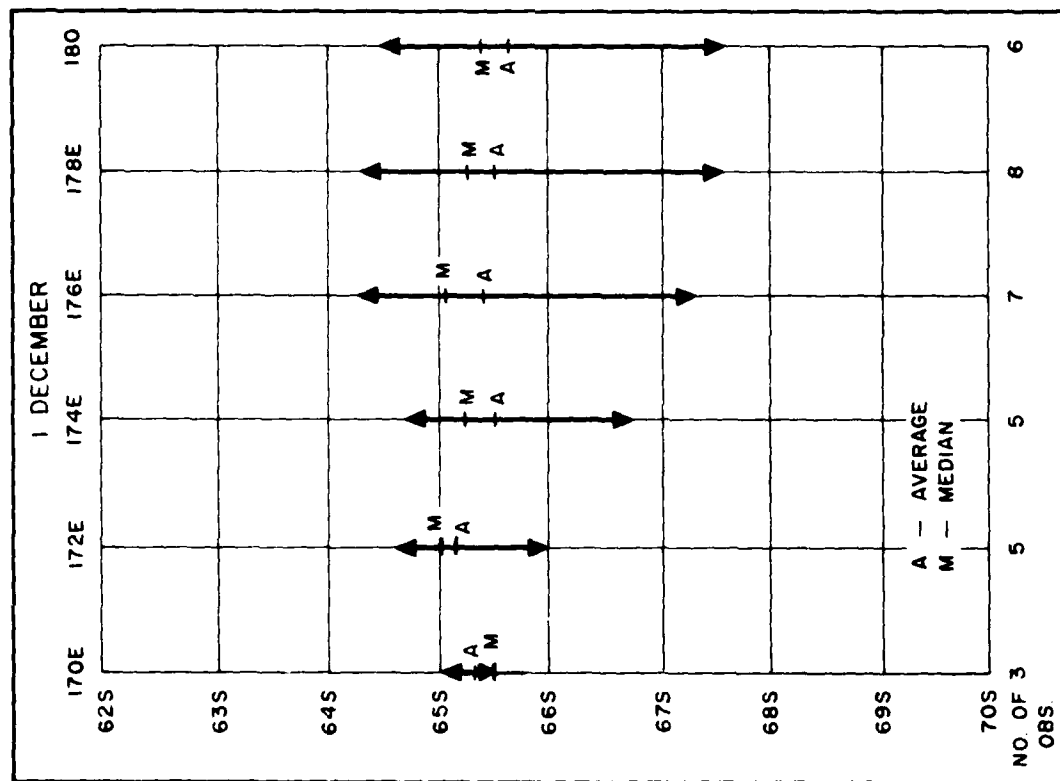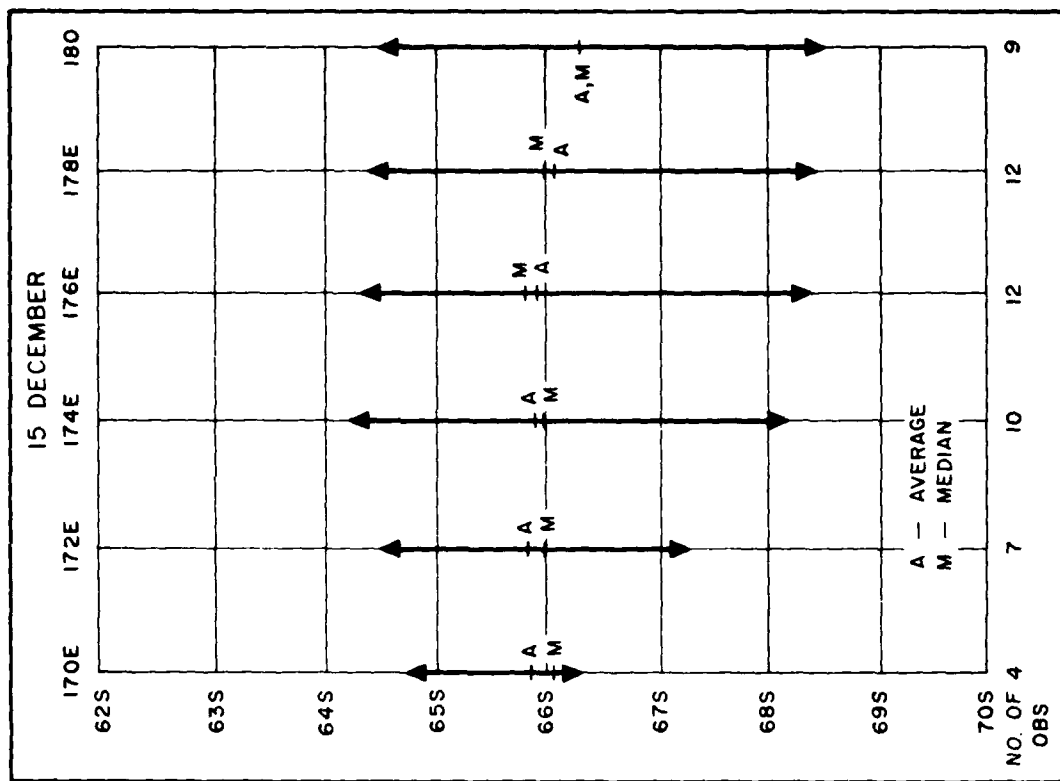
FIGURE 7. AVERAGE, MEDIAN, AND LATITUDE RANGES OF THE NORTH PACK EDGE, WESTERN ROSS SEA, 1 DECEMBER, 15 DECEMBER (DF I – DF 71).
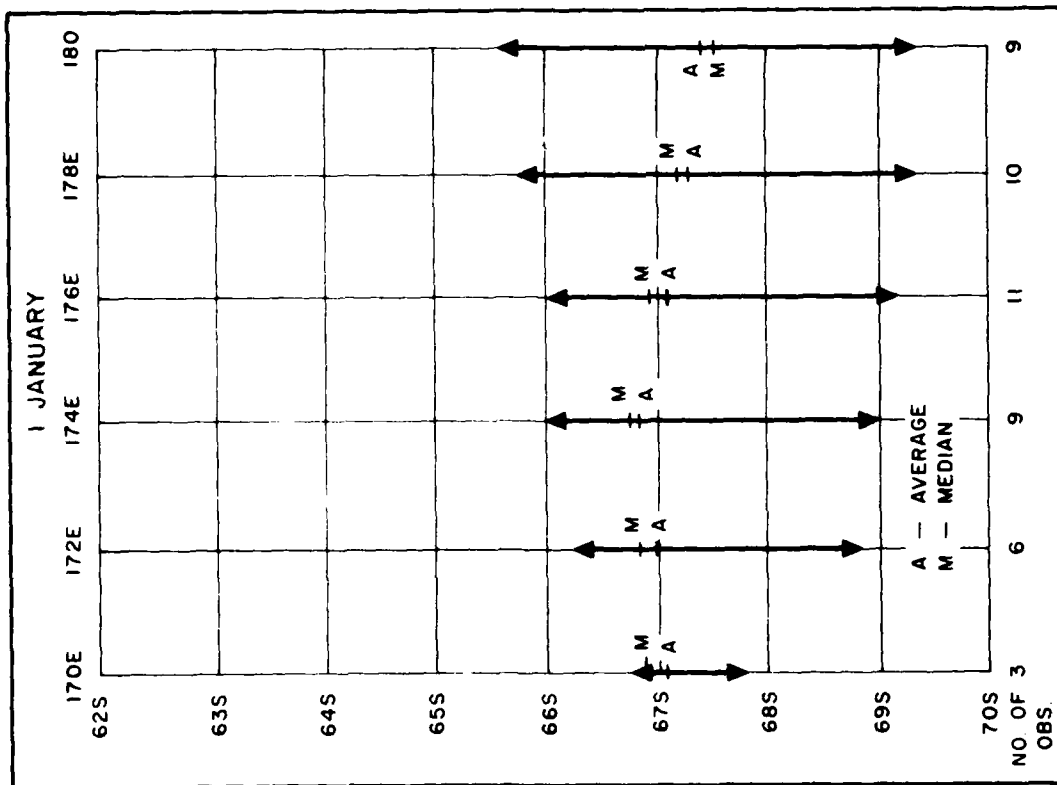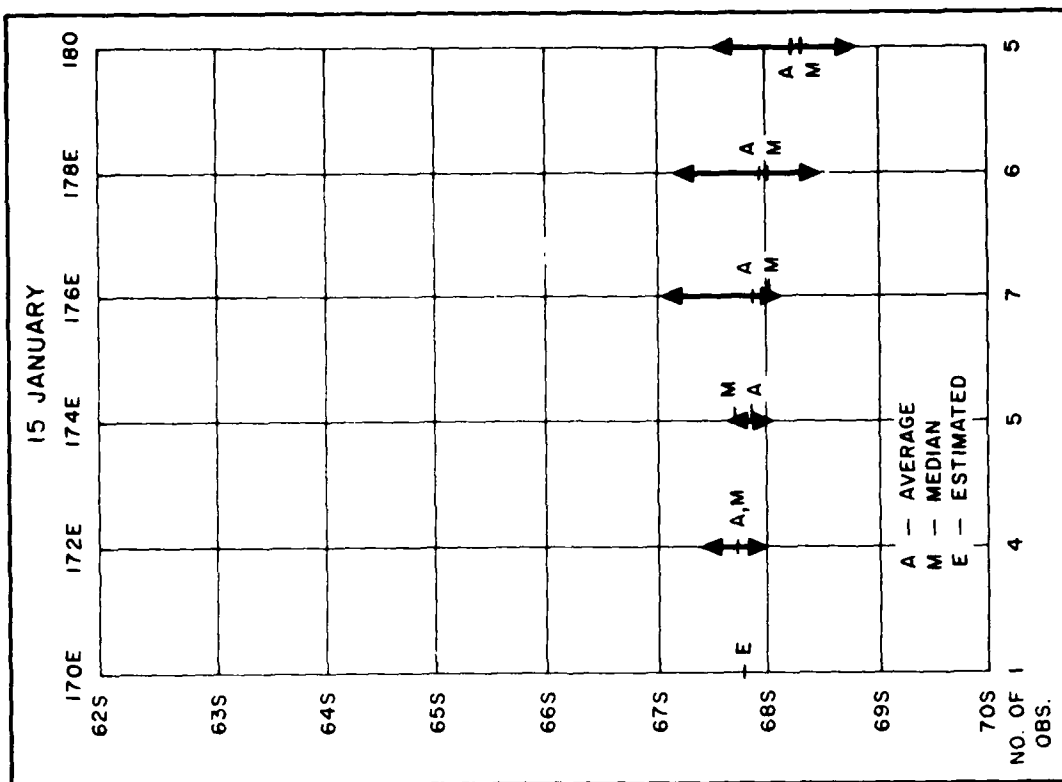
FIGURE 8. AVERAGE, MEDIAN, AND LATITUDE RANGES OF THE NORTH PACK EDGE, WESTERN ROSS SEA, 1 JANUARY, 15 JANUARY (DF I – DF 71).
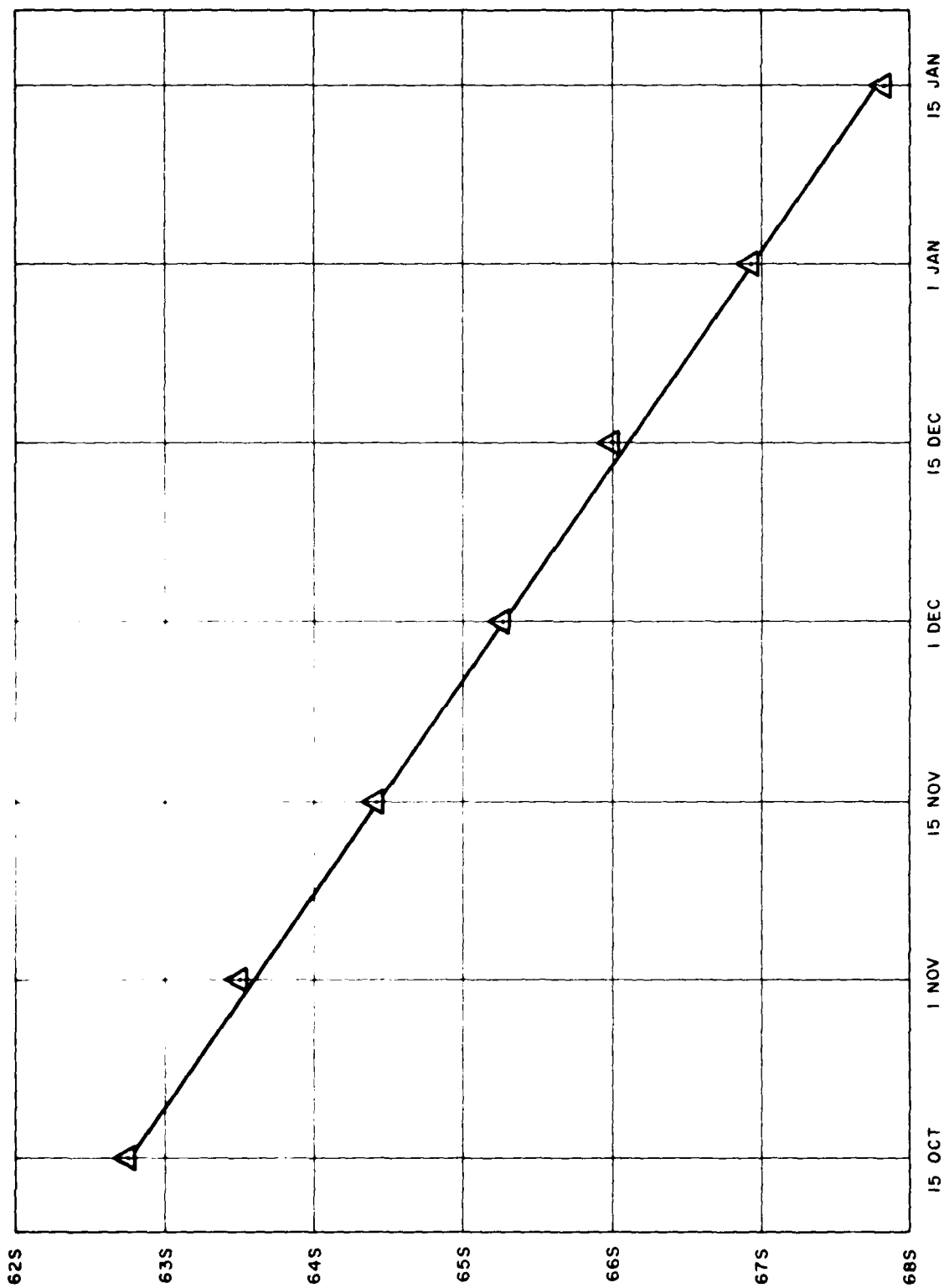
FIGURE 9. OVERALL NORTH PACK EDGE RECESSION, WESTERN ROSS SEA,
15 OCTOBER – 15 JANUARY (DF I – DF 71).

FIGURE 11. AVERAGE, MEDIAN, AND LATITUDE
RANGES OF THE SOUTH PACK EDGE,
WESTERN ROSS SEA, 15 NOVEMBER
(DF I – DF 71).
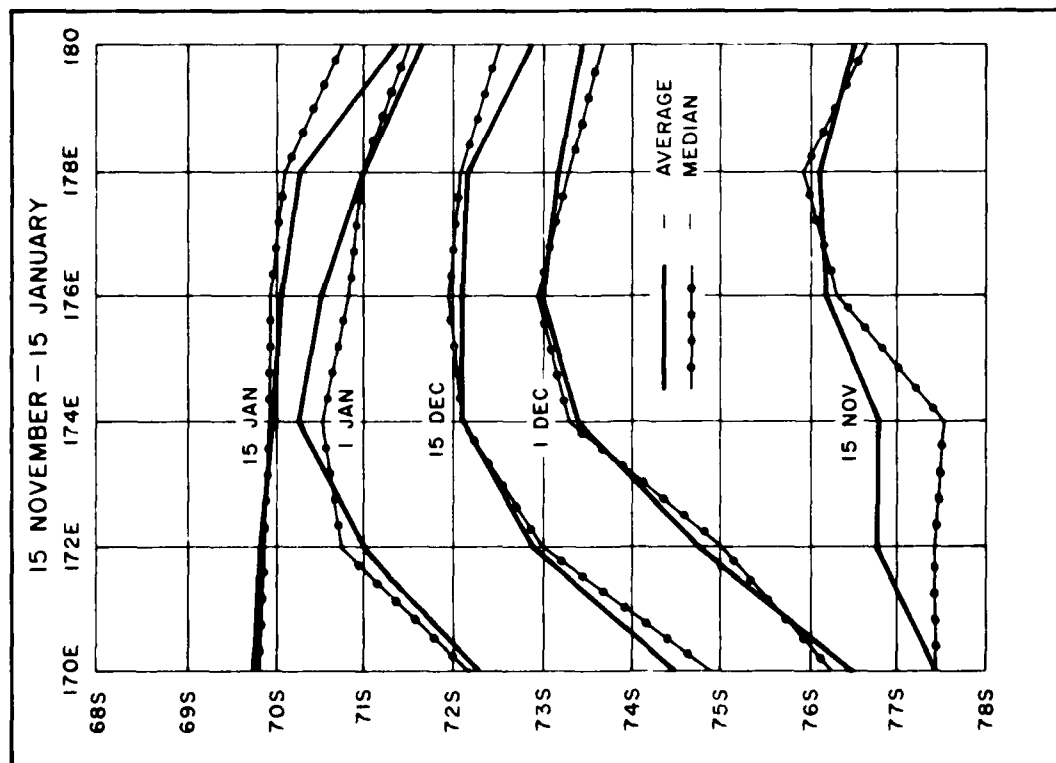
FIGURE 10. AVERAGE AND MEDIAN LATITUDES
OF THE SOUTH PACK EDGE, WESTERN
ROSS SEA, 15 NOVEMBER – 15 JANUARY
(DF I – DF 71)
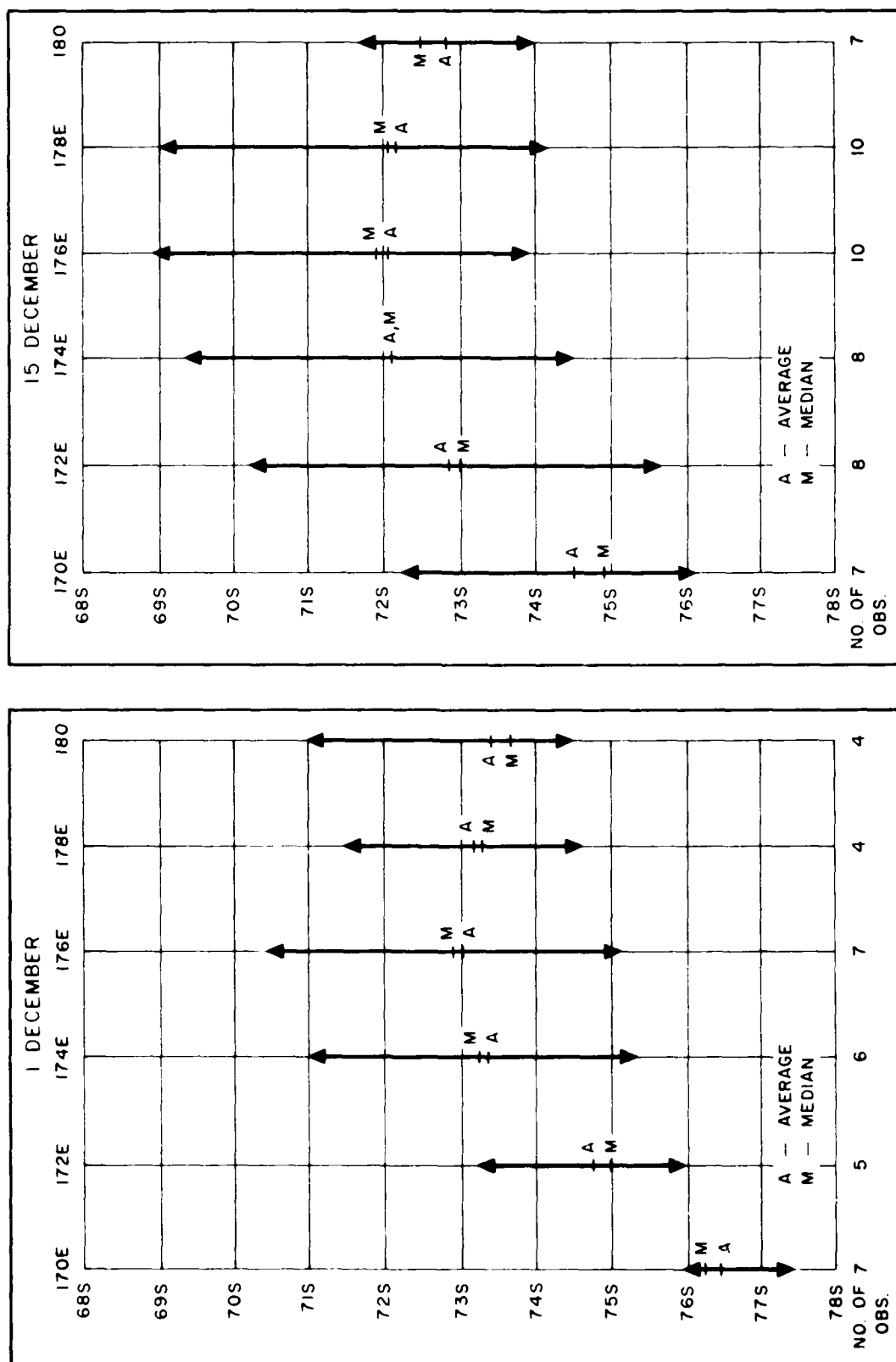
FIGURE 12. AVERAGE, MEDIAN, AND LATITUDE RANGES OF THE SOUTH PACK EDGE, WESTERN ROSS SEA, 1 DECEMBER, 15 DECEMBER (DF 1—DF 71)

72
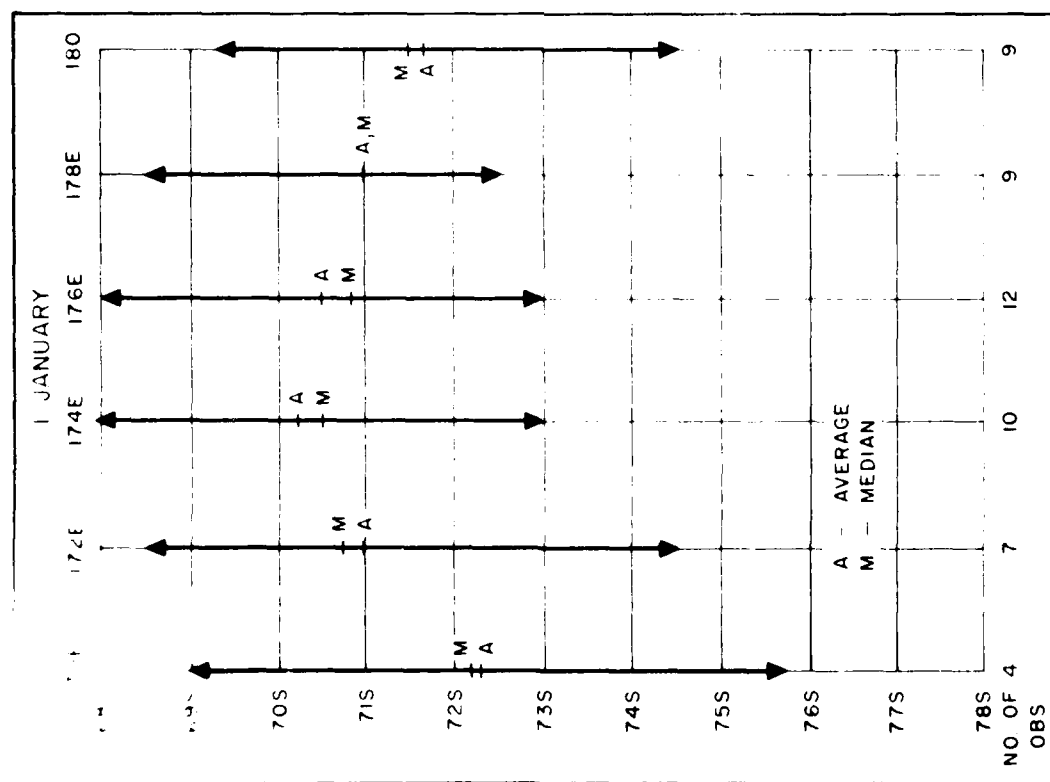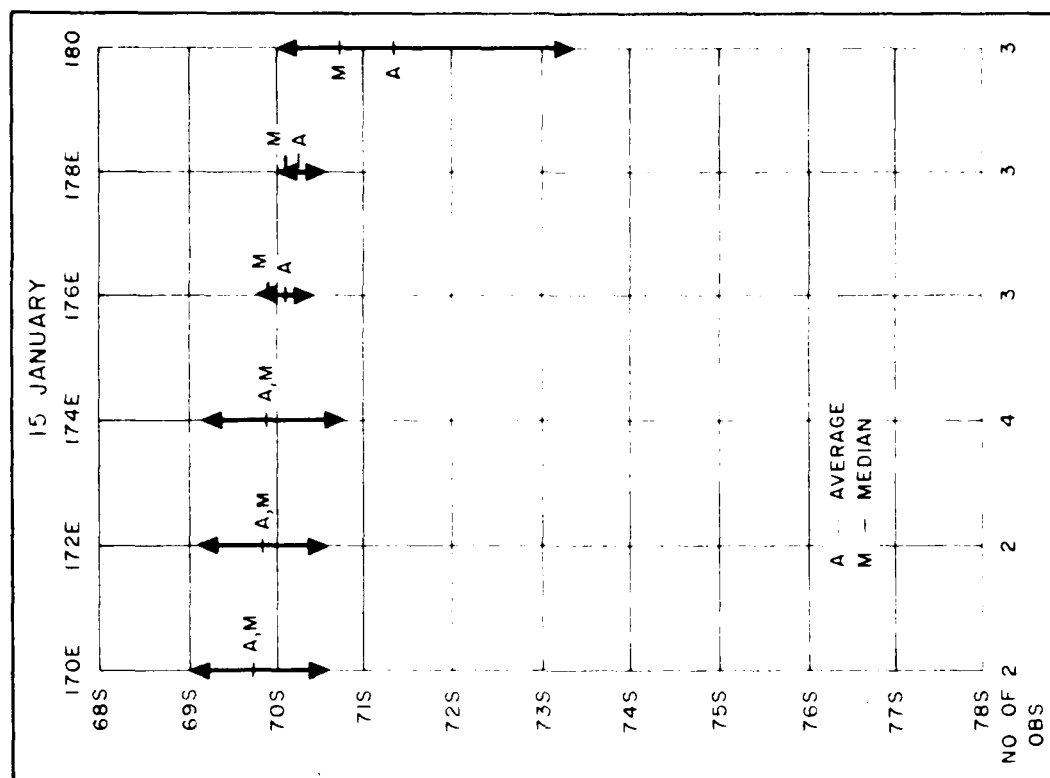
FIGURE 13 AVERAGE, MEDIAN, AND LATITUDE RANGES OF THE SOUTH PACK EDGE, WESTERN ROSS SEA,
1 JANUARY, 15 JANUARY (DF I – DF 71)

73
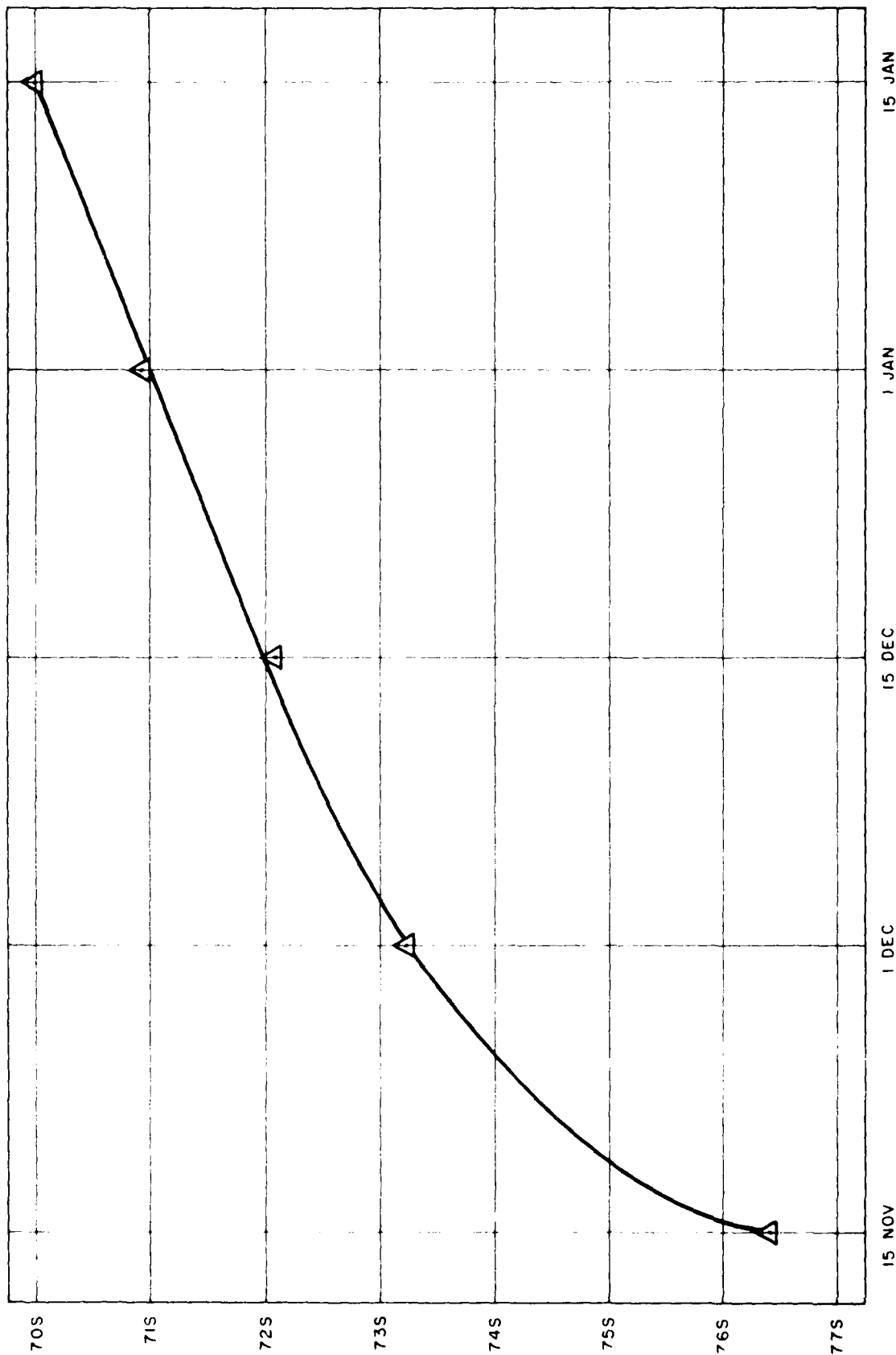
FIGURE 14 OVERALL SOUTH PACK EDGE RECESSION, WESTERN ROSS SEA
15 NOVEMBER – 15 JANUARY (DF I – DF 71)

74
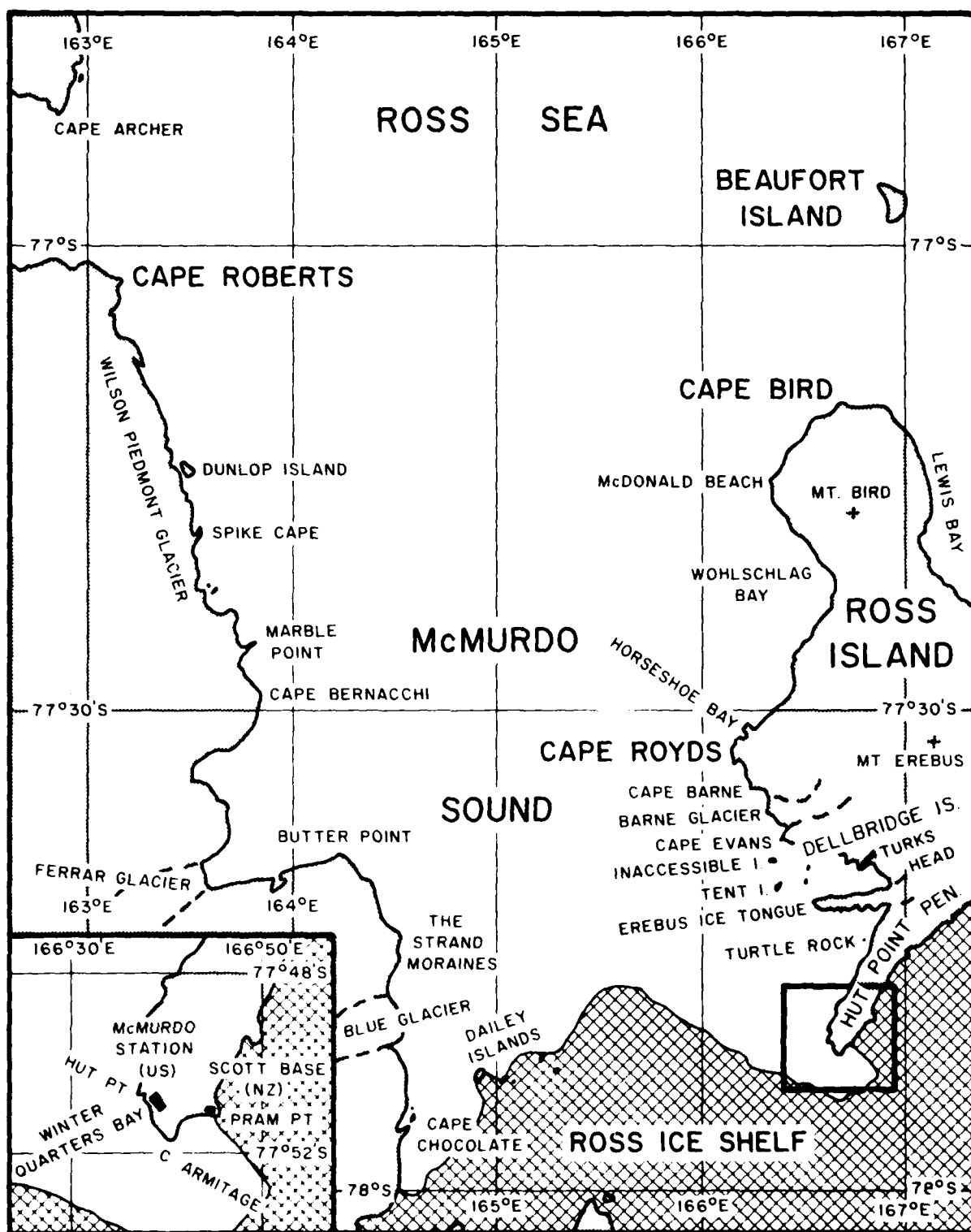
FIGURE 15 PLACE NAMES, McMURDO SOUND

Map labels:

ROSS SEA

CAPE ARCHER

163°E 164°E 165°E 166°E 167°E

BEAUFORT ISLAND

77°S 77°S

CAPE ROBERTS

CAPE BIRD

WILSON PIEDMONT GLACIER

DUNLOP ISLAND

McDONALD BEACH MT. BIRD

SPIKE CAPE

LEWIS BAY

WOHLSCHLAG BAY

ROSS ISLAND

MARBLE POINT

McMURDO

HORSESHOE BAY

CAPE BERNACCHI

77°30'S 77°30'S

CAPE ROYDS MT EREBUS

SOUND CAPE BARNE
BARNE GLACIER
CAPE EVANS DELLBRIDGE IS.
INACCESSIBLE I. TURKS
TENT I. HEAD
EREBUS ICE TONGUE
TURTLE ROCK

BUTTER POINT

FERRAR GLACIER
163°E 164°E

THE STRAND MORAINES

166°30'E 166°50'E
77°48'S
BLUE GLACIER
DAILEY ISLANDS
HUT POINT PEN.

McMURDO STATION (US)
HUT PT
SCOTT BASE (NZ)
WINTER QUARTERS BAY
PRAM PT
C ARMITAGE
77°52'S

CAPE CHOCOLATE
ROSS ICE SHELF

78°S 78°S
165°E 166°E 167°E

75

FIGURE 16. FAST-ICE EXTENT IN THE APPROACHES TO McMURDO STATION (DF I – DF 60).
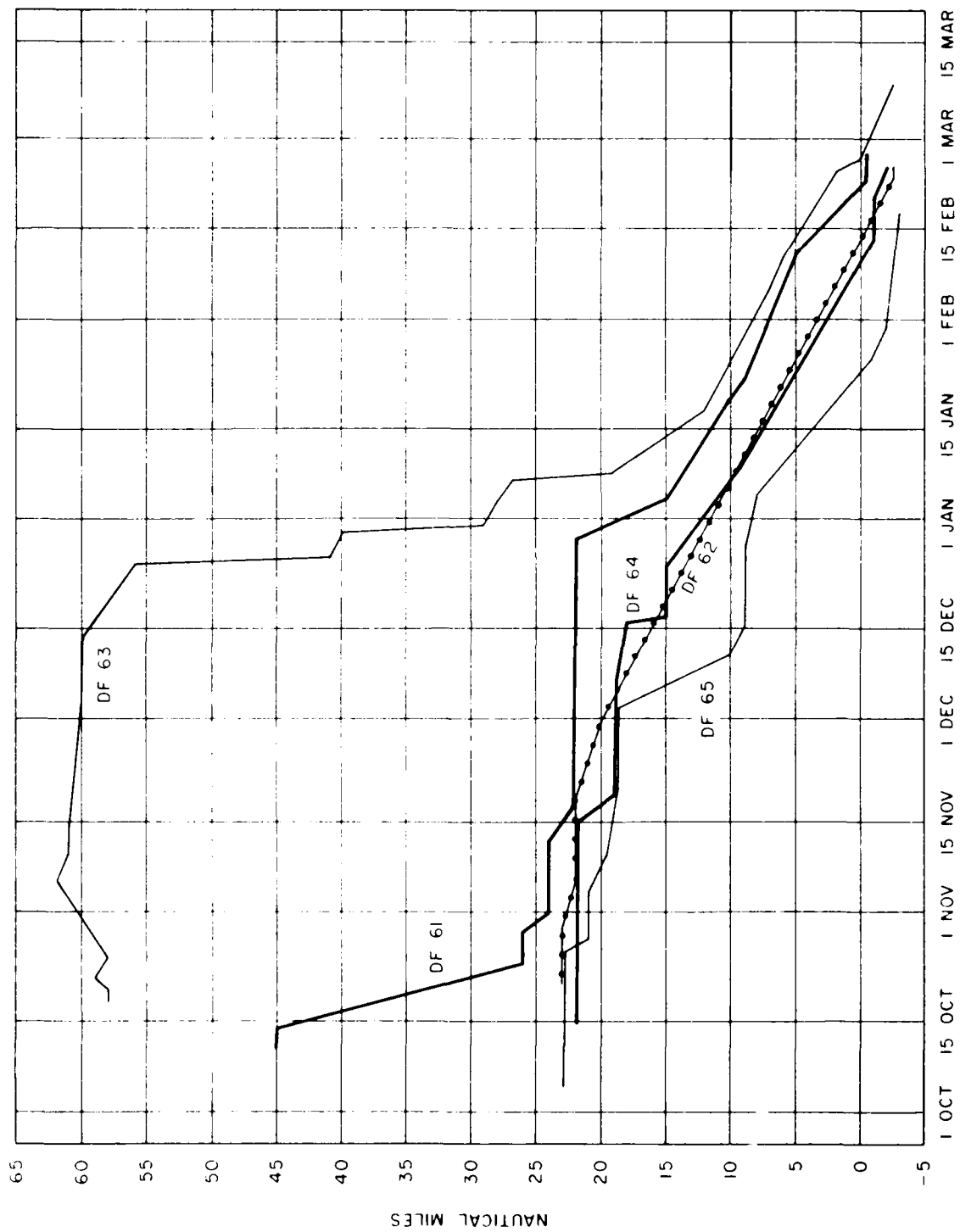
FIGURE 17 FAST-ICE EXTENT IN THE APPROACHES TO McMURDO STATION (DF 61–DF 65).

77
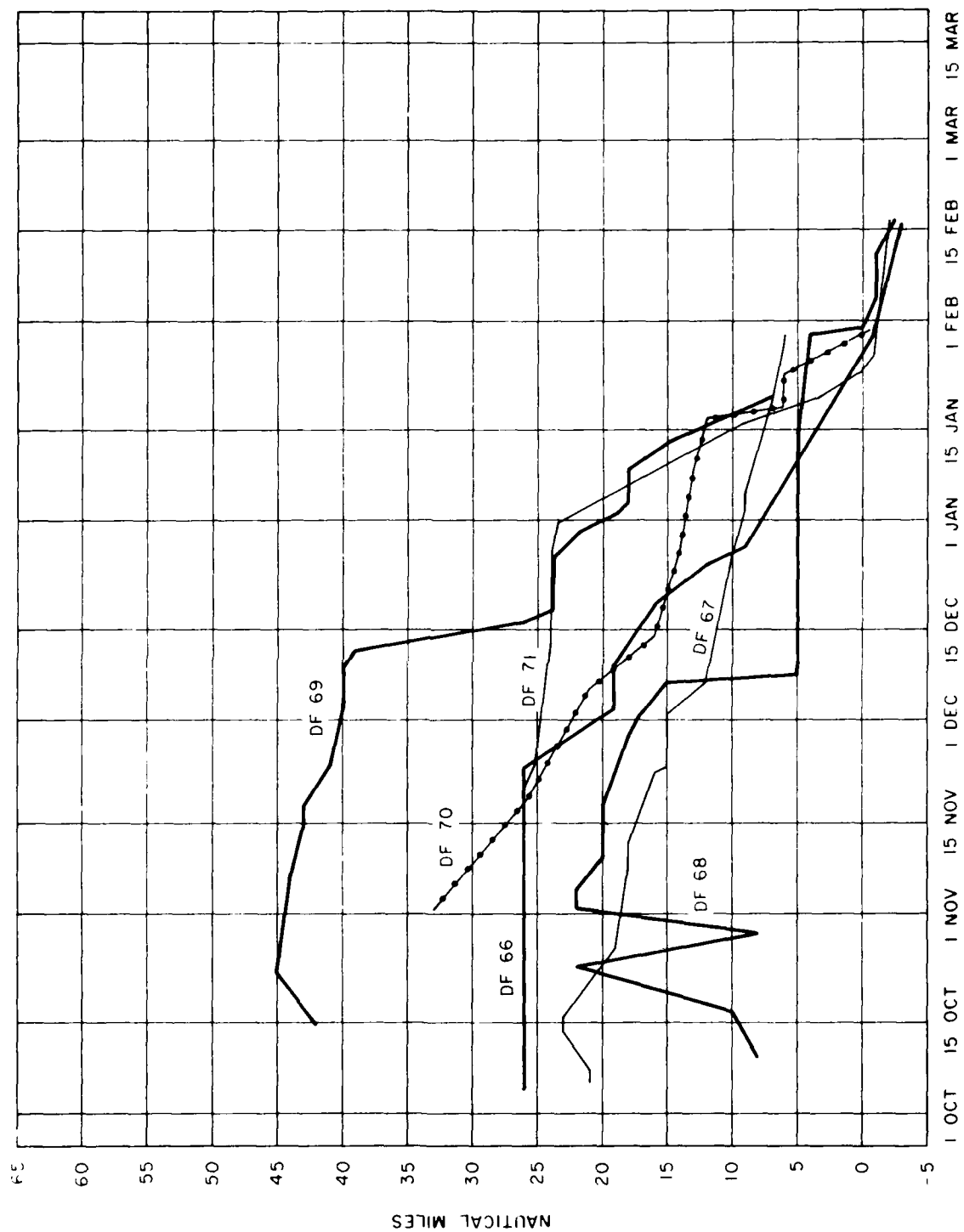
FIGURE 18. FAST-ICE EXTENT IN THE APPROACHES TO McMURDO STATION (DF 66 – DF 71).

78
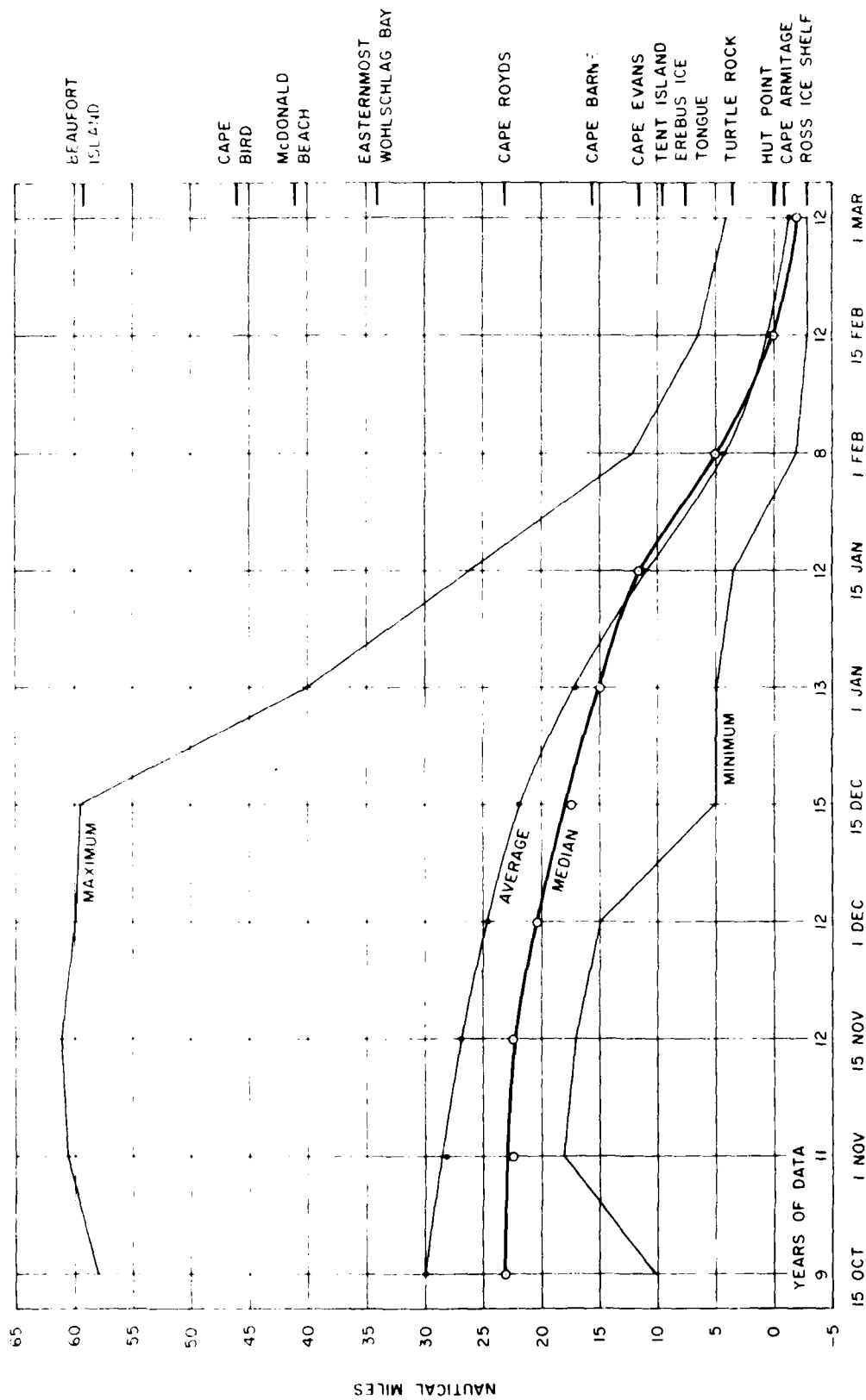
FIGURE 19. AVERAGE, MEDIAN, MAXIMUM, AND MINIMUM EXTENTS OF FAST ICE AT HALF-MONTHLY INTERVALS IN THE APPROACHES TO McMURDO STATION (DF I - DF 71).
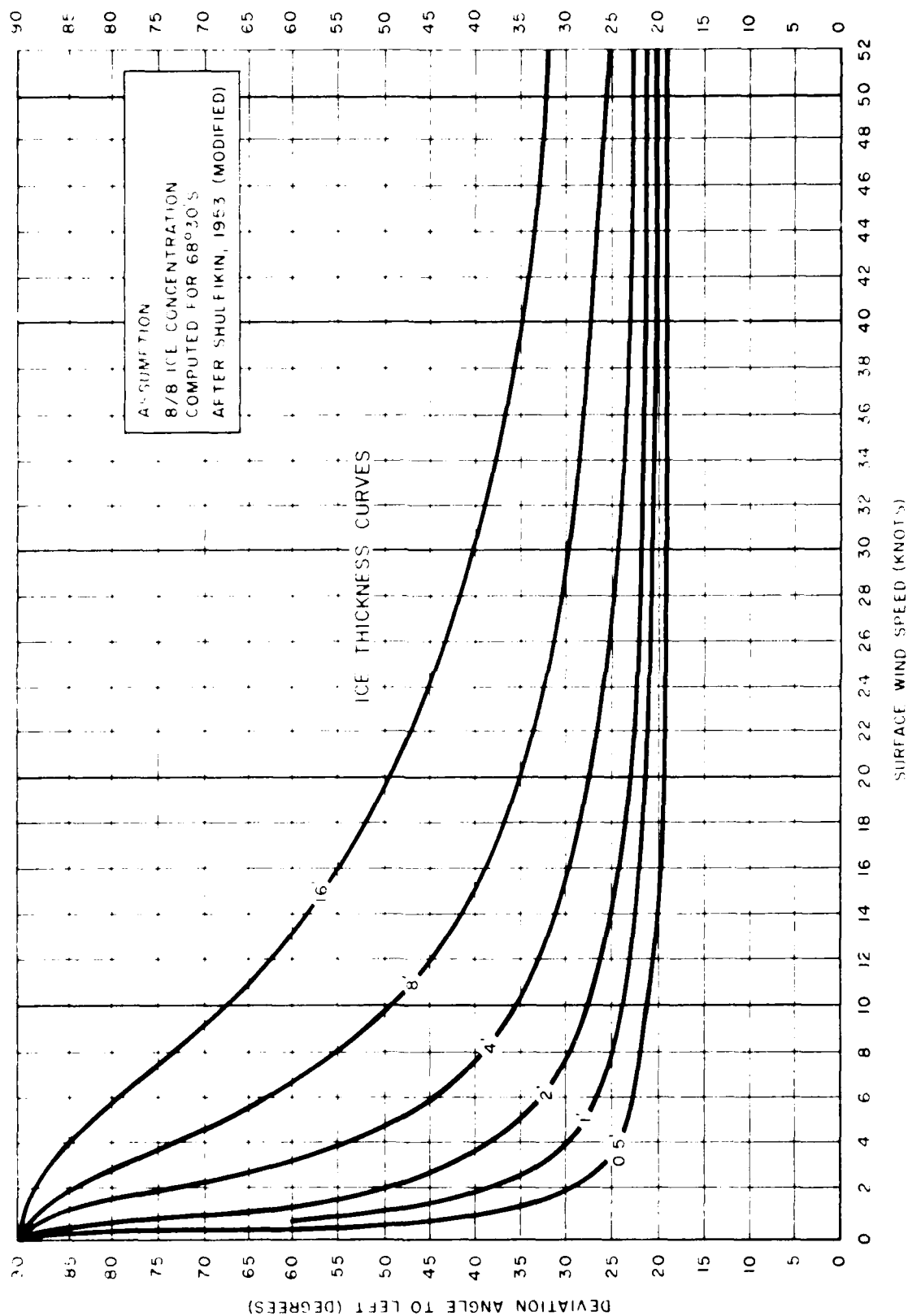
FIGURE 20 ICE DRIFT DIRECTION FOR VARYING WIND SPEED AND ICE THICKNESS.
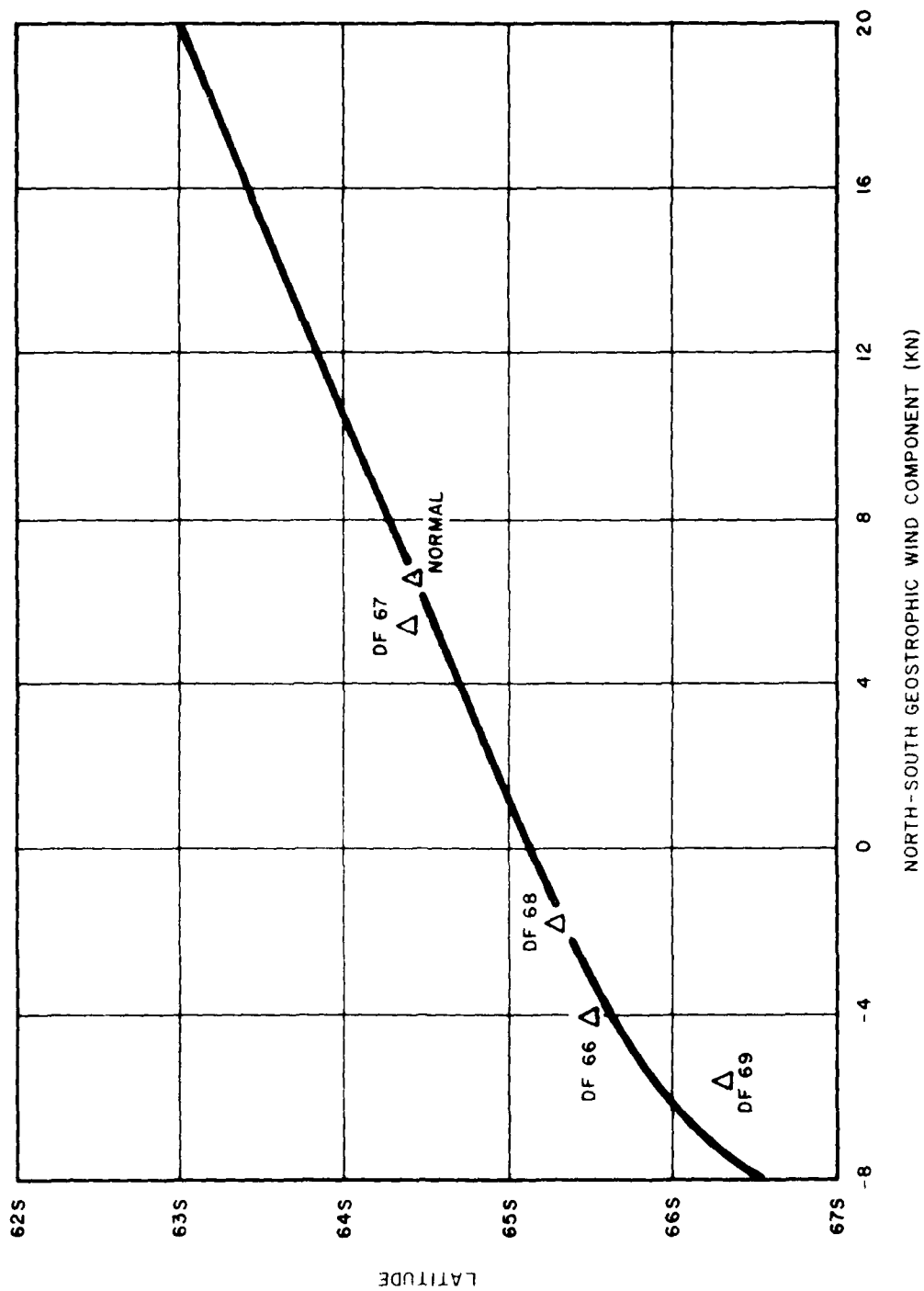
FIGURE 21. AVERAGE 15-DAY NORTH (−) — SOUTH (+) GEOSTROPHIC WIND COMPONENT, MID-JULY TO MID-SEPTEMBER AT 70°S, 175°E RELATED TO LATITUDE OF THE NORTH PACK EDGE ON 15 NOVEMBER.
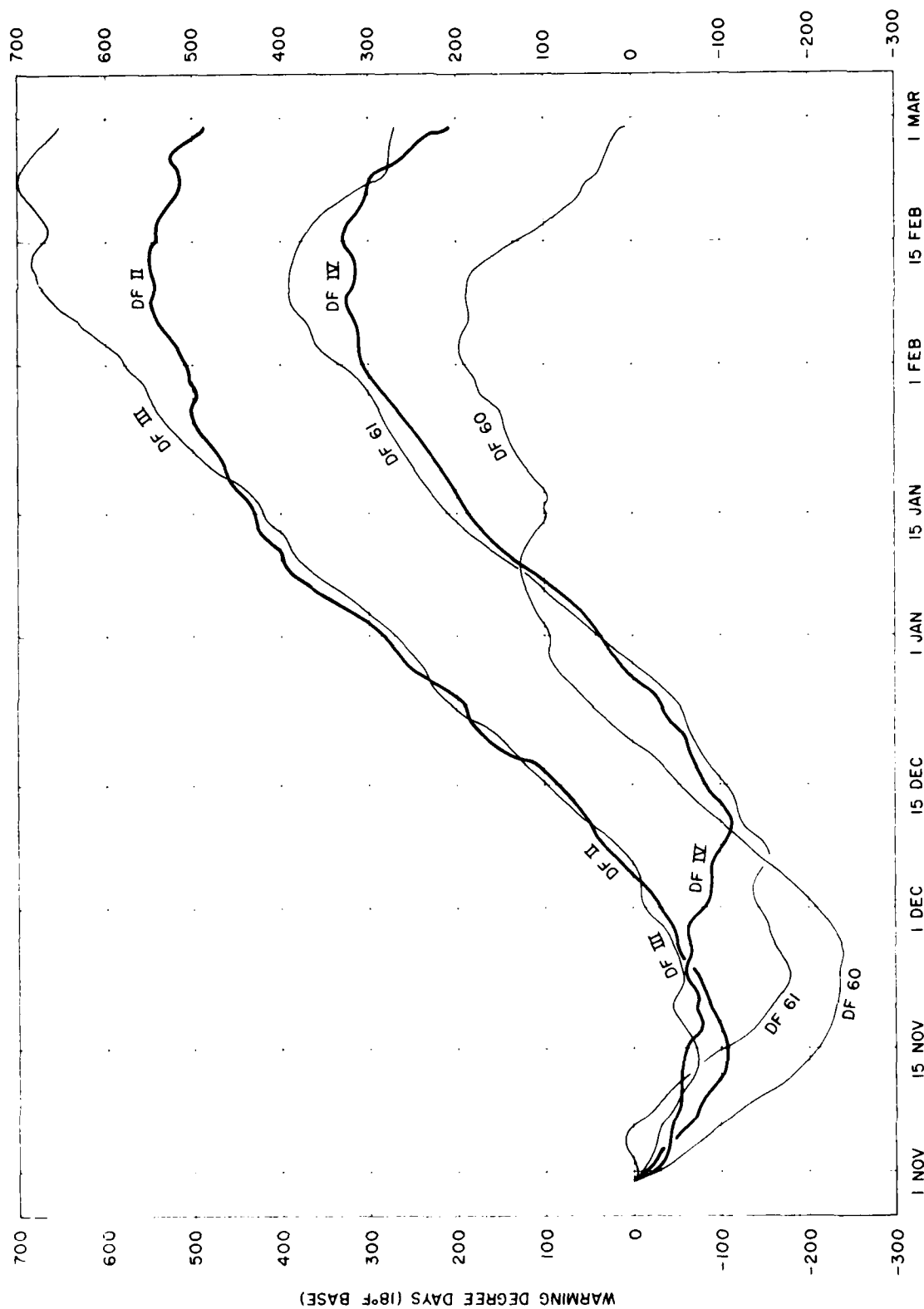
FIGURE 22. ACCUMULATED WARMING DEGREE DAYS AT McMURDO STATION (DF II – DF 61)

WARMING DEGREE DAYS (18°F BASE)
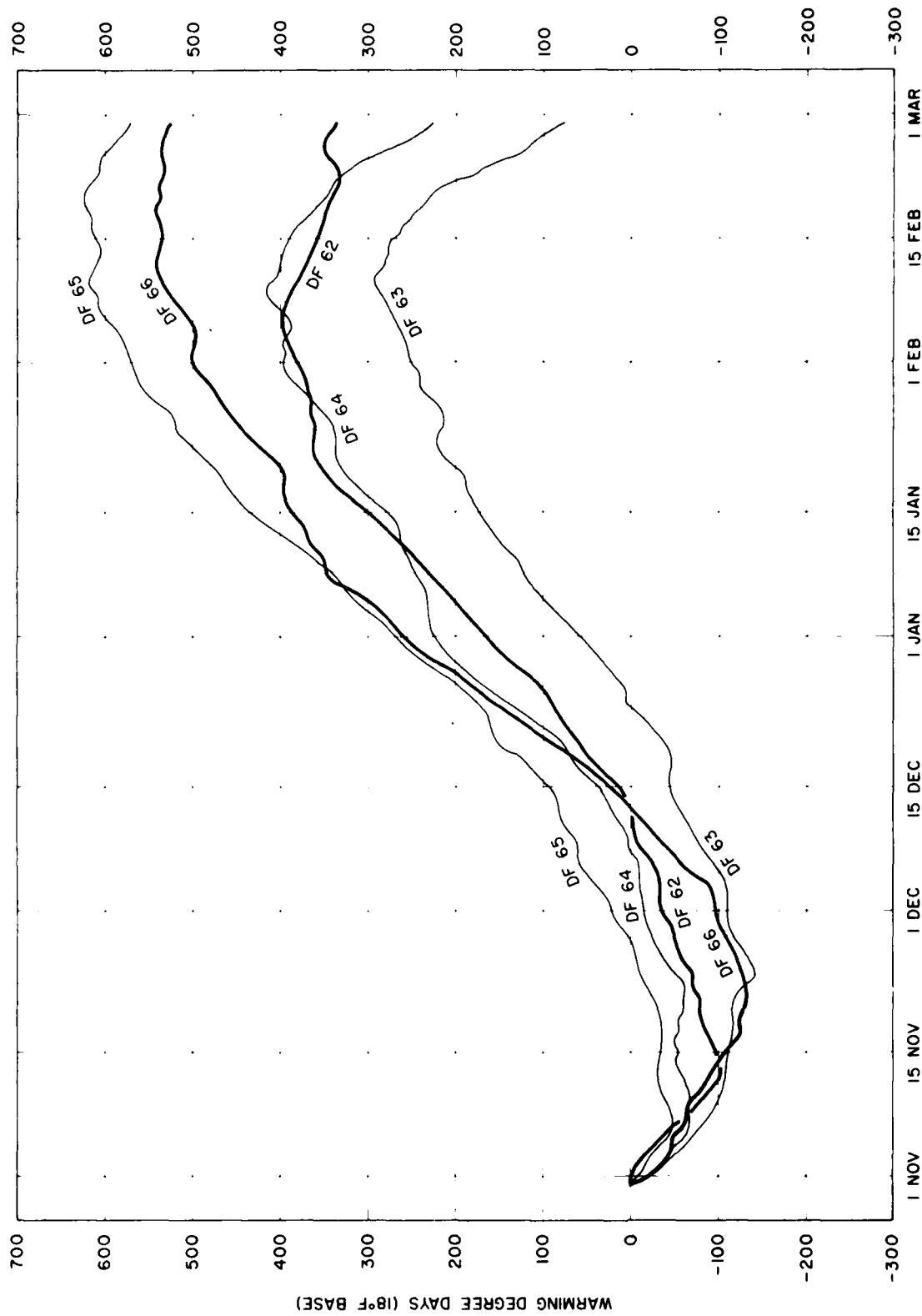
FIGURE 23. ACCUMULATED WARMING DEGREE DAYS AT McMURDO STATION (DF 62 – DF 66).

WARMING DEGREE DAYS (18°F BASE)
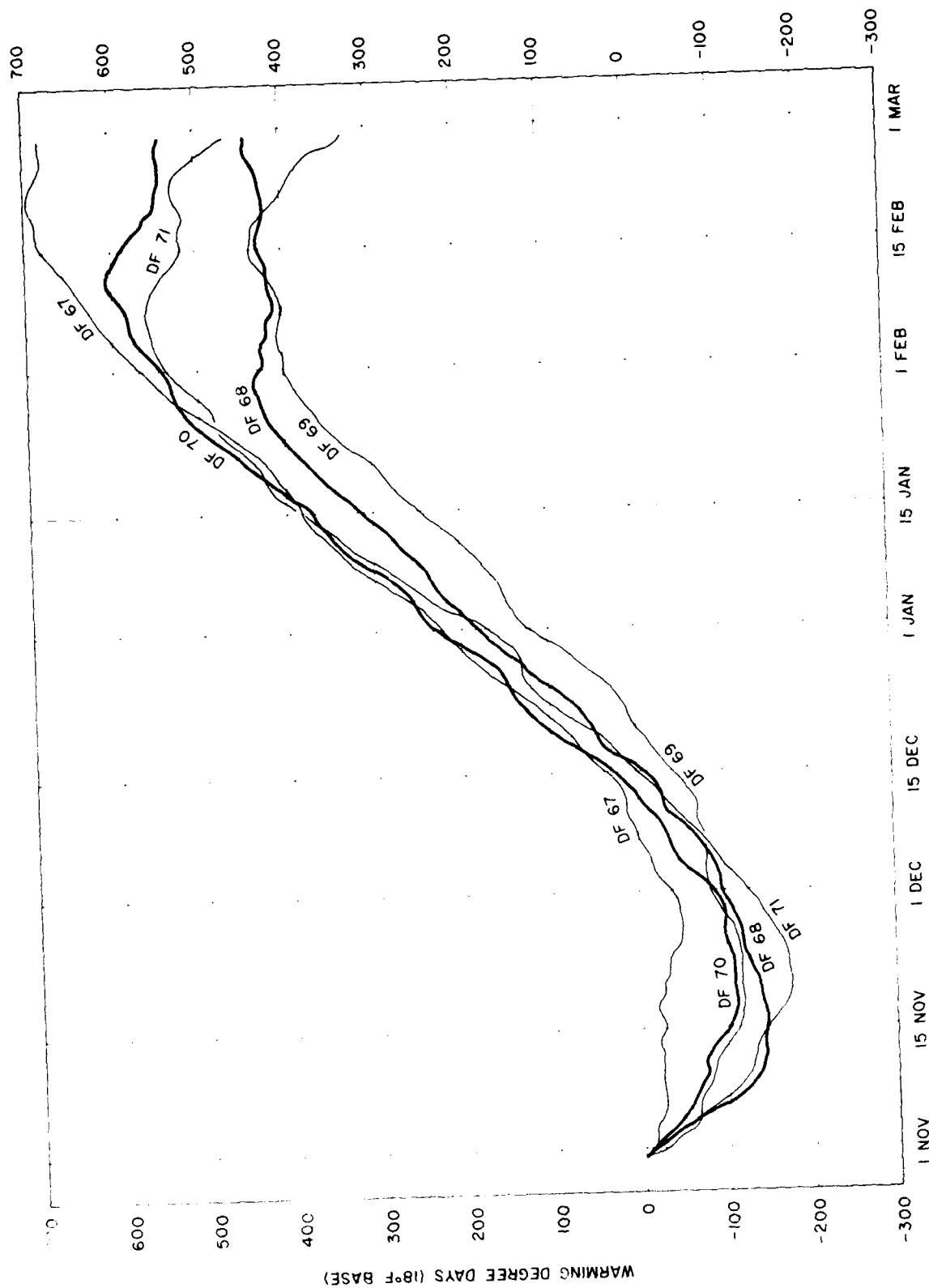
FIGURE 24 ACCUMULATED WARMING DEGREE DAYS AT McMURDO STATION (DF 67 – DF 71).

84
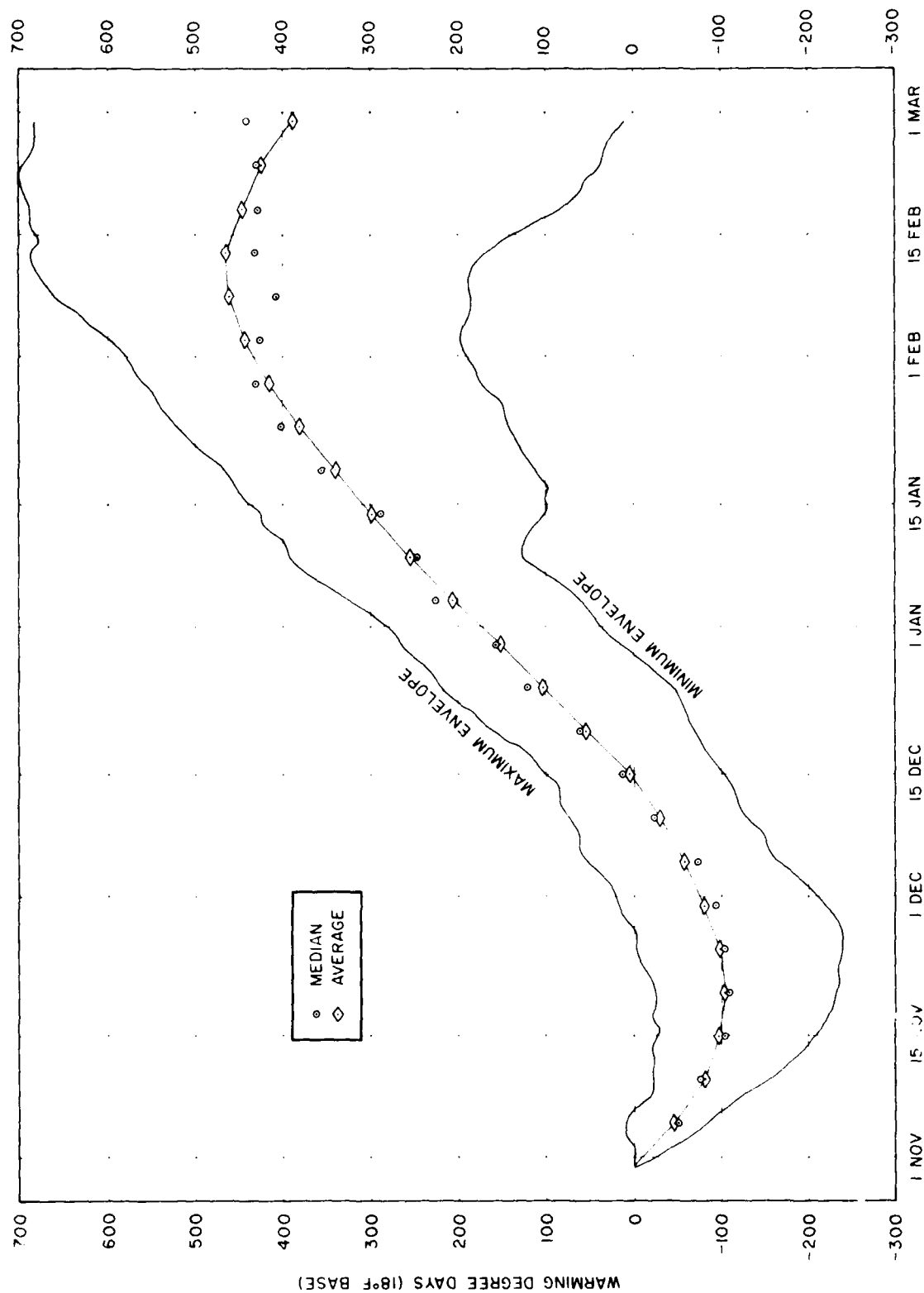
FIGURE 25. AVERAGE AND MEDIAN VALUES, AND MAXIMUM AND MINIMUM ENVELOPES OF ACCUMULATED WARMING DEGREE DAYS AT McMURDO STATION (DF II – DF 71).

$$W = 90/1.75 \, V_0^{0.656}$$

V_0 is surface wind speed in m/sec
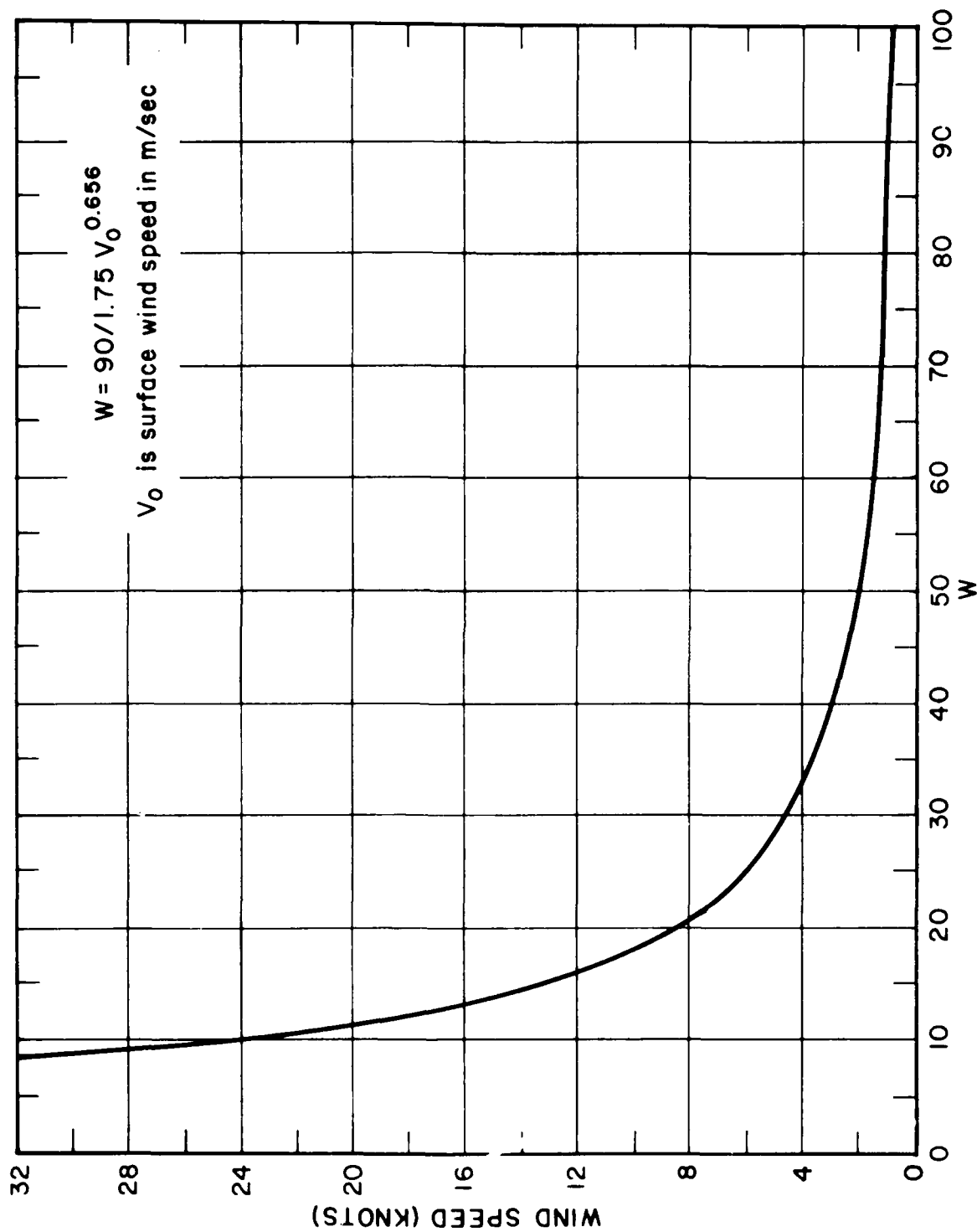
FIGURE 26. WIND SPEED (KN) RELATED TO WIND TERM W

86
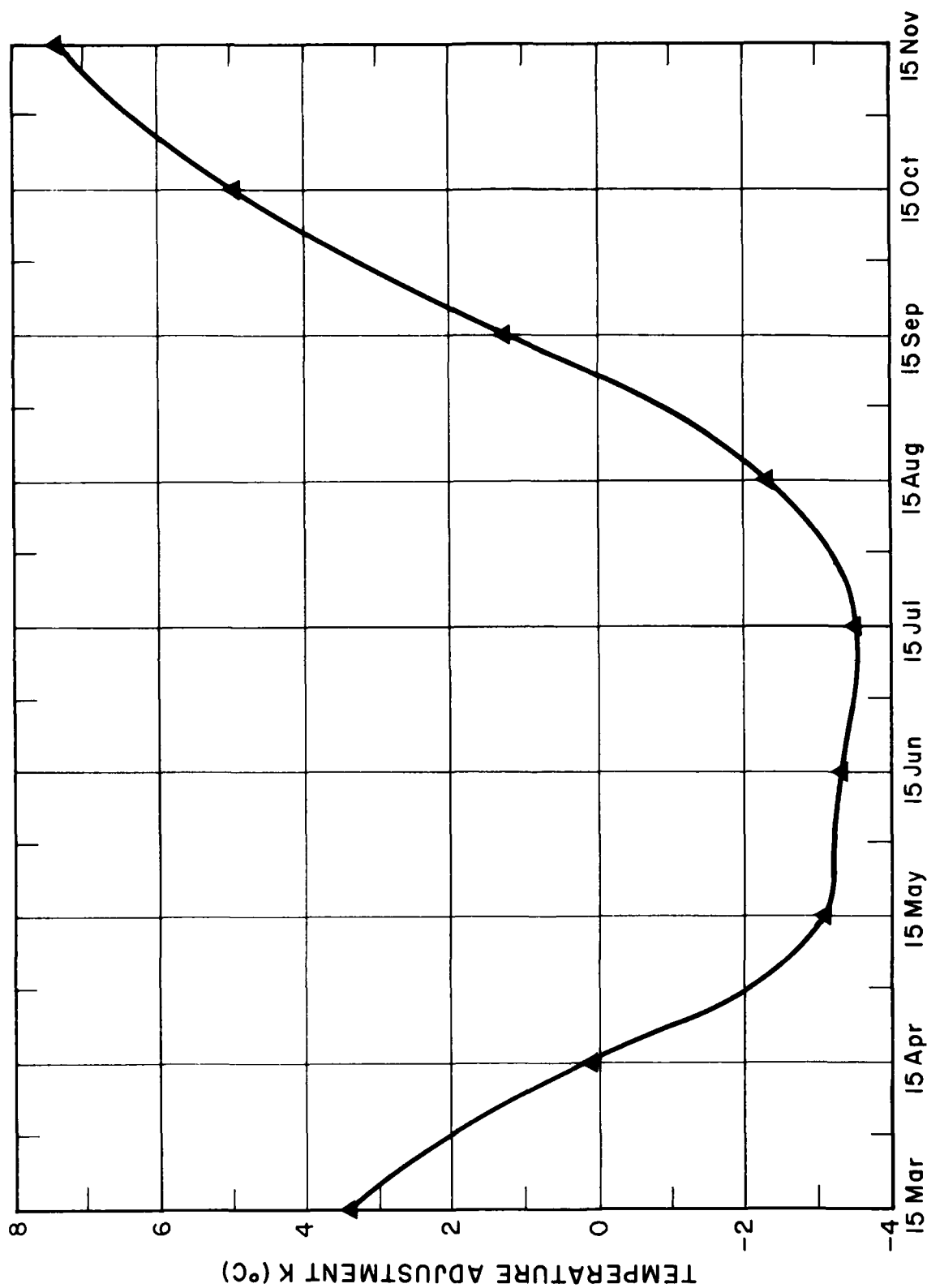
FIGURE 27. SEASONAL VARIATION OF TEMPERATURE ADJUSTMENT K

87

APPENDIX A

Mean Monthly Sea Level Pressure (Mb),

Ross Sea
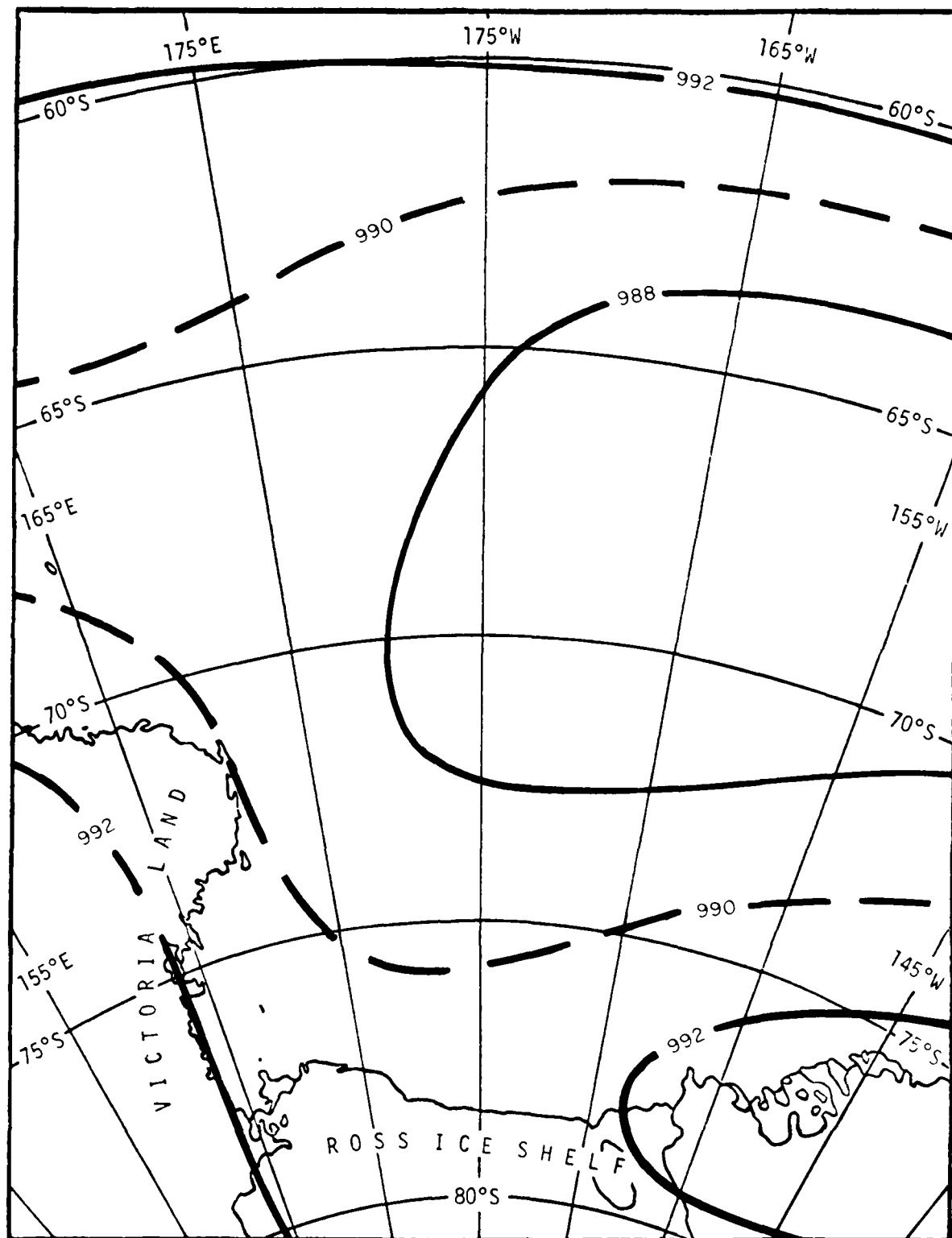
FIGURE A-1. MEAN SEA LEVEL PRESSURE (MB), JANUARY
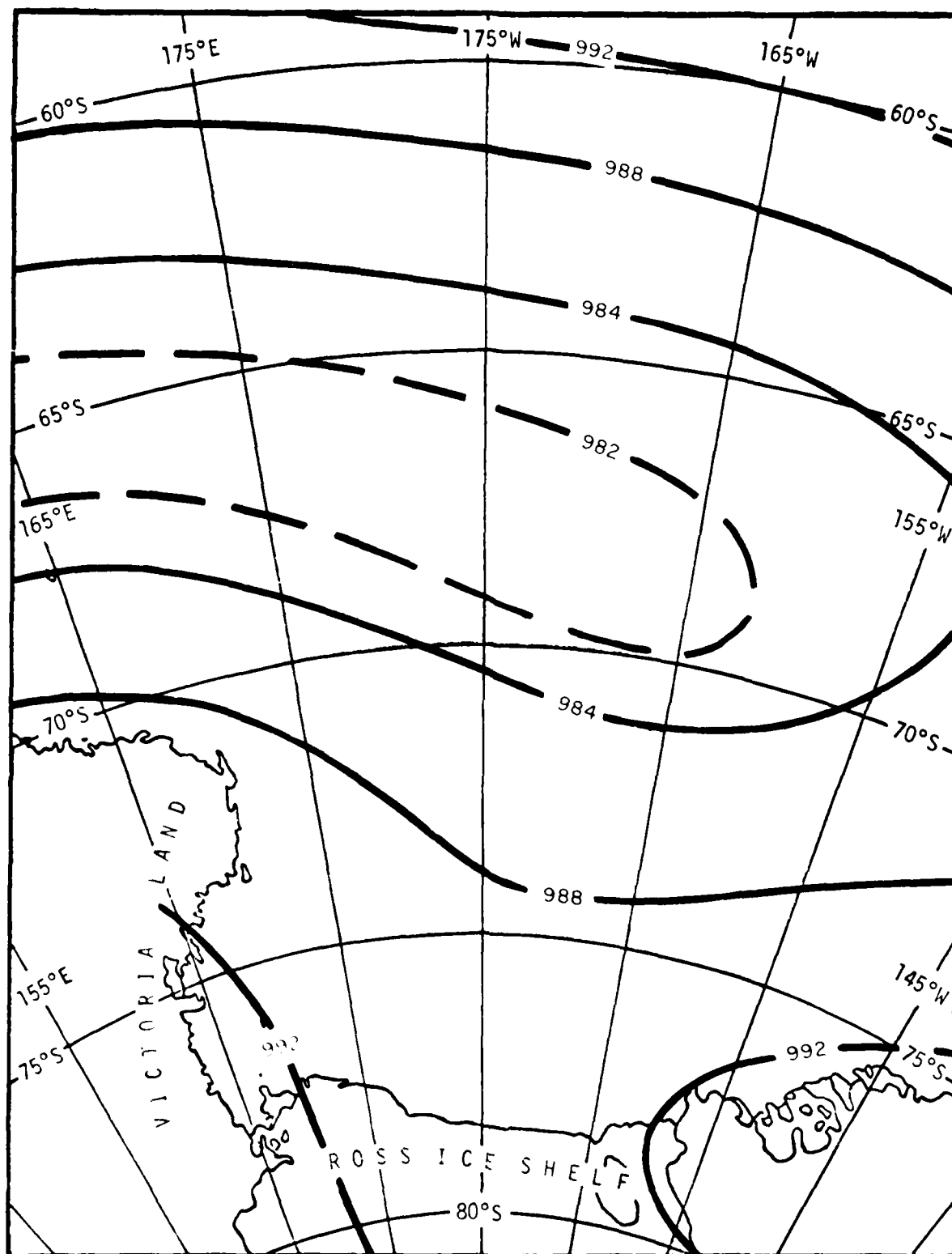
FIGURE A-2 MEAN SEA LEVEL PRESSURE (MB), FEBRUARY
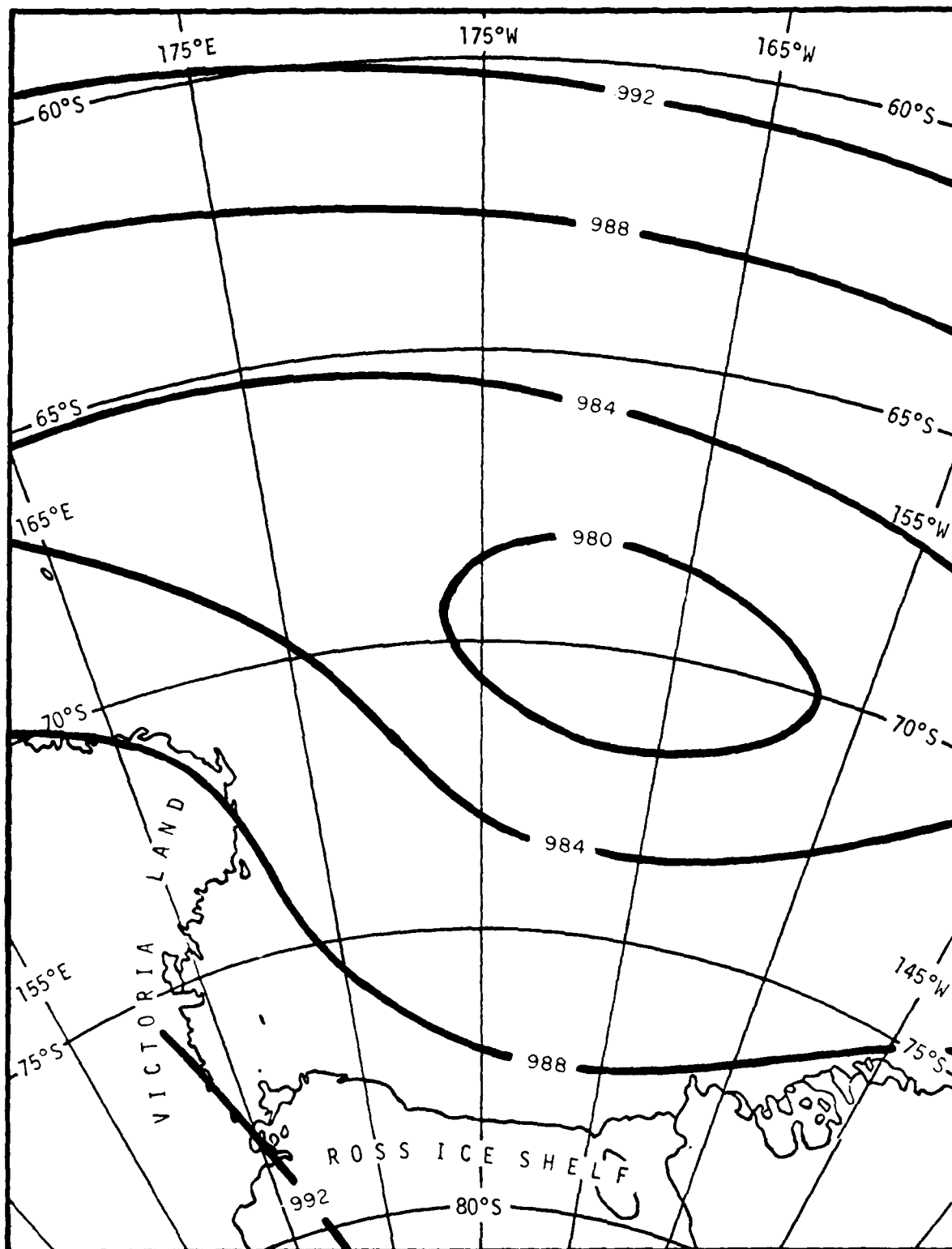
FIGURE A-3. MEAN SEA LEVEL PRESSURE (MB), MARCH
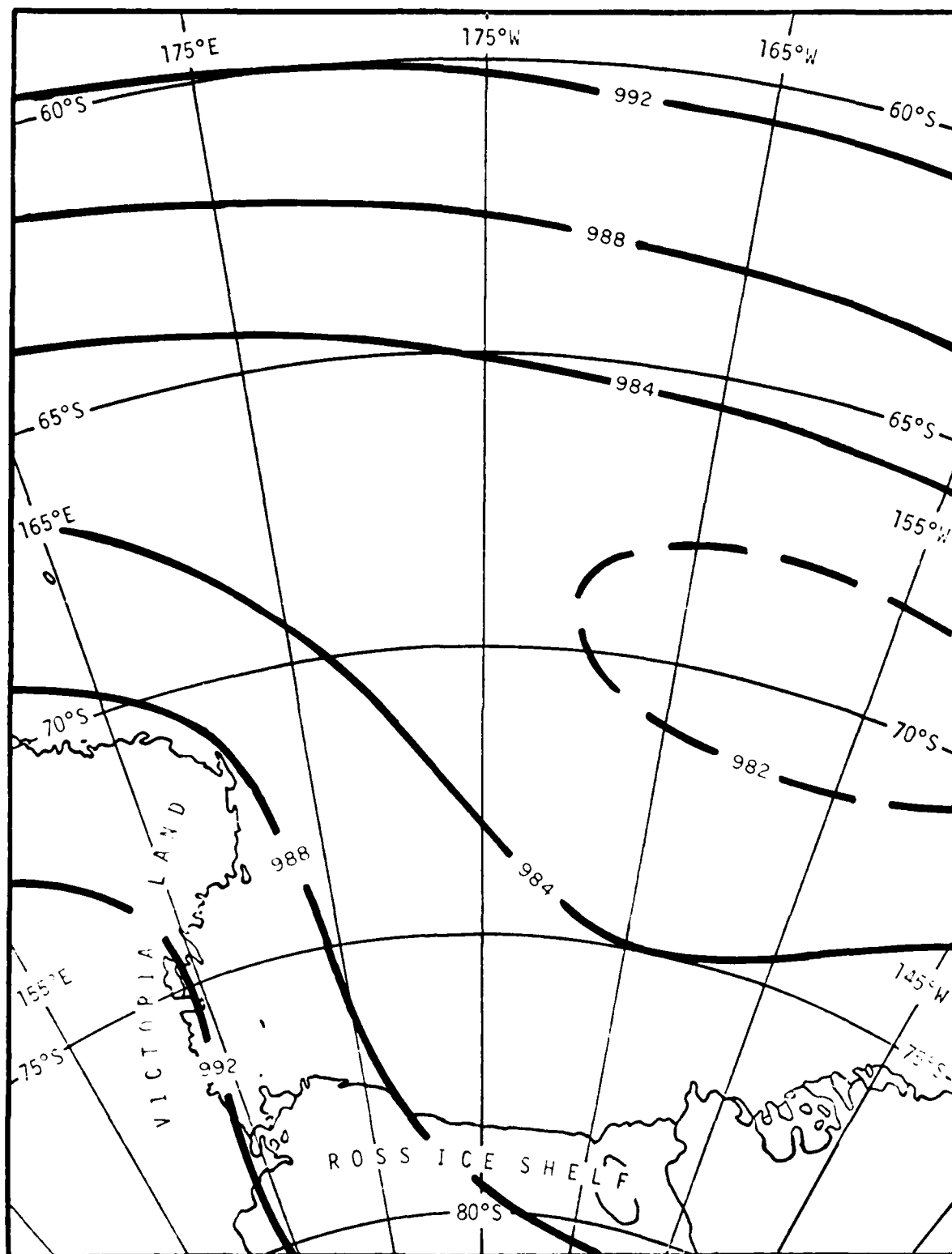
FIGURE A-4. MEAN SEA LEVEL PRESSURE (MB), APRIL
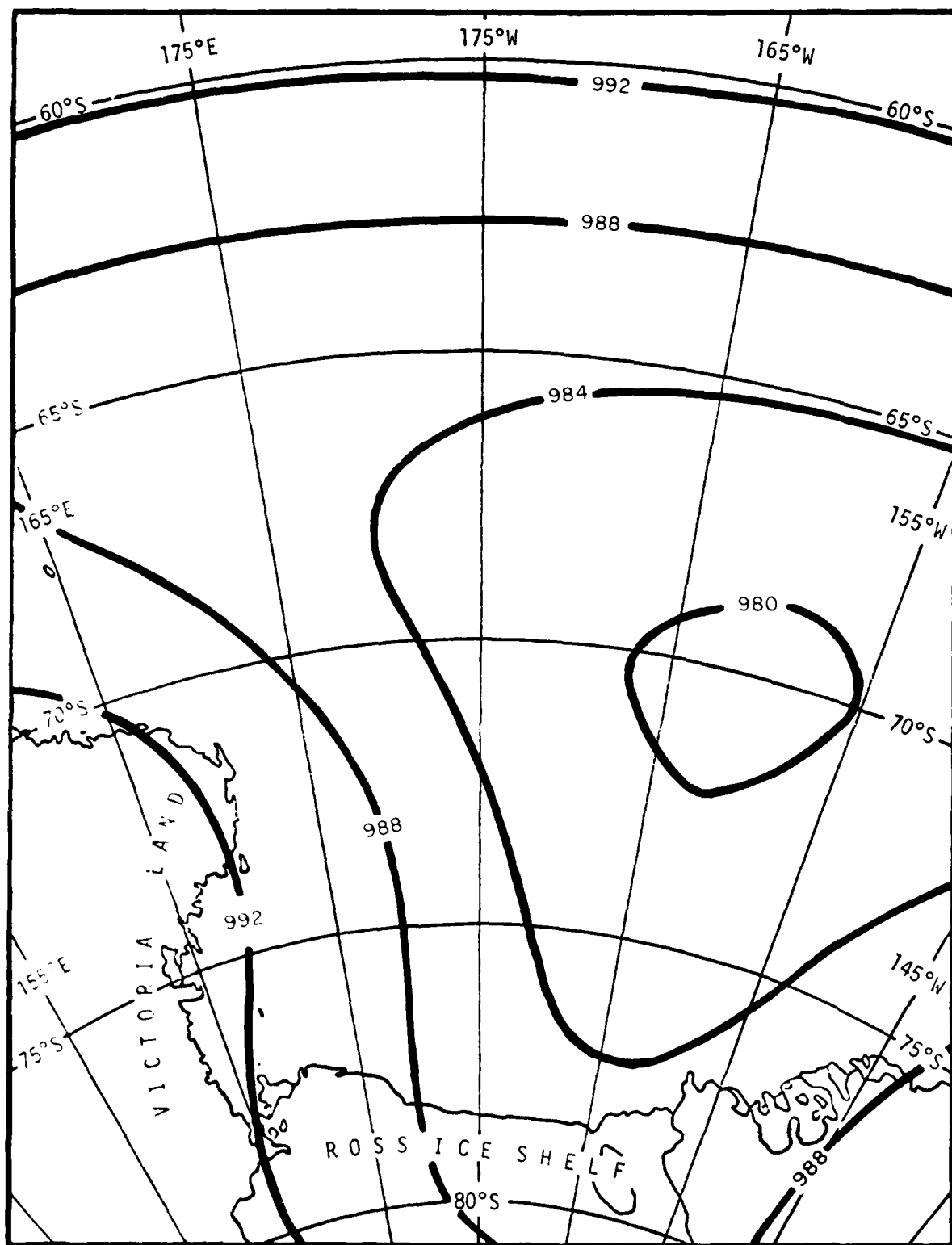
FIGURE A-5. MEAN SEA LEVEL PRESSURE (MB), MAY
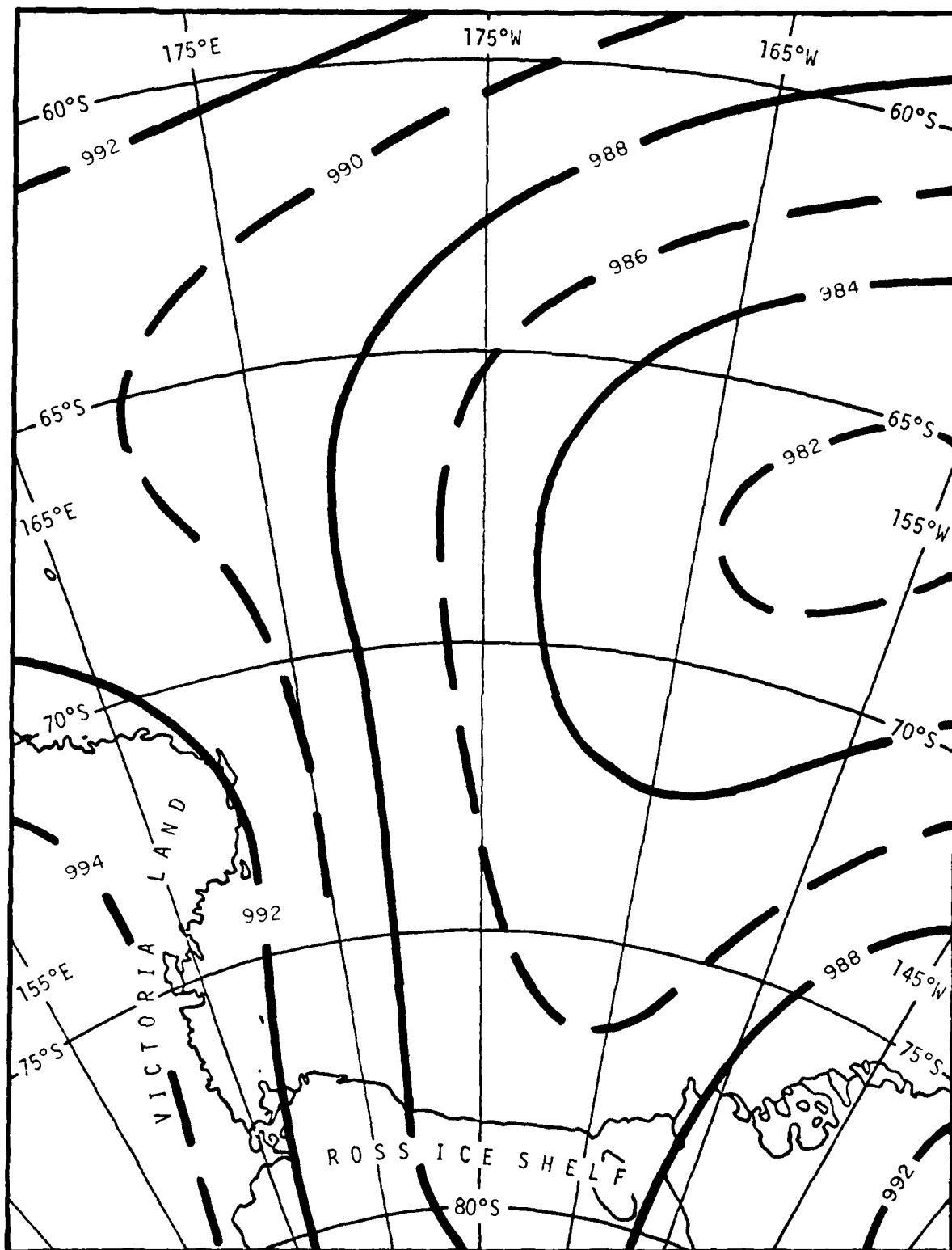
FIGURE A-6. MEAN SEA LEVEL PRESSURE (MB), JUNE
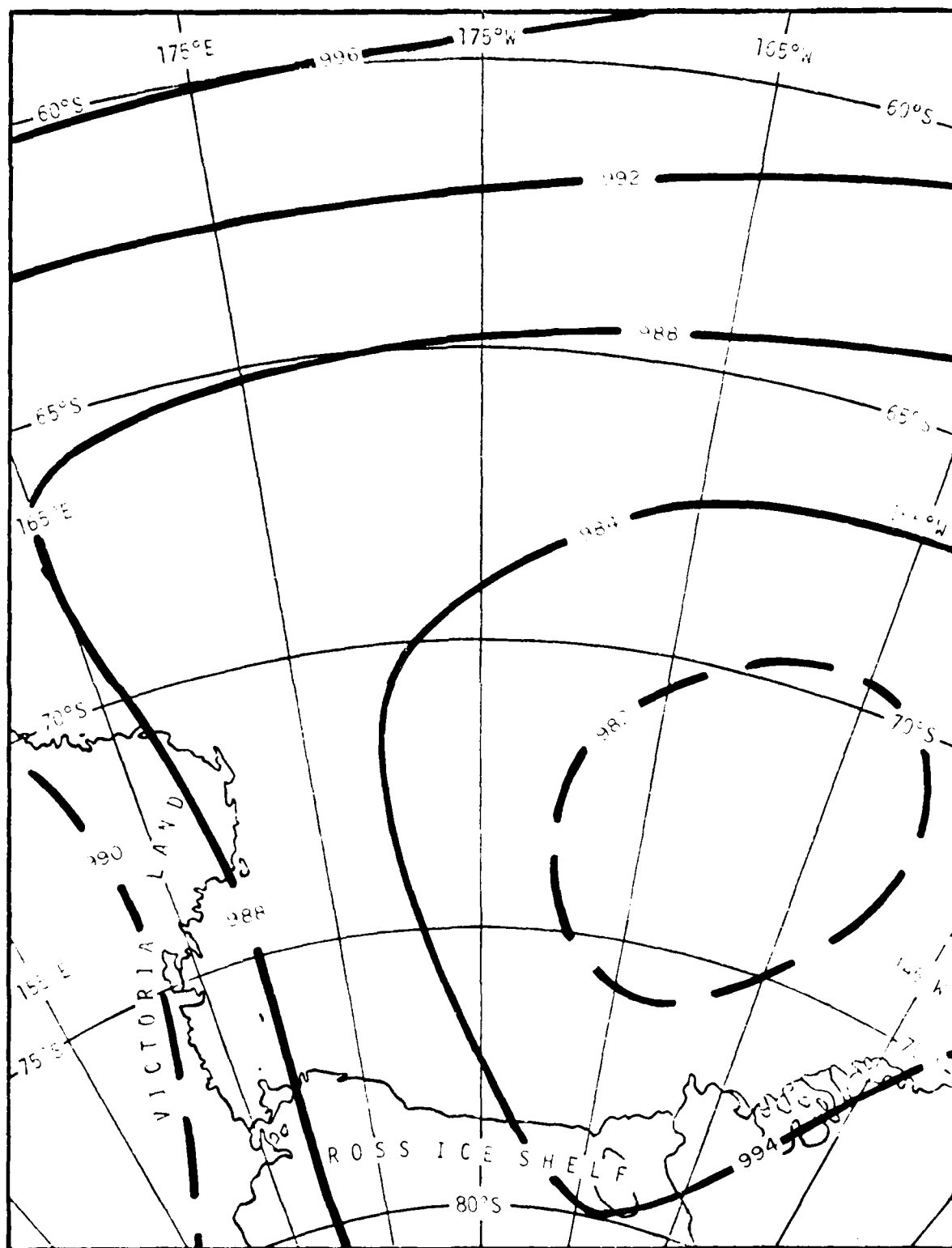
FIGURE A-7 MEAN SEA LEVEL PRESSURE (MB), JULY
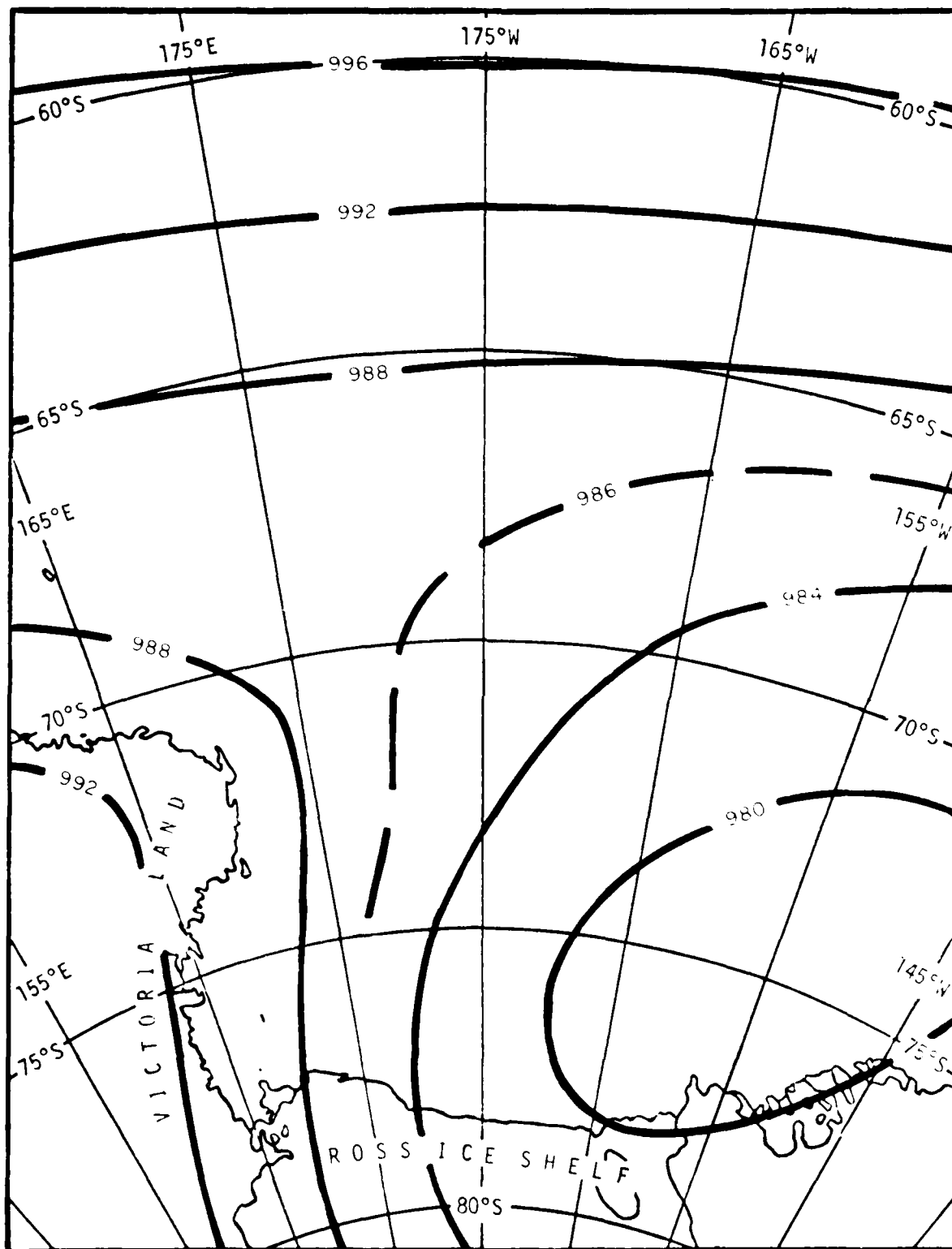
FIGURE A-8 MEAN SEA LEVEL PRESSURE (MB), AUGUST
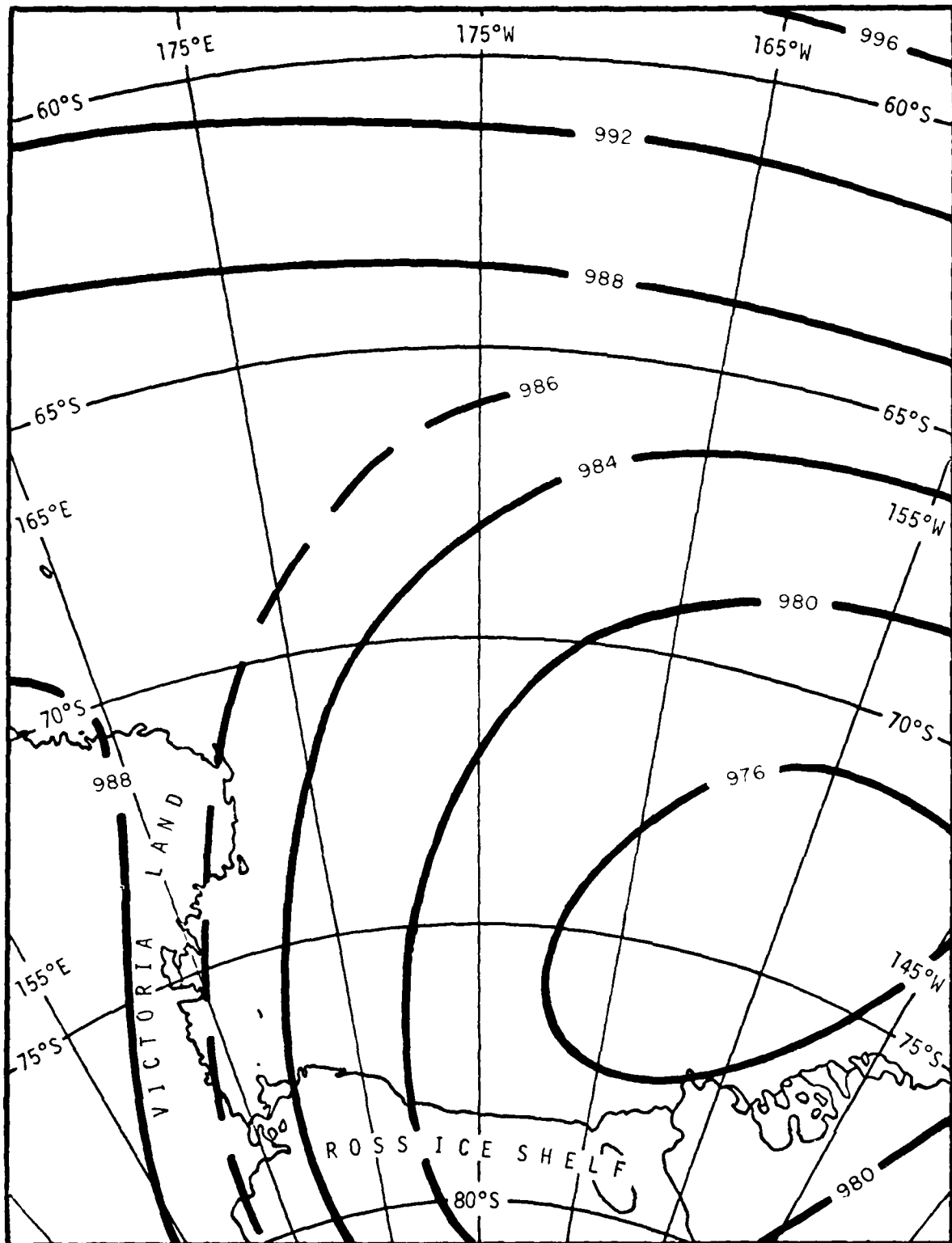
FIGURE A-9. MEAN SEA LEVEL PRESSURE (MB), SEPTEMBER
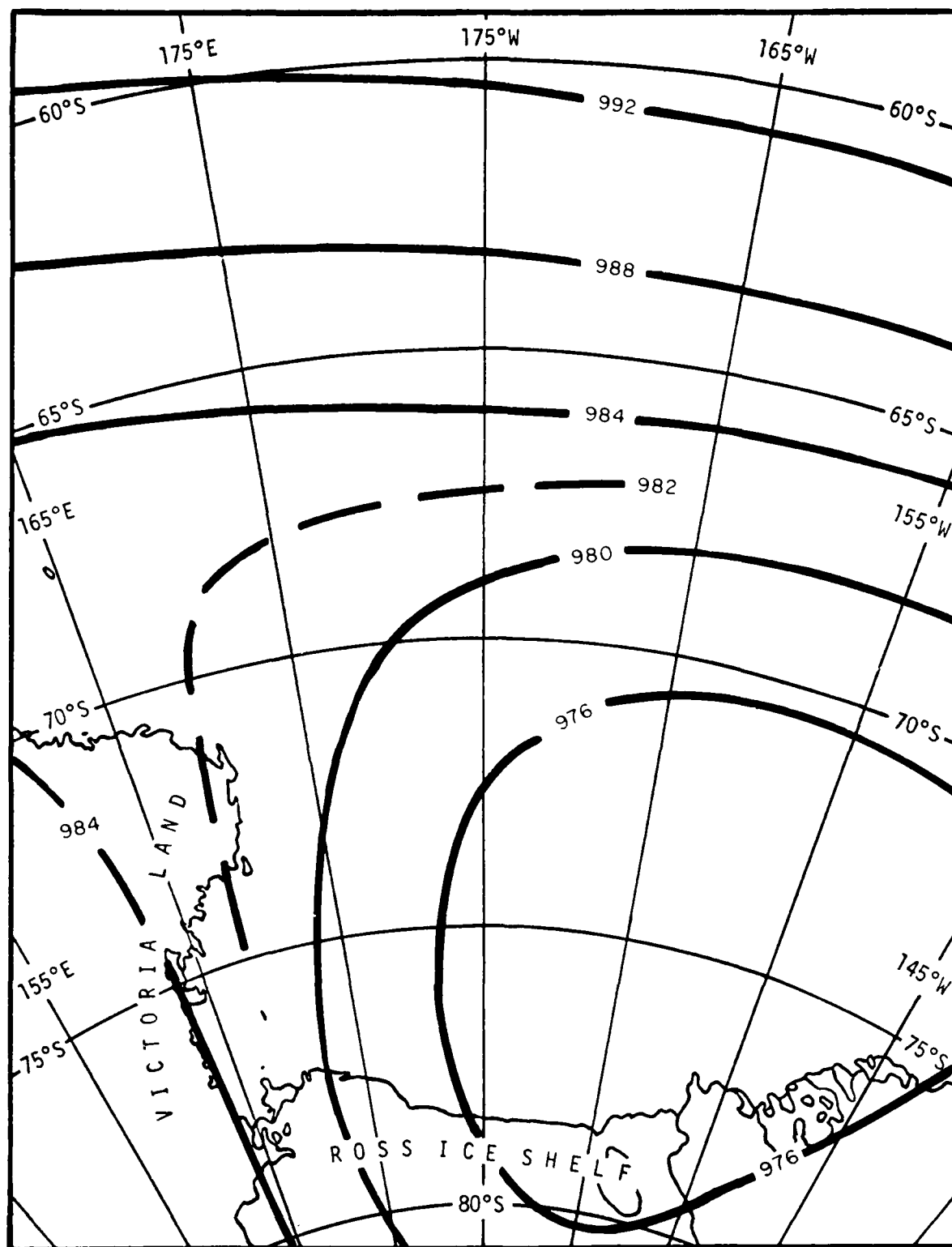
FIGURE A-IO. MEAN SEA LEVEL PRESSURE (MB), OCTOBER

99
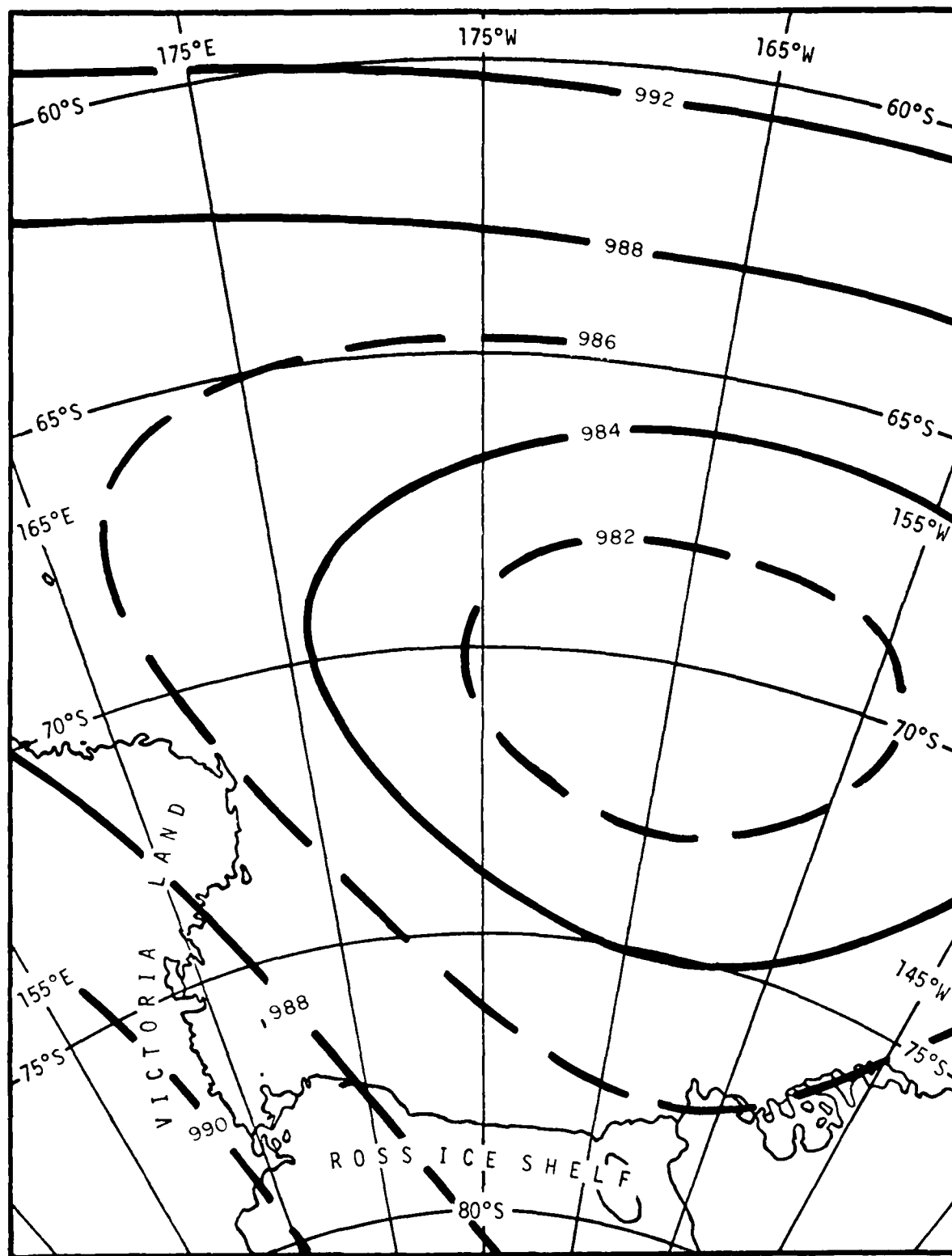
FIGURE A-11 MEAN SEA LEVEL PRESSURE (MB), NOVEMBER
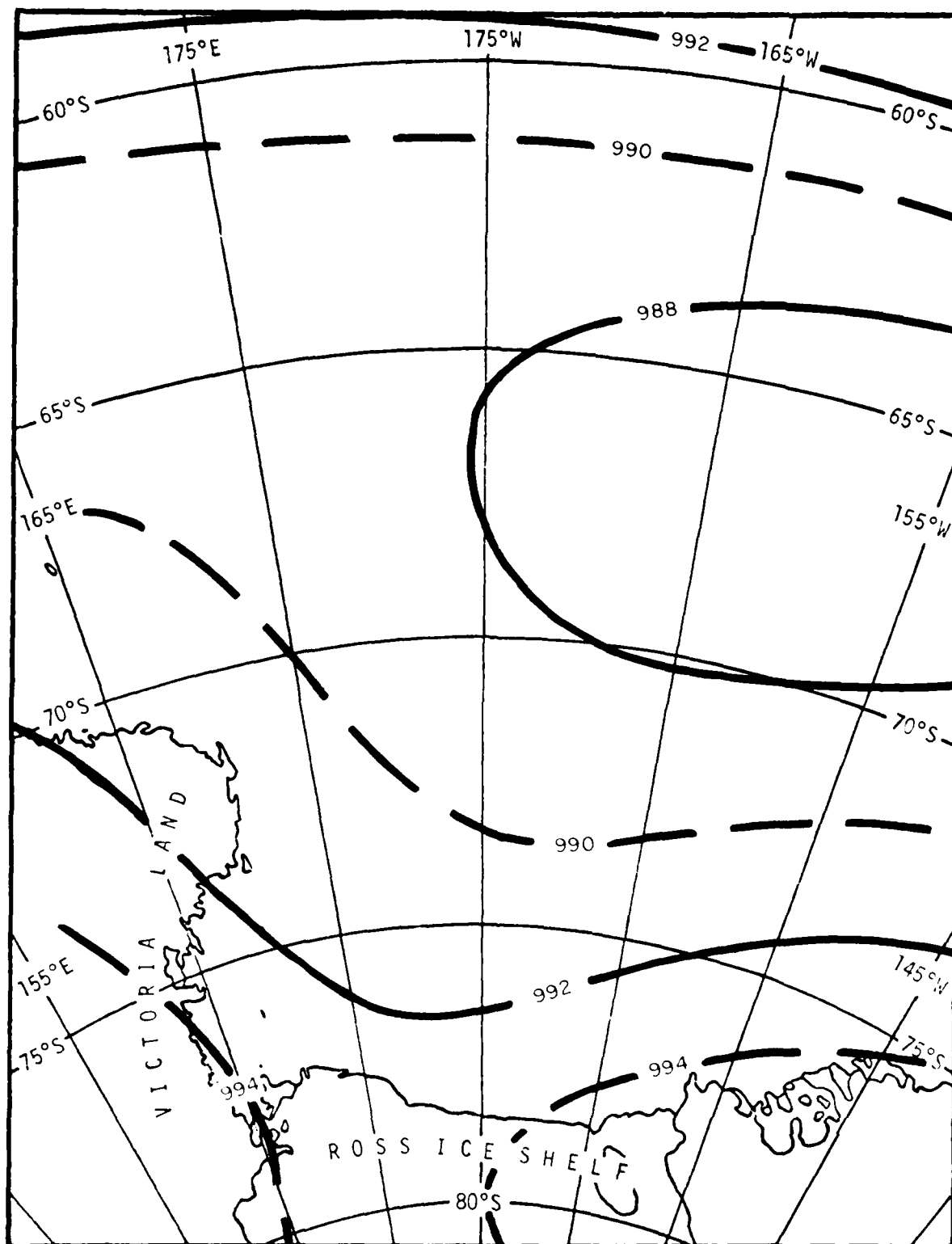
FIGURE A-12 MEAN SEA LEVEL PRESSURE (MB), DECEMBER

APPENDIX B

Mean Monthly Surface Air Temperature (°C),

Ross Sea
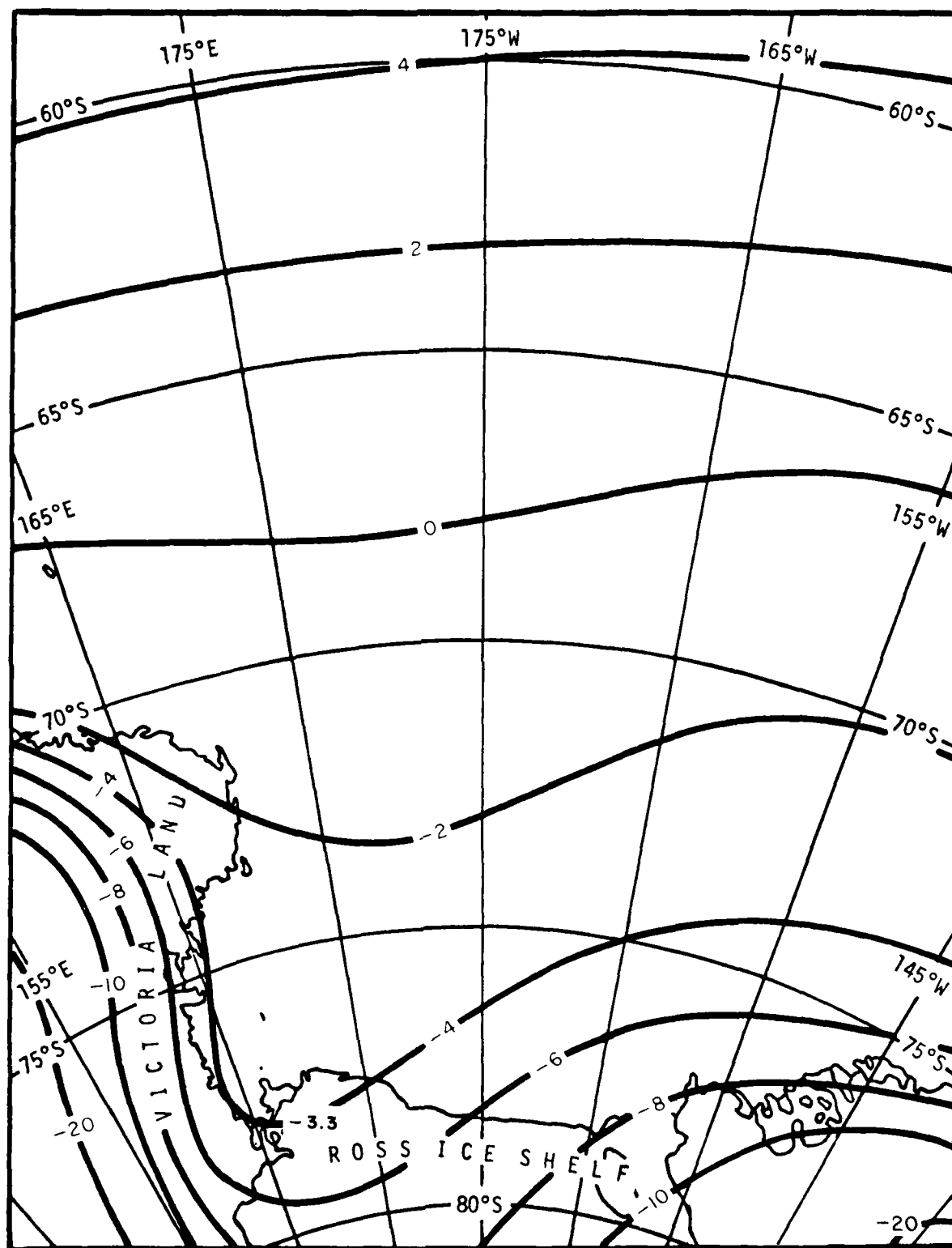
FIGURE B-I MEAN MONTHLY SURFACE AIR TEMPERATURE (°C), JANUARY
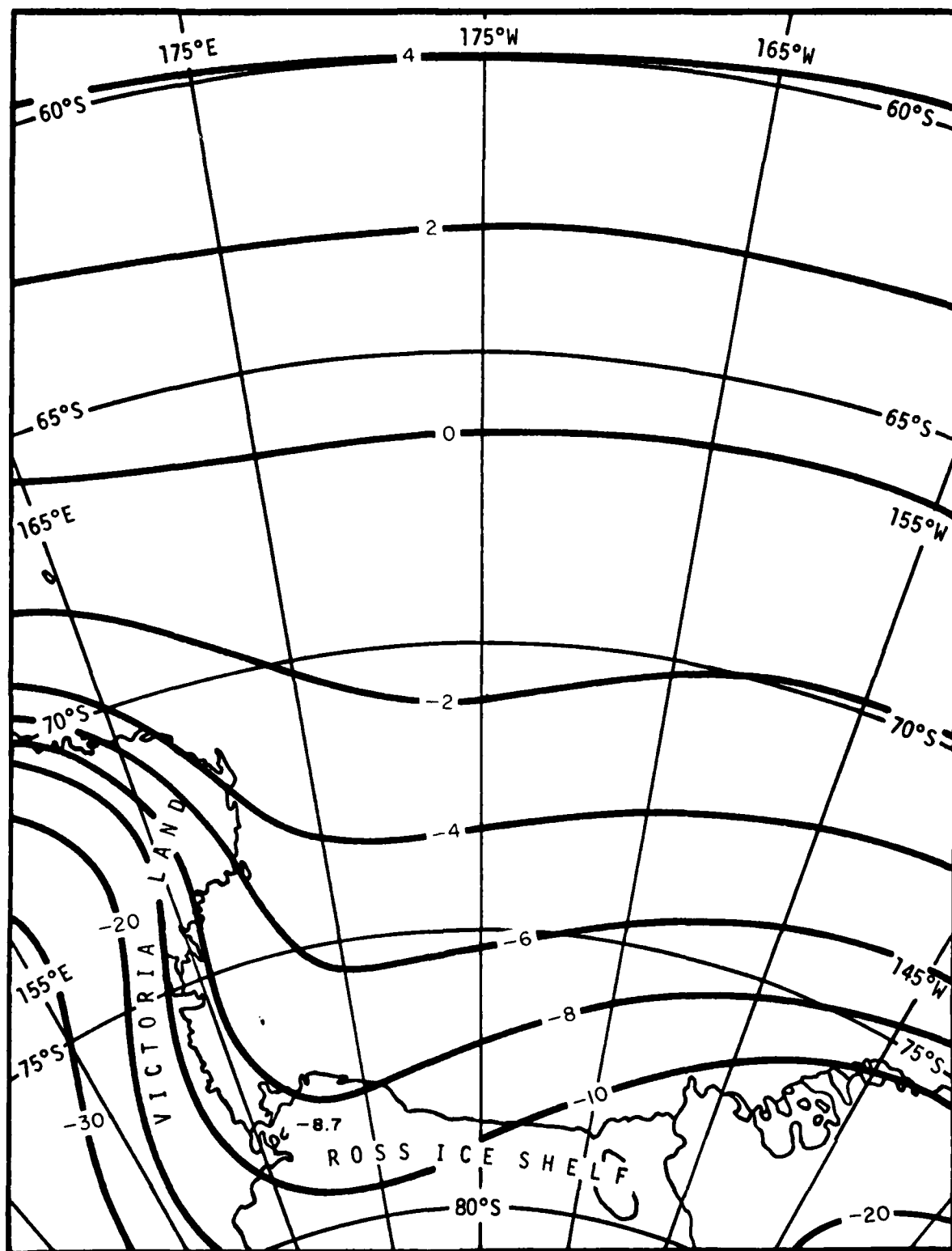
FIGURE B-2. MEAN MONTHLY SURFACE AIR TEMPERATURE (°C), FEBRUARY
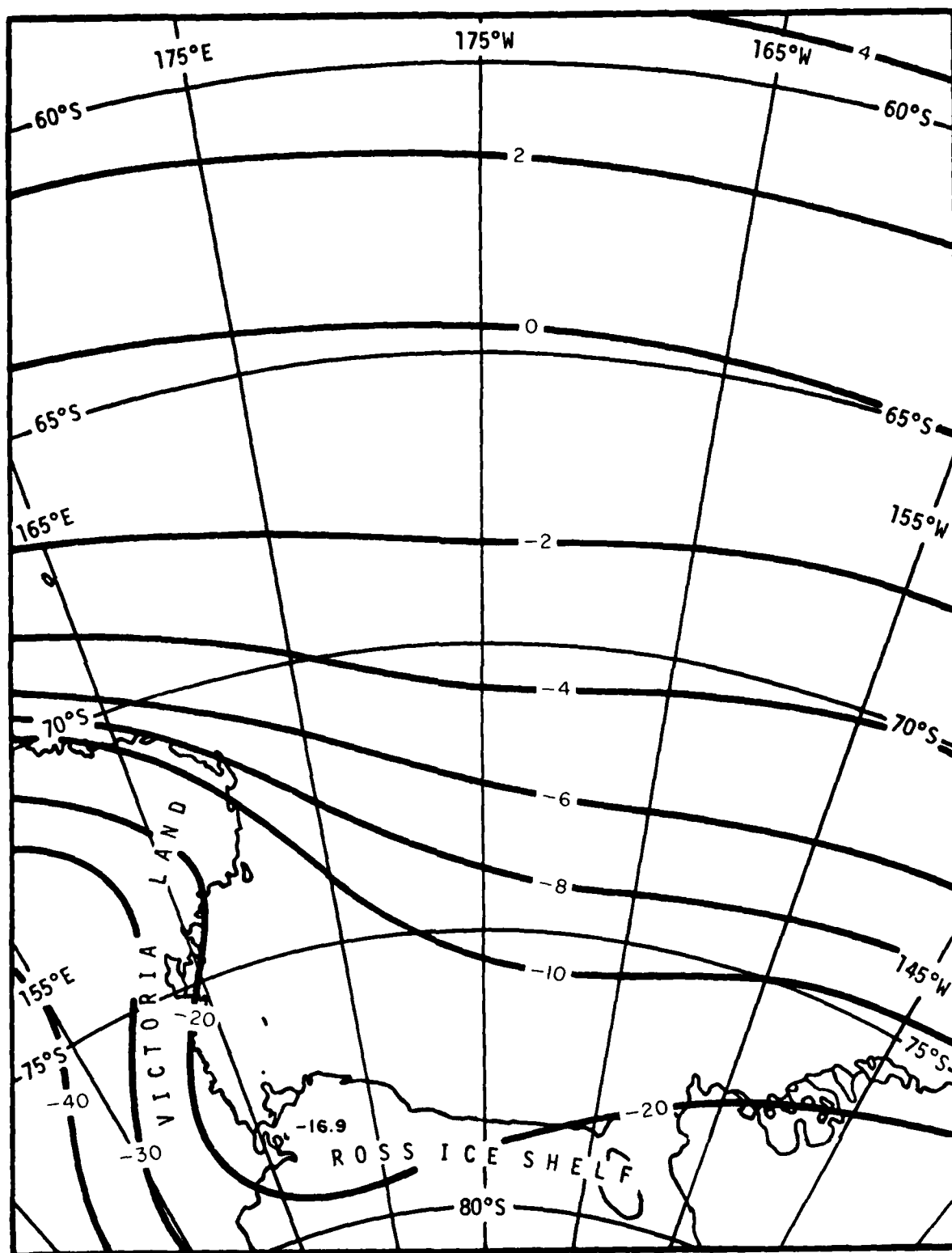
FIGURE B-3. MEAN MONTHLY SURFACE AIR TEMPERATURE (°C), MARCH

106
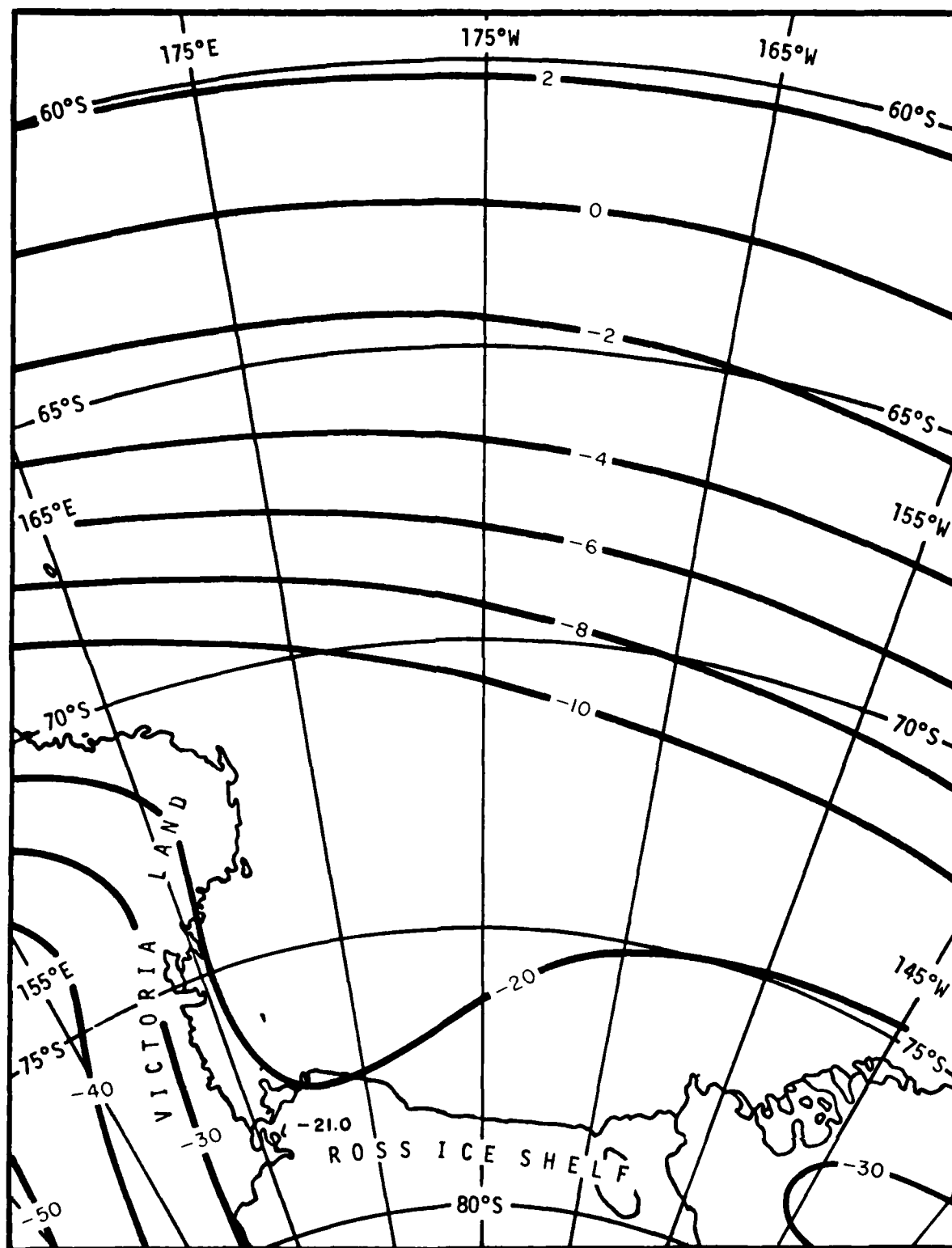
FIGURE B-4. MEAN MONTHLY SURFACE AIR TEMPERATURE (°C), APRIL
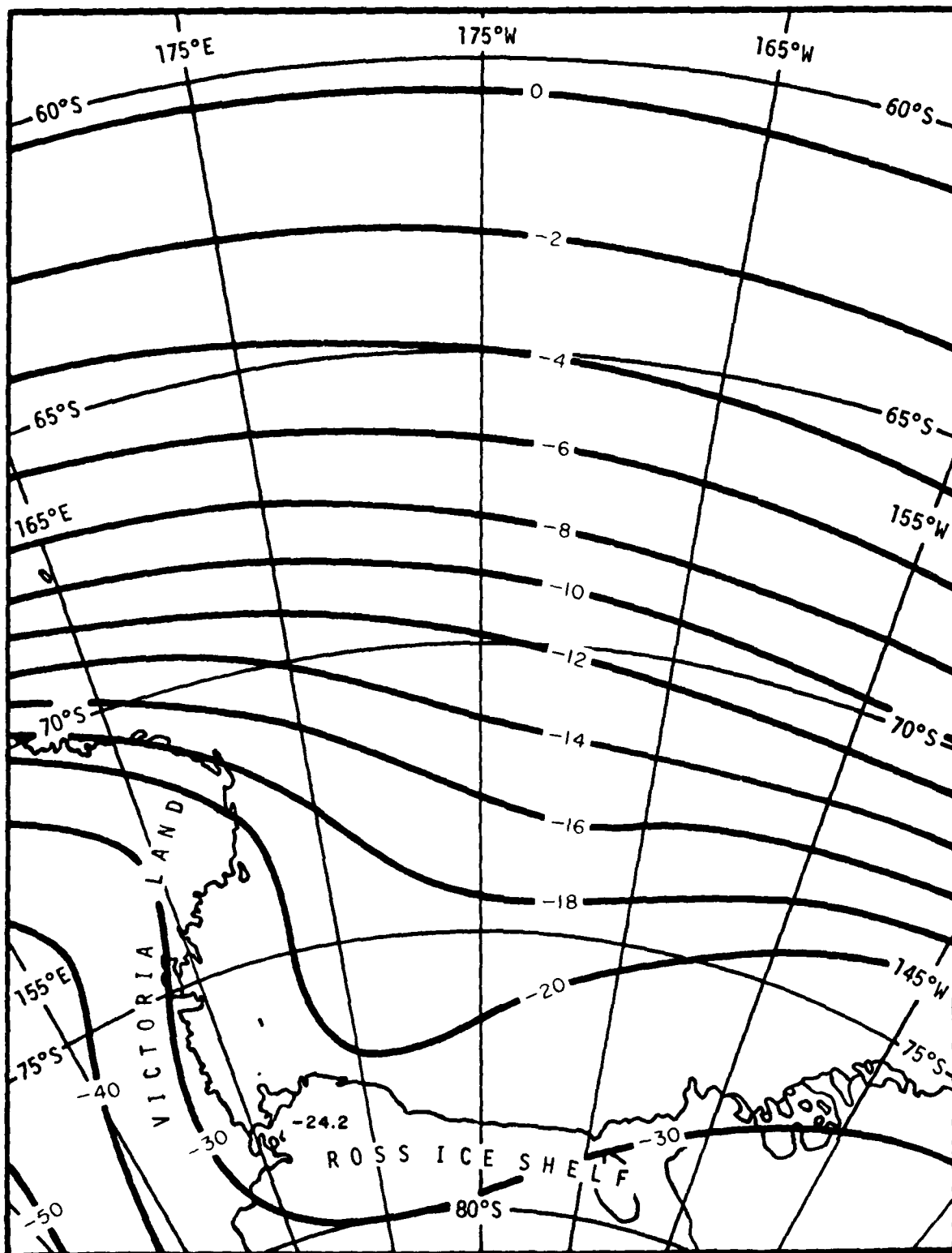
FIGURE B-5. MEAN MONTHLY SURFACE AIR TEMPERATURE (°C), MAY
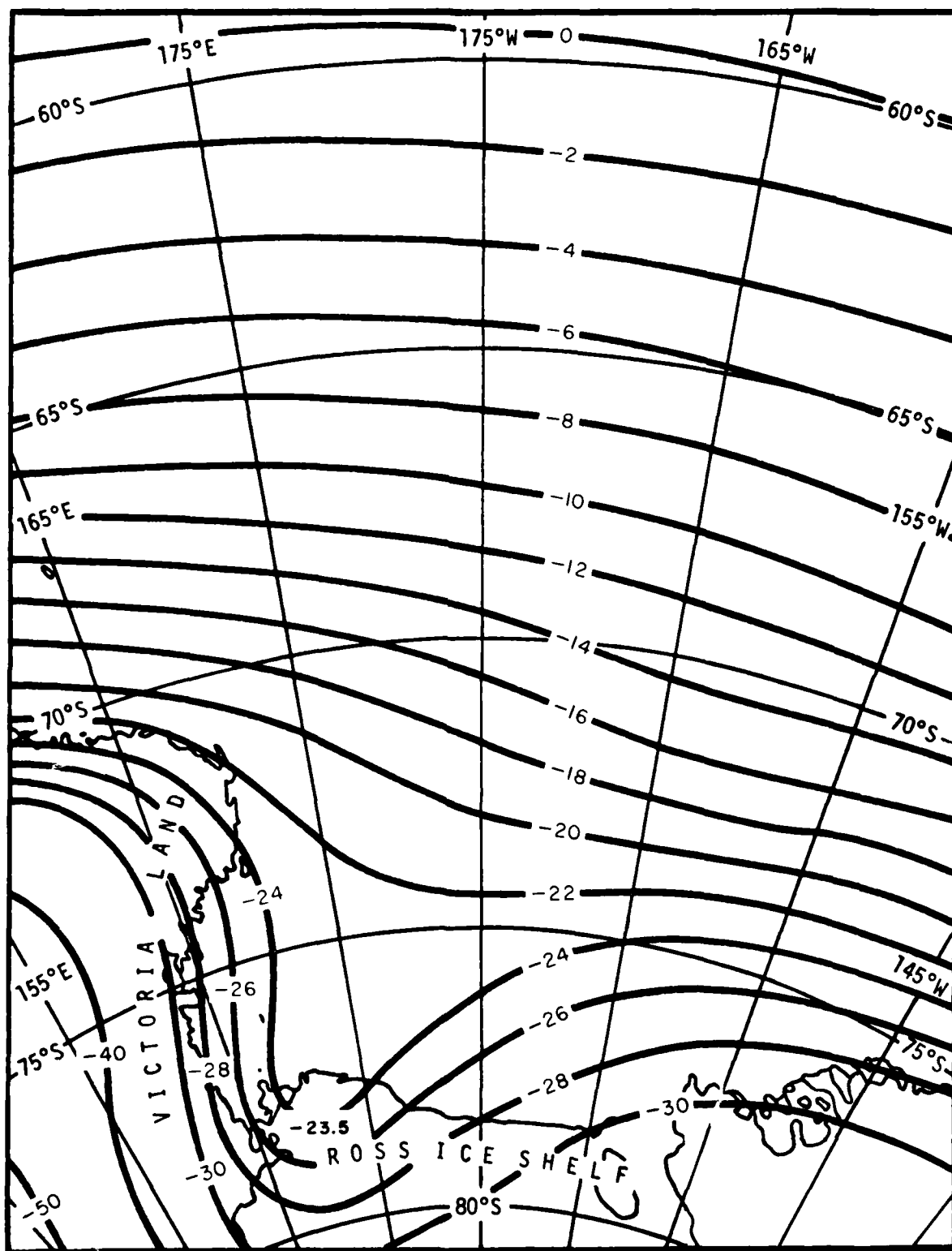
FIGURE B-6. MEAN MONTHLY SURFACE AIR TEMPERATURE (°C), JUNE
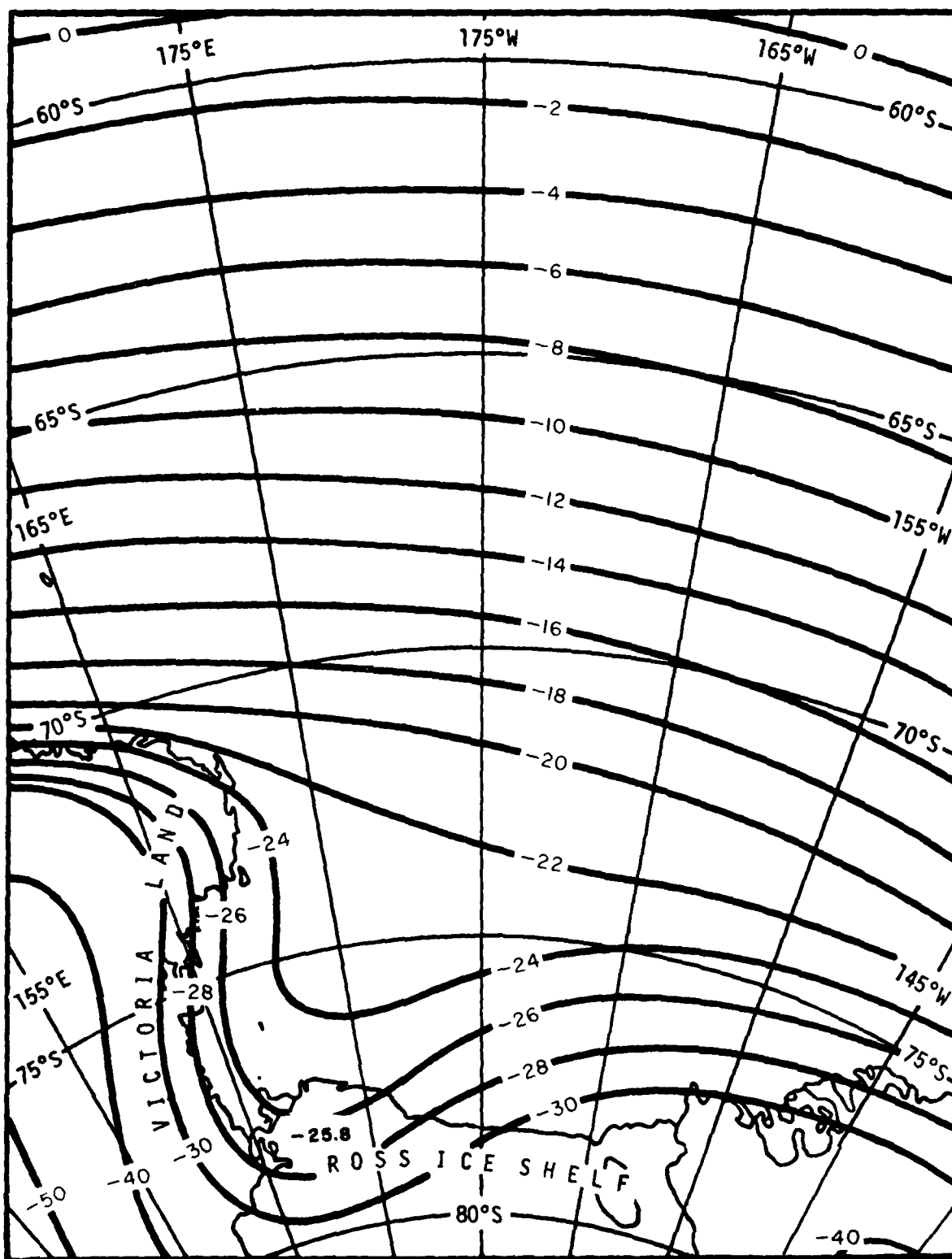
FIGURE B-7. MEAN MONTHLY SURFACE AIR TEMPERATURE (°C), JULY

110
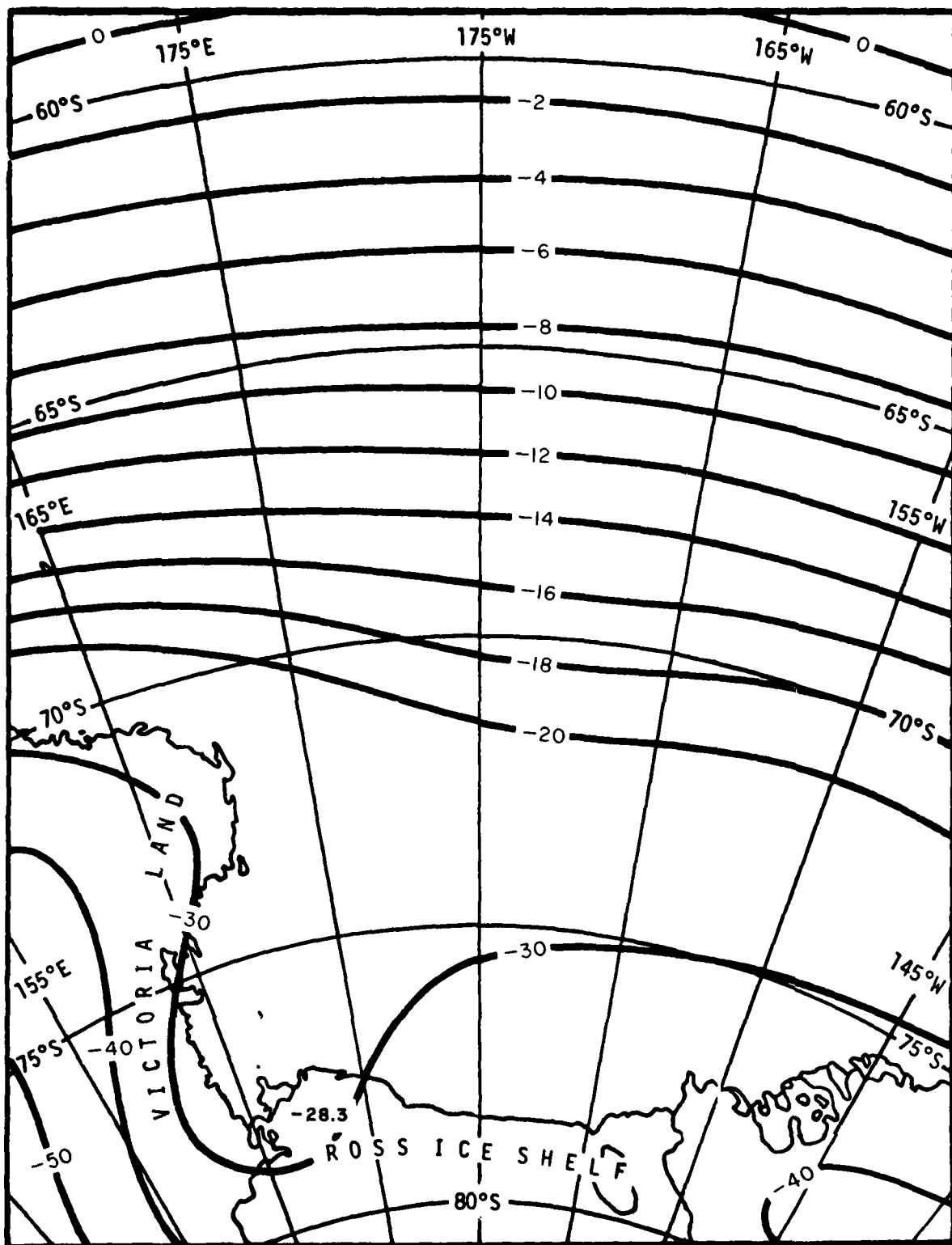
FIGURE B-8. MEAN MONTHLY SURFACE AIR TEMPERATURE (°C), AUGUST

111
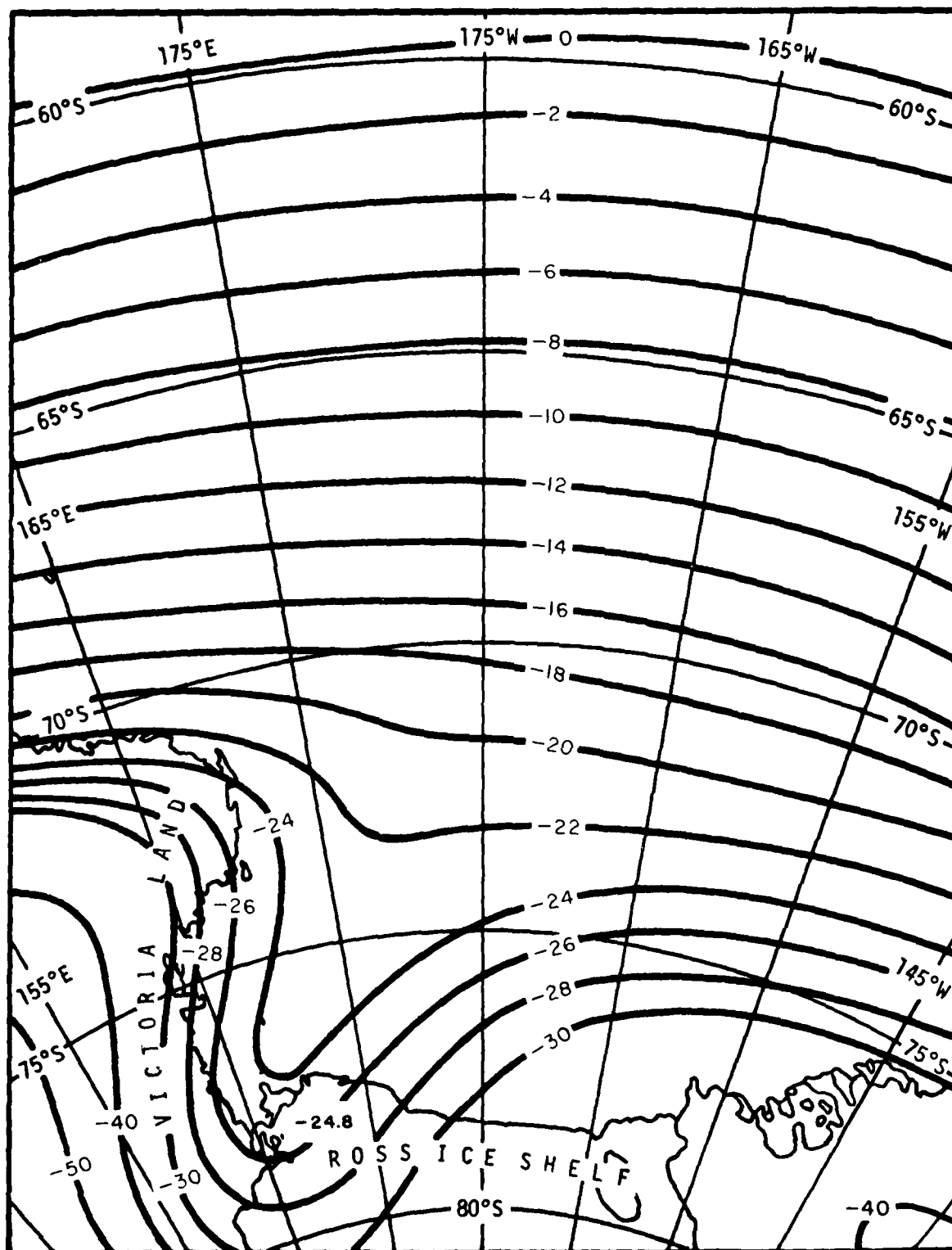
FIGURE B-9. MEAN MONTHLY SURFACE AIR TEMPERATURE (°C), SEPTEMBER
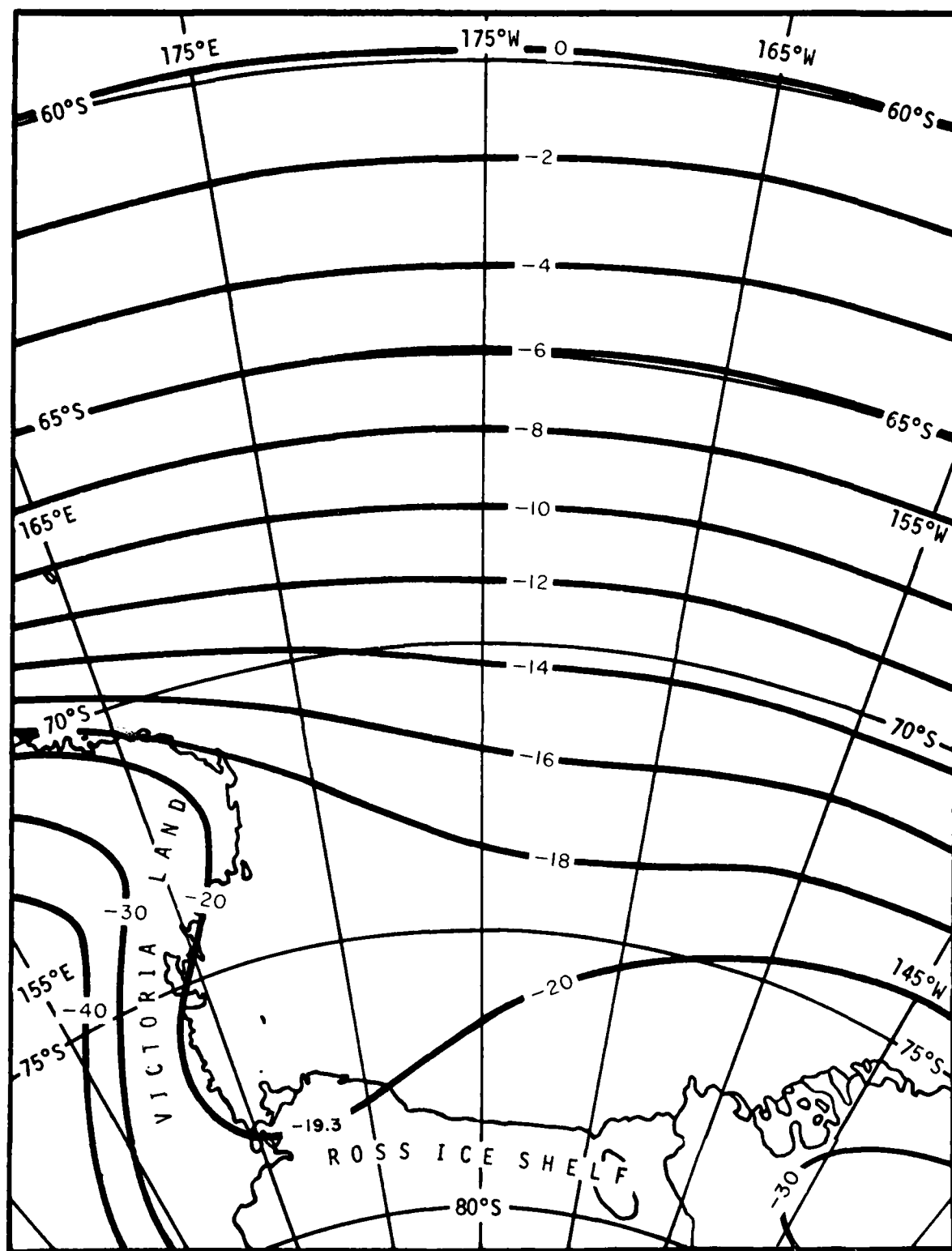
FIGURE B-10. MEAN MONTHLY SURFACE AIR TEMPERATURE (°C), OCTOBER

113
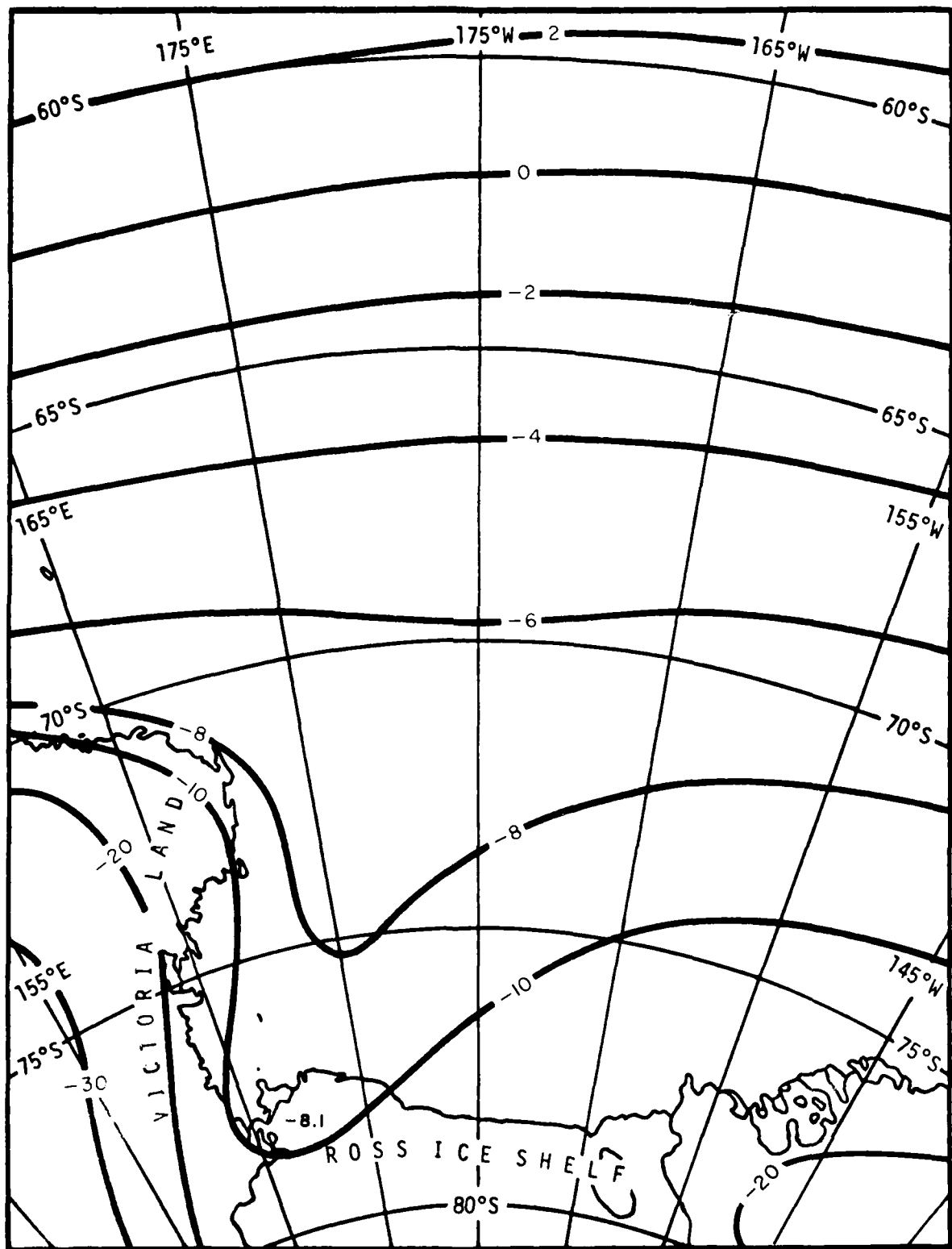
FIGURE B-11 MEAN MONTHLY SURFACE AIR TEMPERATURE (°C), NOVEMBER
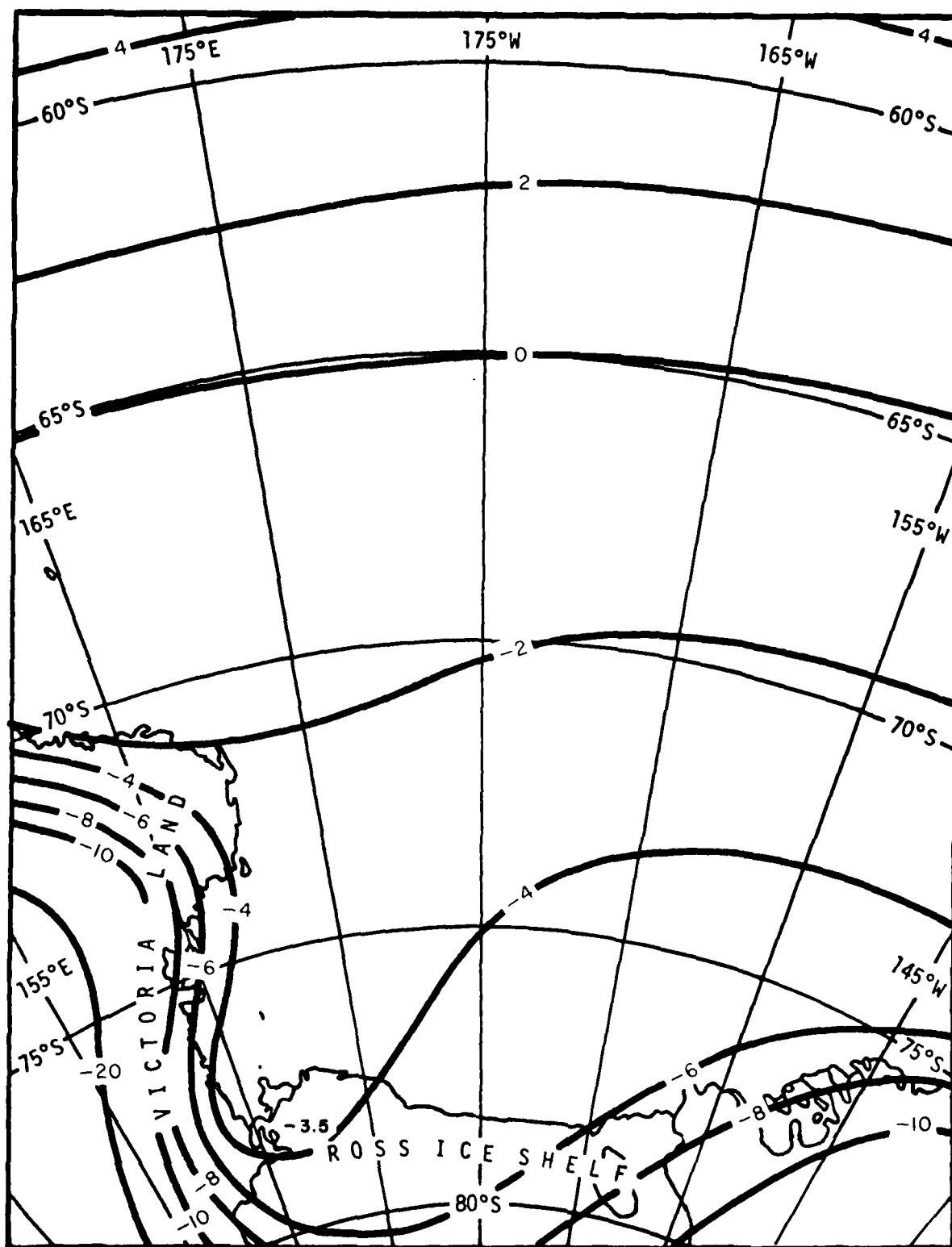
FIGURE B-12. MEAN MONTHLY SURFACE AIR TEMPERATURE (°C), DECEMBER

115

APPENDIX C

Mean Half-Monthly Pack Ice Concentration and

Large Floe-Size Percentage, Western Ross Sea,

October - January (DF 62 - DF 69)
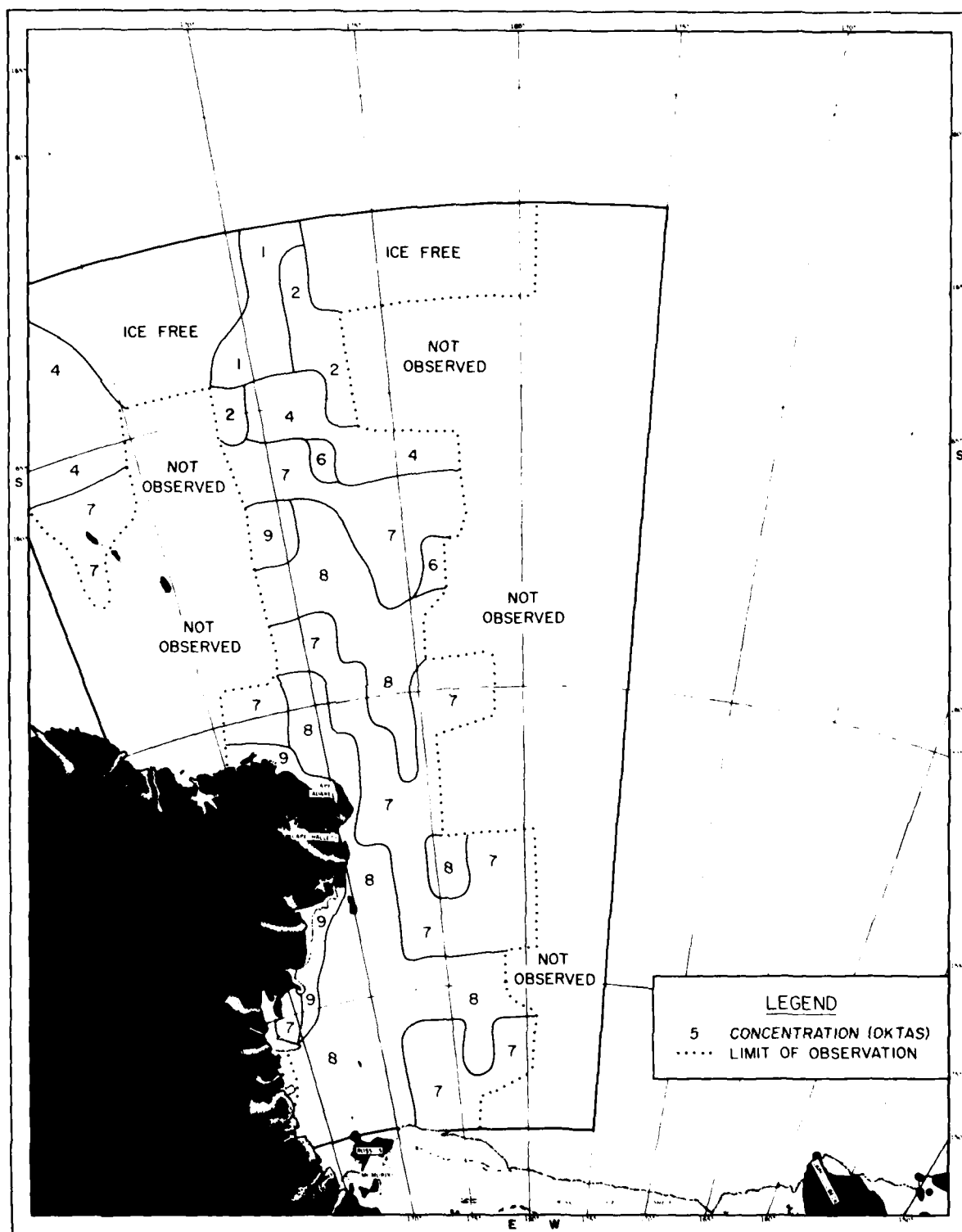
FIGURE C-1. ICE CONCENTRATION 1-15 OCTOBER
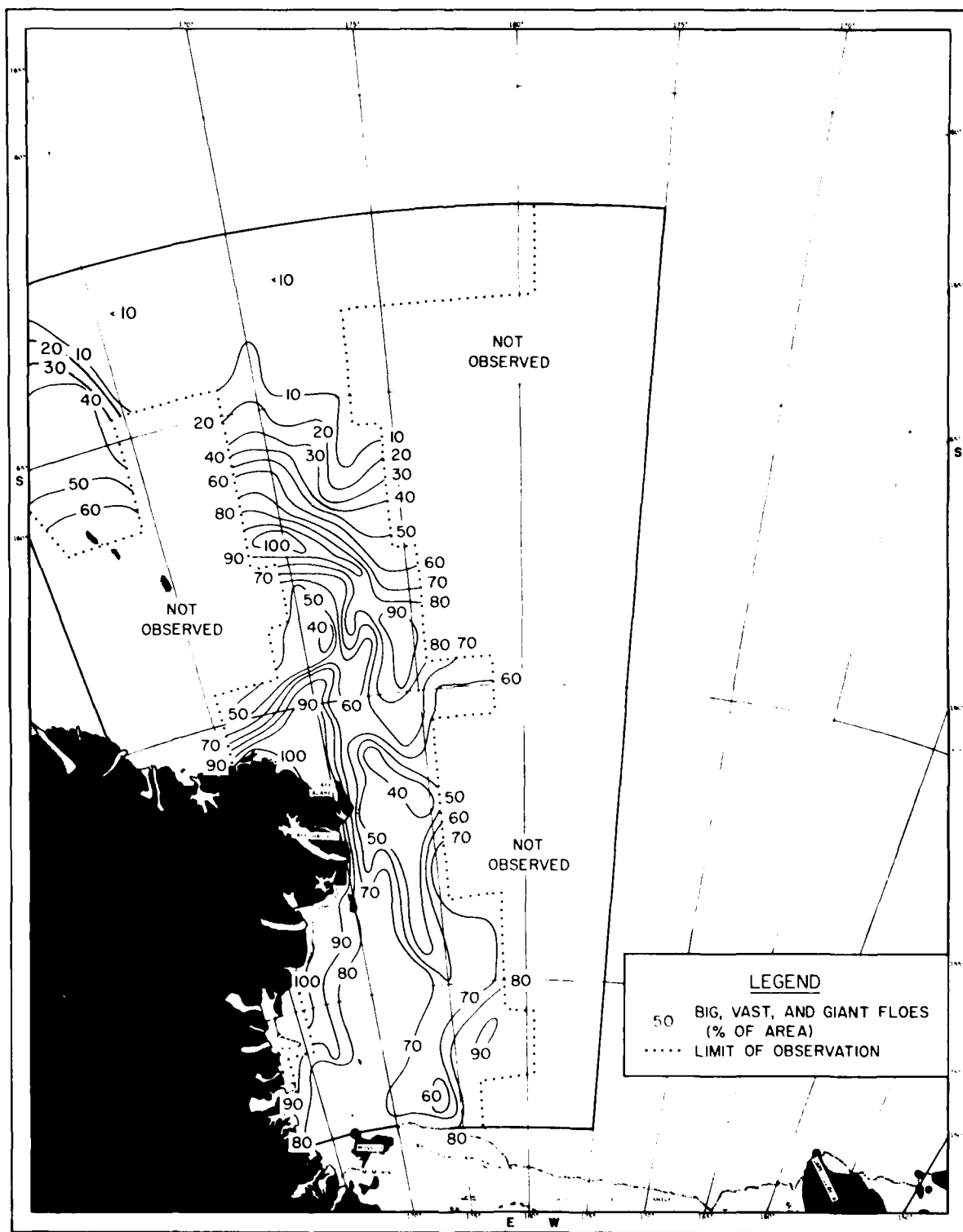
FIGURE C-2. FLOE SIZE 1-15 OCTOBER

119
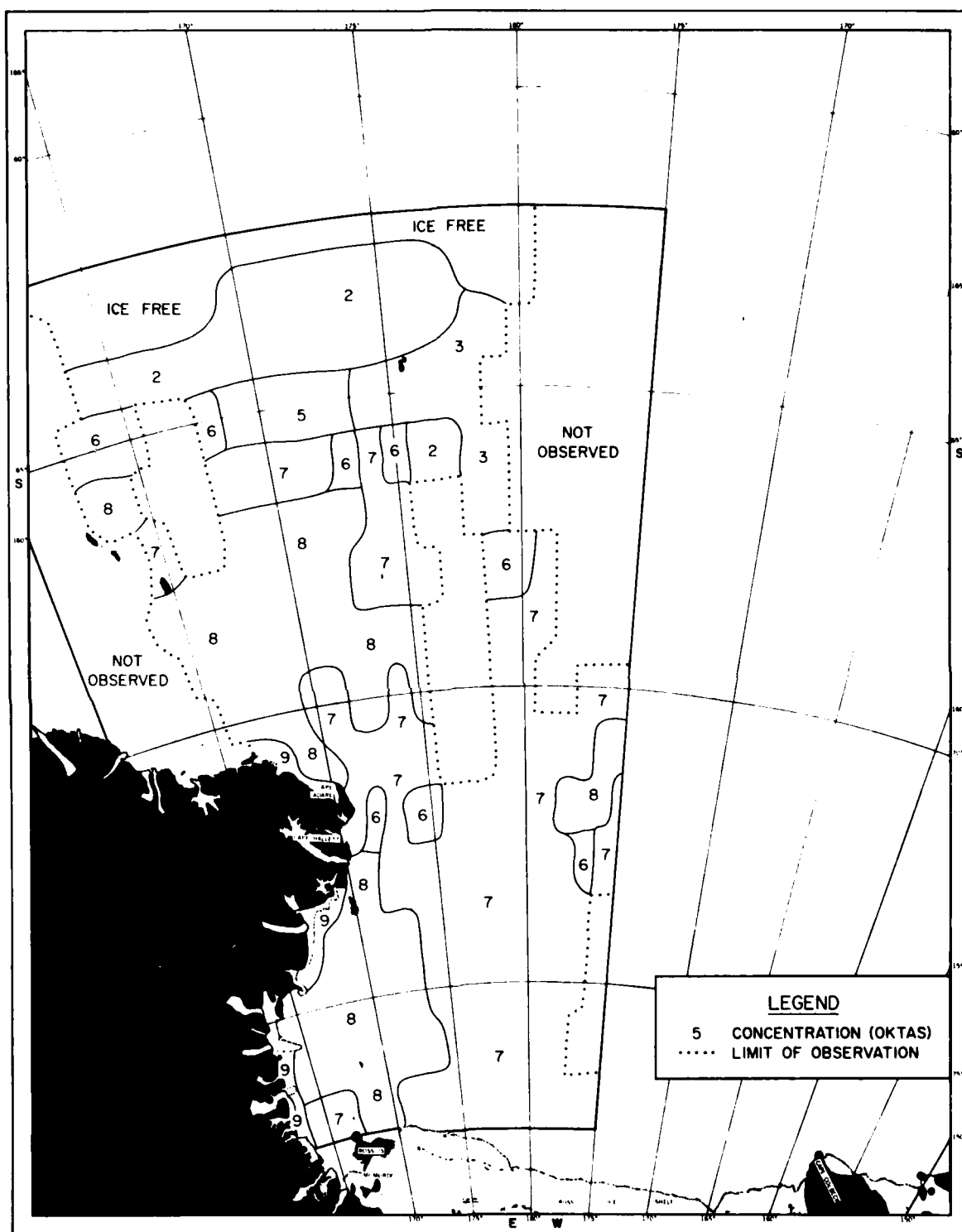
FIGURE C-3. ICE CONCENTRATION 16-31 OCTOBER

120
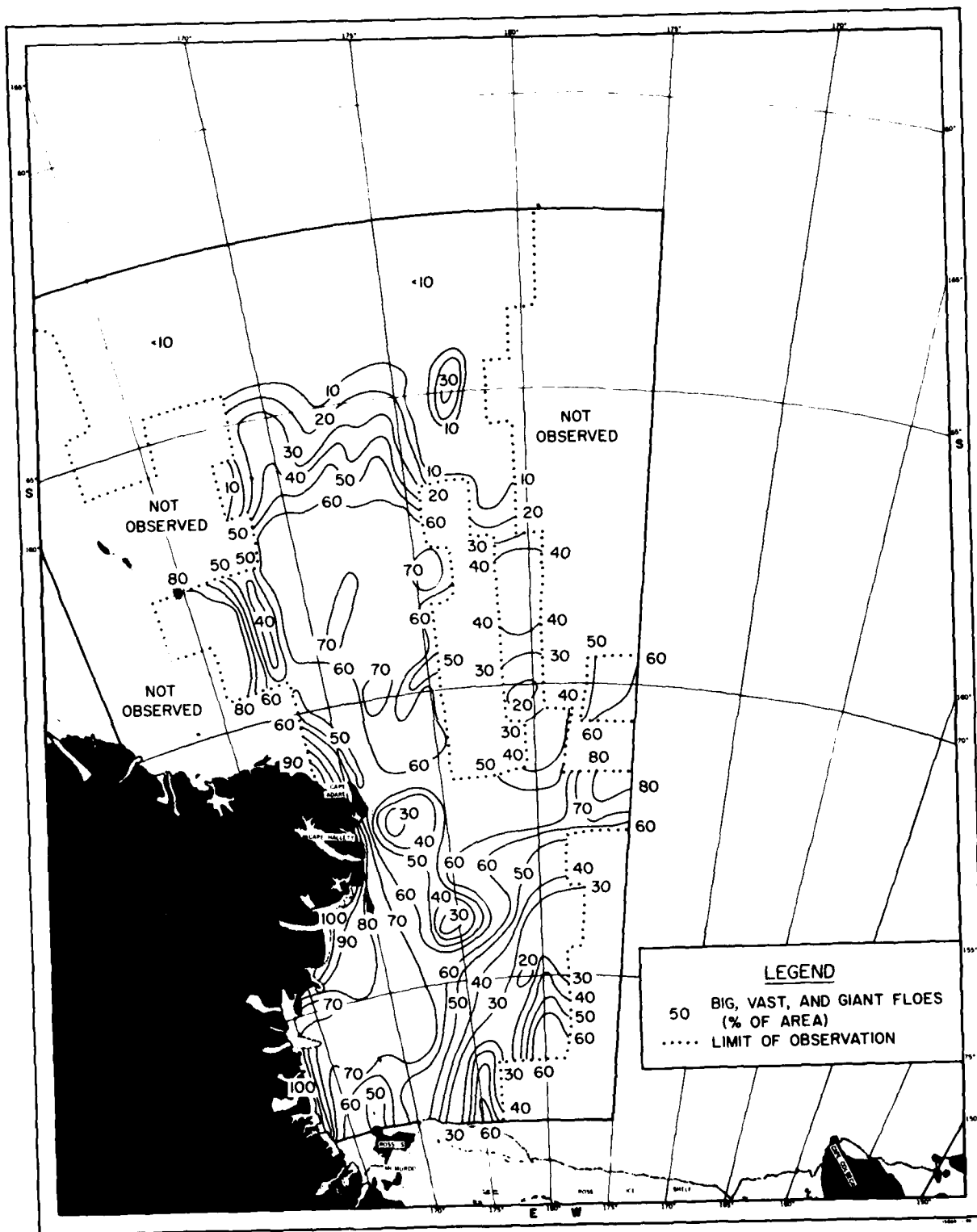
FIGURE C-4. FLOE SIZE 16-31 OCTOBER

121
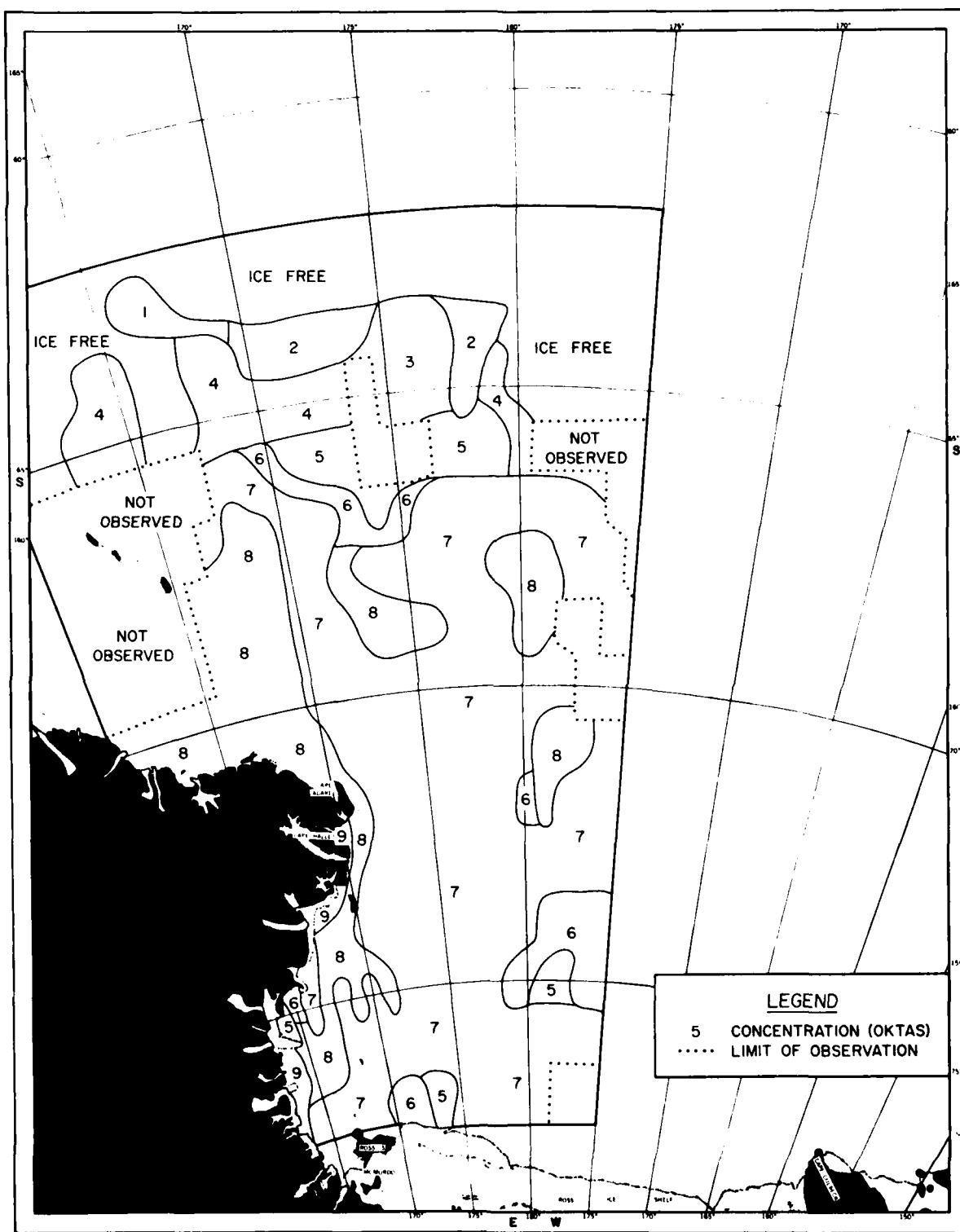
FIGURE C-5. ICE CONCENTRATION 1-15 NOVEMBER
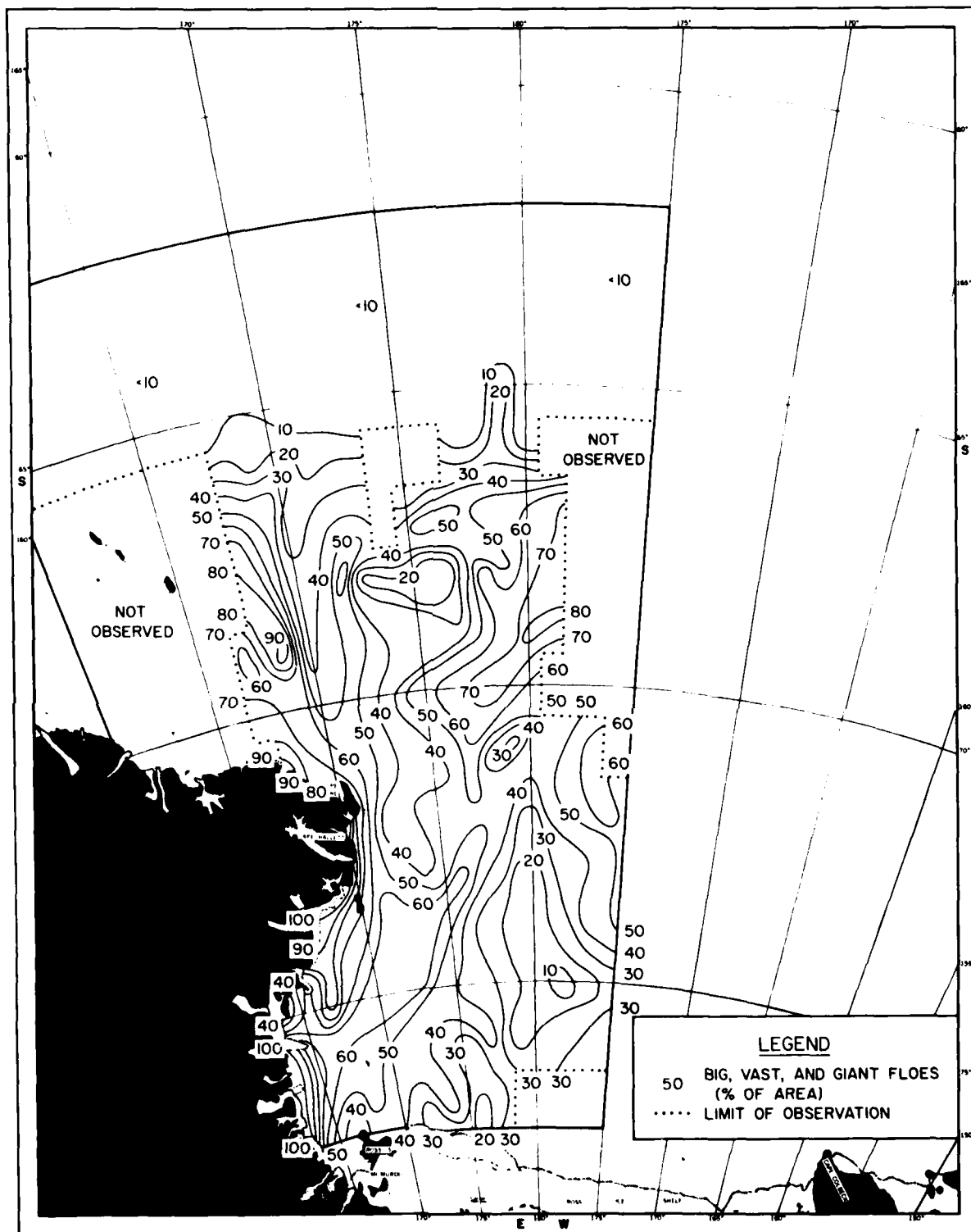
FIGURE C-6. FLOE SIZE I-15 NOVEMBER

123
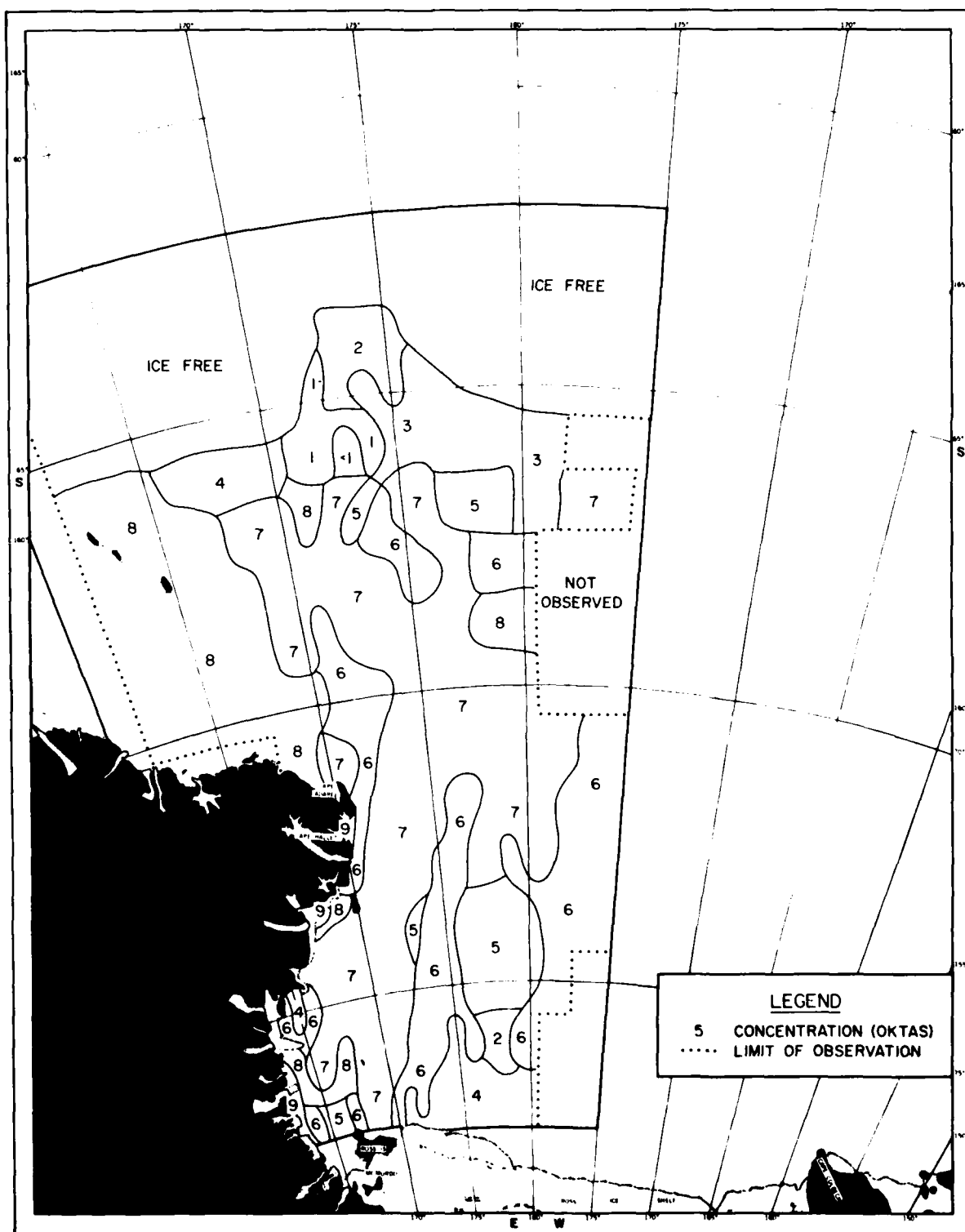
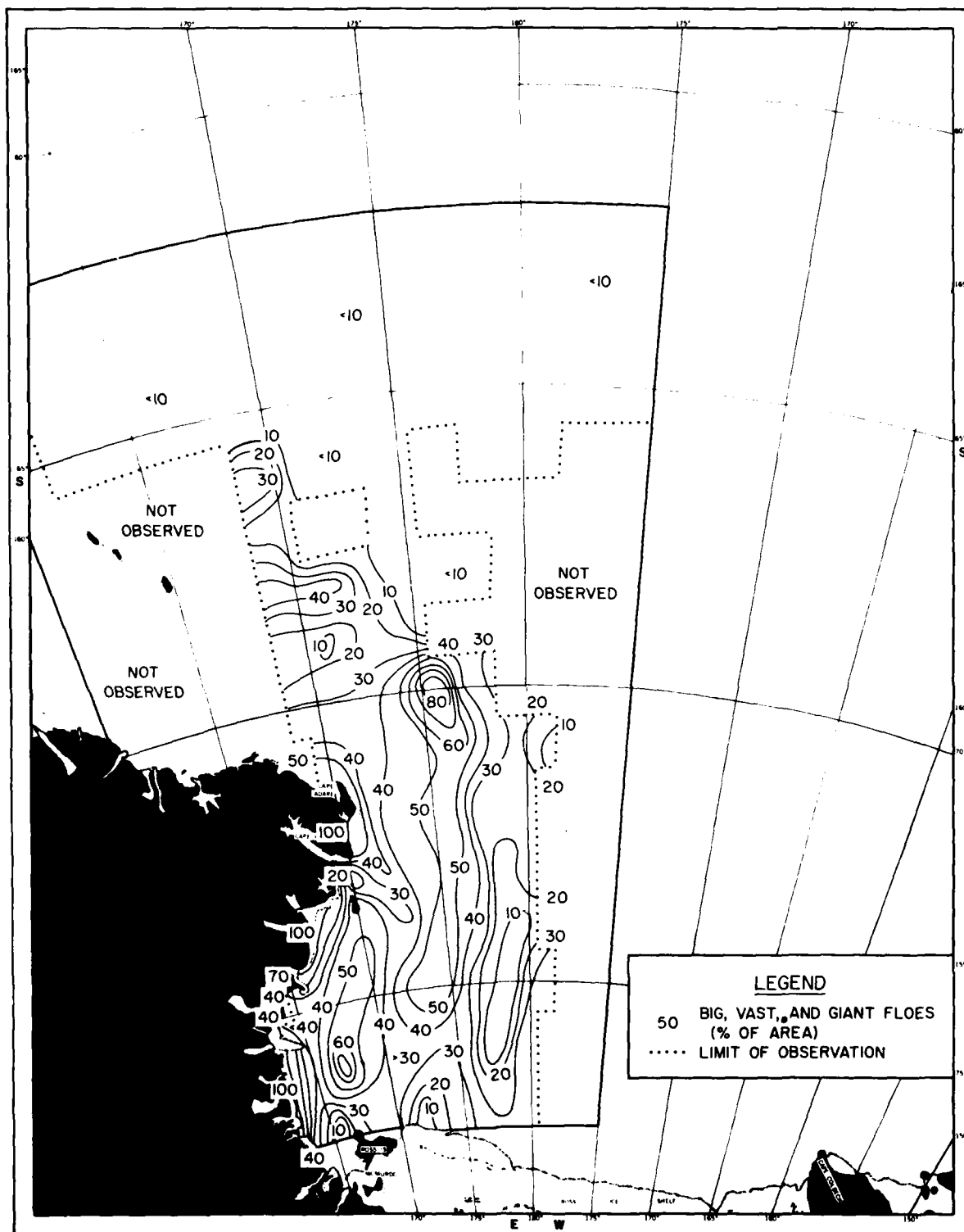FIGURE C-7 ICE CONCENTRATION 16-30 NOVEMBER
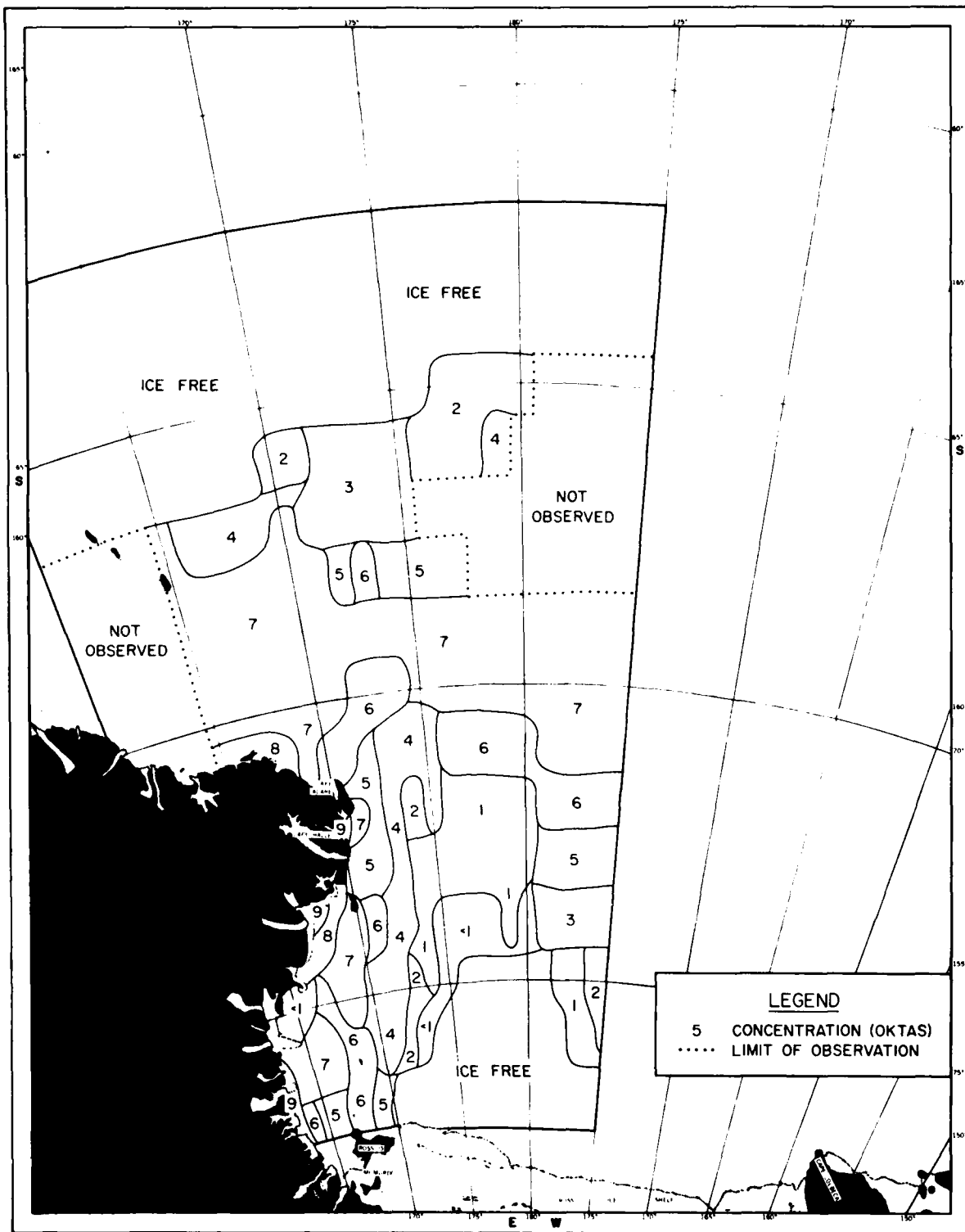
124

FIGURE C-8. FLOE SIZE 16-30 NOVEMBER
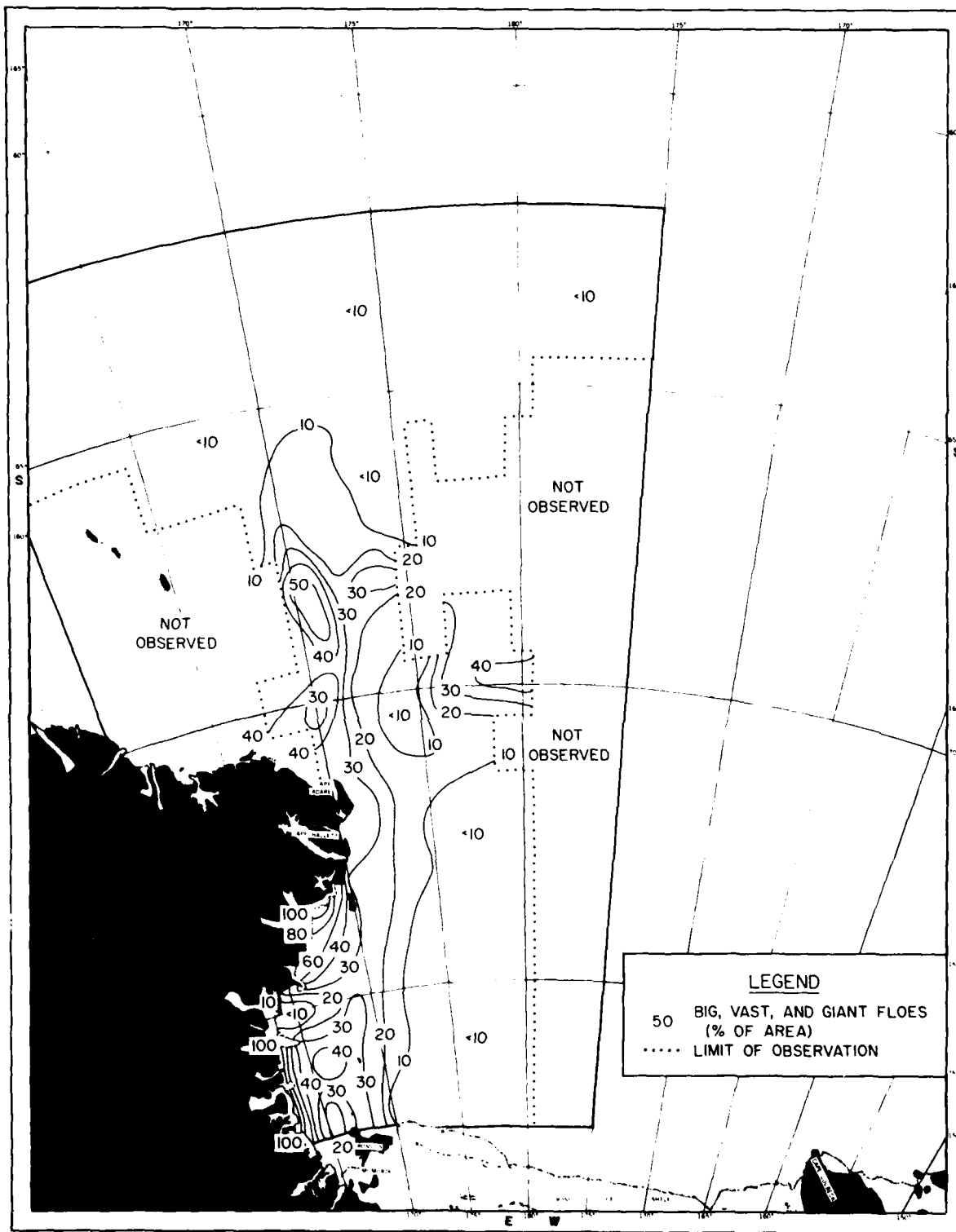
FIGURE C-9. ICE CONCENTRATION 1-15 DECEMBER

FIGURE C-10. FLOE SIZE 1-15 DECEMBER

127

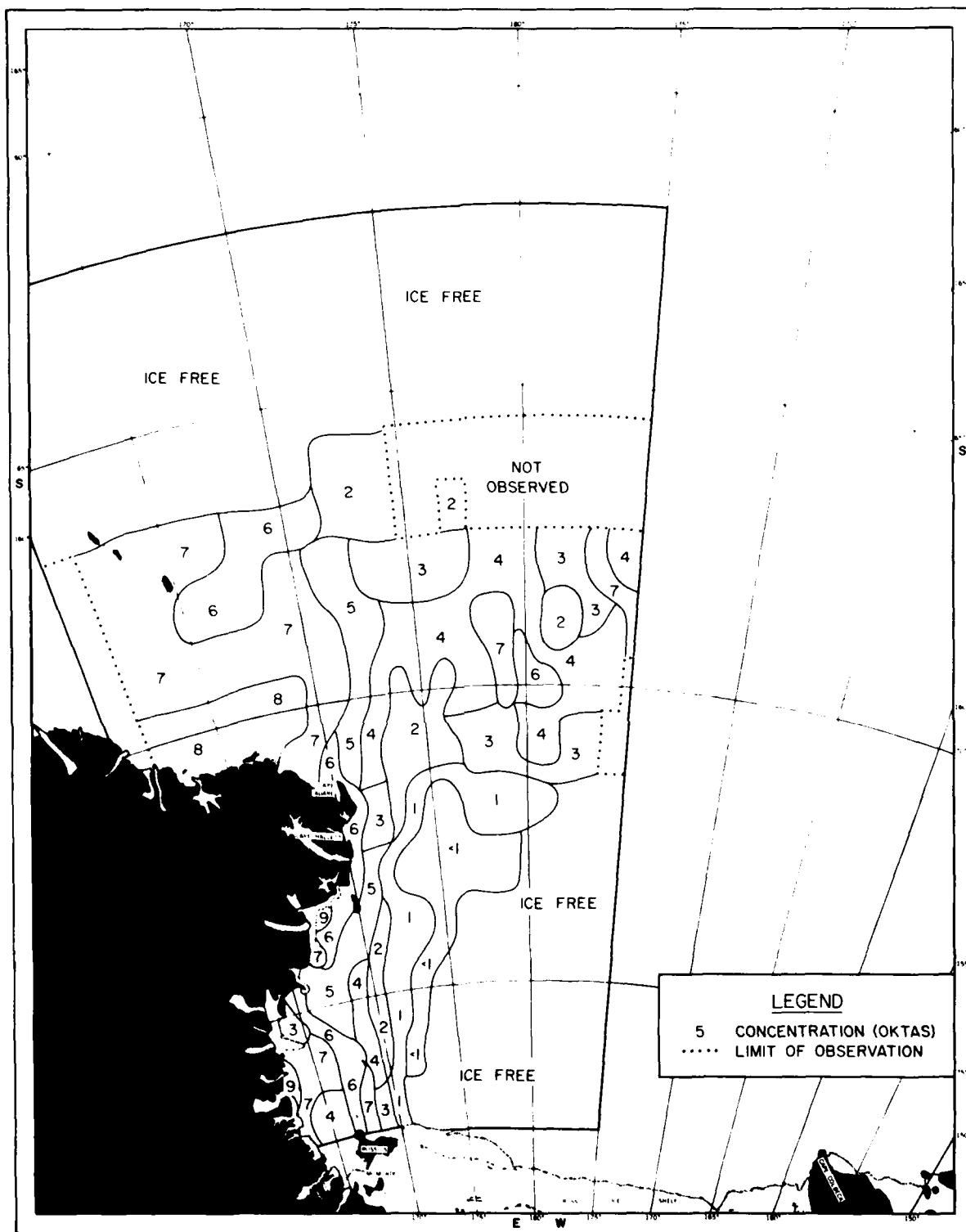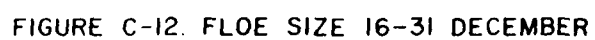FIGURE C-11. ICE CONCENTRATION 16-31 DECEMBER

128

FIGURE C-12. FLOE SIZE 16-31 DECEMBER
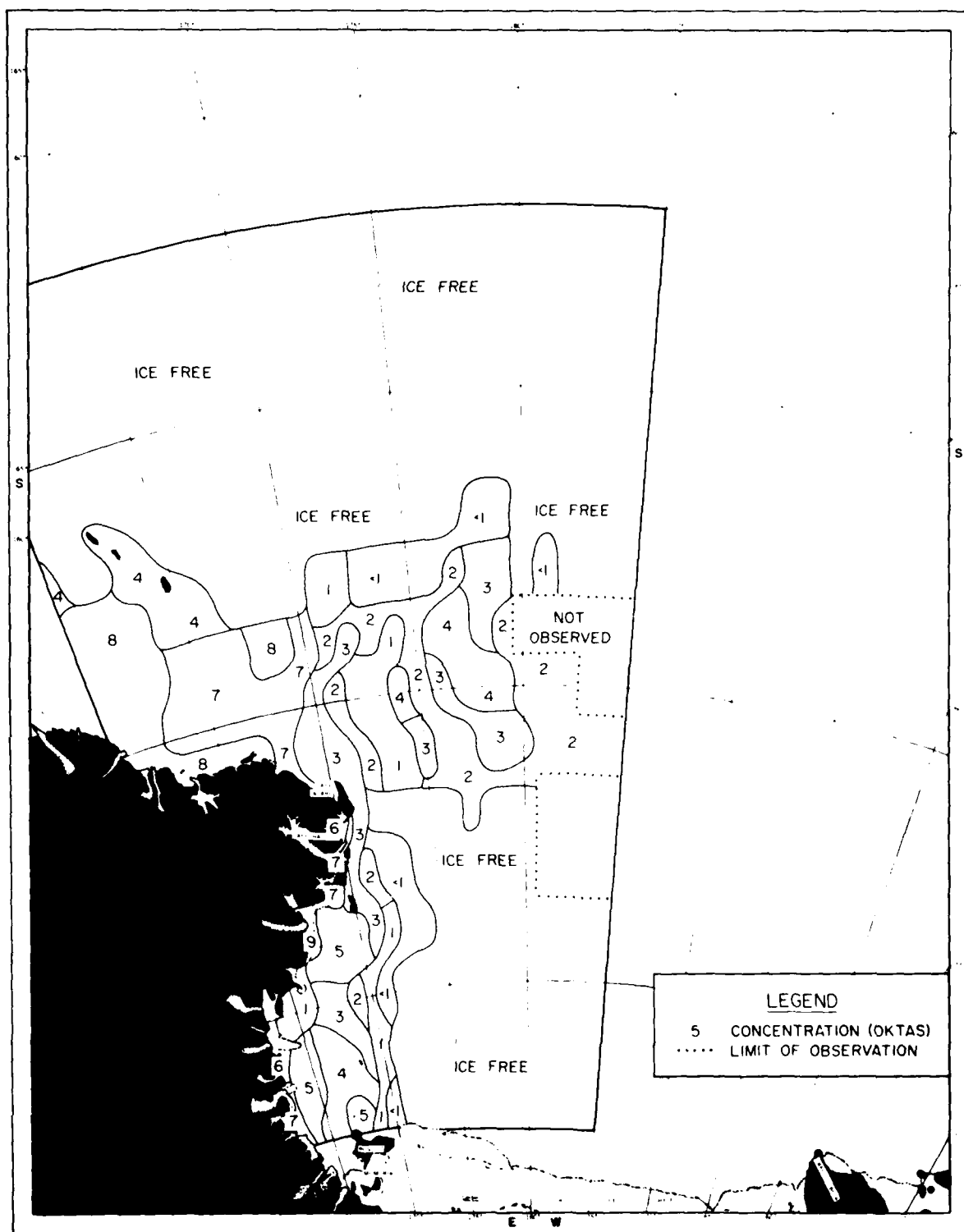
FIGURE C-13. ICE CONCENTRATION 1-15 JANUARY

130

<10

<10

<10

<10

<10

10

NOT
OBSERVED

NOT
OBSERVED

<10

20
10

50

50

100

10

<10

10

<10

20

50

70 30

S

S

E W

LEGEND

50   BIG, VAST, AND GIANT FLOES
(% OF AREA)

····· LIMIT OF OBSERVATION

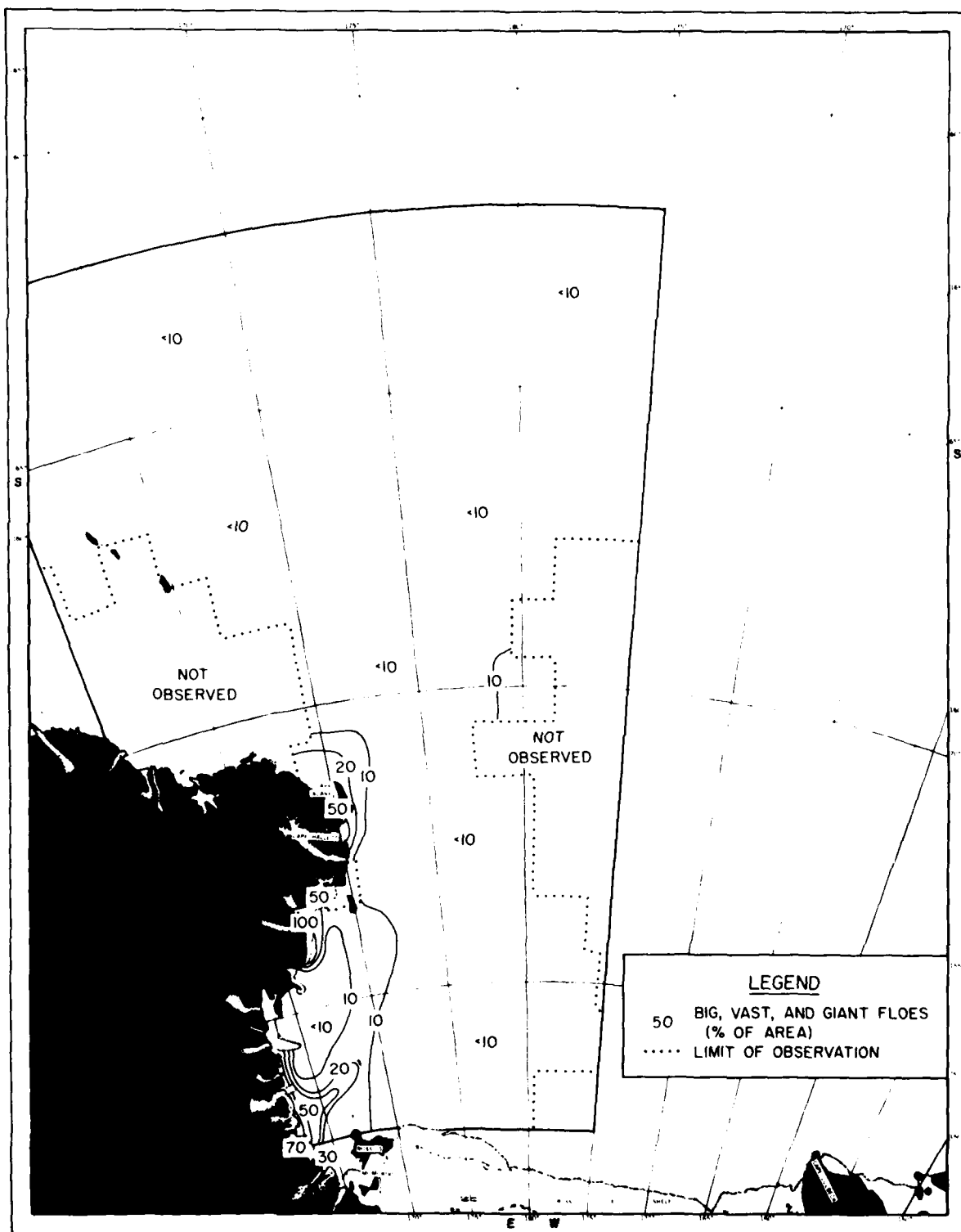FIGURE C-14. FLOE SIZE 1-15 JANUARY

131

FIGURE C-15. ICE CONCENTRATION 16-31 JANUARY

DISTRIBUTION LIST

NAVY

NATTC
USNA/ANNA
NAVSHIPRANDCEN
CNO/OP987T1
COMNAVWEASERV
NRL Codes 2027, 8040, and 8310
FLEWEAFAC
COMSC
OCEANAV
ONR/Code 460
FLEWEACEN
FLENUMWEACEN
NAVPGSCOL, 3 copies
VXE-6

OSU
SIO/UC

FOREIGN

INO/Argentina
SDHN/Argentina
SMAA/Argentina
DEAES/Canada
ORI/UT/Japan
JMA/Japan
OD/UA New Zealand
NRL/New Zealand
NZOI/New Zealand

OTHER GOVERNMENT AGENCIES

USCGTC/MSS
USCG/PSD
COMUSCG
USCGOU
USCGC POLAR STAR
USCGC BURTON ISLAND
USCGC EDISTO
USCGC GLACIER
USCGC NORTHWIND
USCGC WESTWIND
USCGC STATEN ISLAND
NOAA/OTC
NOAA/NOS
NOAA/EMP
NOAA/Library
NOAA/NESS
JCS/J3-38
USAF/ETAC
GPO/PDD
DDC, 12 copies
NCC

UNIVERSITIES

MIT/DOCS
MRL/UC
MLDS/SUNY, STONY BROOK
CMES/LU
EPS/UP
DES/AU
VIMS
OI/FSU

REPORT DOCUMENTATION PAGE

READ INSTRUCTIONS
BEFORE COMPLETING FORM

1. REPORT NUMBER	2. GOVT ACCESSION NO.	3. RECIPIENT'S CATALOG NUMBER
NOO SP-265	AD-A102093	

4. TITLE *(and Subtitle)*	5. TYPE OF REPORT & PERIOD COVERED
WESTERN ROSS SEA AND MCMURDO SOUND ICE FORECASTING GUIDE	SPECIAL PUBLICATION
	6. PERFORMING ORG. REPORT NUMBER

7. AUTHOR(s)	8. CONTRACT OR GRANT NUMBER(s)
R. J. PERCHAL	

9. PERFORMING ORGANIZATION NAME AND ADDRESS	10. PROGRAM ELEMENT, PROJECT, TASK AREA & WORK UNIT NUMBERS
NAVAL OCEANOGRAPHIC OFFICE (NAVOCEANO) WASHINGTON, D.C. 20373	

11. CONTROLLING OFFICE NAME AND ADDRESS	12. REPORT DATE
NAVAL OCEANOGRAPHIC OFFICE (NAVOCEANO) WASHINGTON, D.C. 20373	JUNE 1975
	13. NUMBER OF PAGES
	146

14. MONITORING AGENCY NAME & ADDRESS *(if different from Controlling Office)*	15. SECURITY CLASS. *(of this report)*
	UNCLASSIFIED
	15a. DECLASSIFICATION/DOWNGRADING SCHEDULE

16. DISTRIBUTION STATEMENT *(of this Report)*

Approved for public release; distribution unlimited.

17. DISTRIBUTION STATEMENT *(of the abstract entered in Block 20, if different from Report)*

18. SUPPLEMENTARY NOTES

19. KEY WORDS *(Continue on reverse side if necessary and identify by block number)*

Ice forecasting guide	North pack edge	Warming degree days
Short-range ice forecasts	South pack edge	Pack edge recession
Long-range ice estimates	Ice growth	Pack concentration
Environmental data	Frost degree days	Ice thickness

20. ABSTRACT *(Continue on reverse side if necessary and identify by block number)*

Procedures for preparing short-range (48-hour) forecasts and long-range (15- and 30-day) estimates of austral summer sea ice conditions in the western Ross Sea and McMurdo Sound are given. Magnitude and direction of short-period ice drift are related to pack concentration, topography, and thickness, surface currents, and forecasted surface wind velocities. Long-period ice estimates are based on analog techniques relating various environmental factors to pack growth, extent, and disintegration as well as

DD FORM 1473 EDITION OF 1 NOV 65 IS OBSOLETE
S/N 0102-014-6601

20.

.using the progression of ice melt indicated by selected historical data. Examples of short-range ice forecasts and long-range estimates are given. Techniques are included for interpreting sea ice from satellite imagery.

Background data on environmental factors of mean storm tracks, mean monthly sea level pressure (winds) and surface air temperature over the Ross Sea and austral summer ice conditions over the western Ross Sea and McMurdo Sound are given. Analyses of historical ice edge data which are based on observations taken over sixteen years from DEEP FREEZE I (1955-56) through DEEP FREEZE 71 (1970-71) indicate median positions of the north and south pack edges at half-monthly intervals from October through January. Ice data also include the range of locations of pack edges, distribution of pack concentrations, percentage of large floe sizes, and ice thickness. Analyses of the thickness and median extent and extremes of fast ice in McMurdo Sound are included. Selection of optimum ice routes is described using mean ice concentrations and the percentage of large floe sizes.

19.

Floe size	Deviation angle	Optimum ice routes
Pack disintegration	Drift distance	Storm tracks
Fast ice extent	Channel clearing	Surface currents
Fast ice dislodgment	Iceberg drift	Satellite ice data